EPRI

Technical Approach to Turbine Missile Probability Assessment

1006451

Technical Approach to Turbine Missile Probability Assessment

1006451

Technical Progress, December 2001

EPRI Project Manager

Steve Hesler

DISCLAIMER OF WARRANTIES AND LIMITATION OF LIABILITIES

THIS DOCUMENT WAS PREPARED BY THE ORGANIZATION(S) NAMED BELOW AS AN ACCOUNT OF WORK SPONSORED OR COSPONSORED BY THE ELECTRIC POWER RESEARCH INSTITUTE, INC. (EPRI). NEITHER EPRI, ANY MEMBER OF EPRI, ANY COSPONSOR, THE ORGANIZATION(S) BELOW, NOR ANY PERSON ACTING ON BEHALF OF ANY OF THEM:

(A) MAKES ANY WARRANTY OR REPRESENTATION WHATSOEVER, EXPRESS OR IMPLIED, (I) WITH RESPECT TO THE USE OF ANY INFORMATION, APPARATUS, METHOD, PROCESS, OR SIMILAR ITEM DISCLOSED IN THIS DOCUMENT, INCLUDING MERCHANTABILITY AND FITNESS FOR A PARTICULAR PURPOSE, OR (II) THAT SUCH USE DOES NOT INFRINGE ON OR INTERFERE WITH PRIVATELY OWNED RIGHTS, INCLUDING ANY PARTY'S INTELLECTUAL PROPERTY, OR (III) THAT THIS DOCUMENT IS SUITABLE TO ANY PARTICULAR USER'S CIRCUMSTANCE; OR

(B) ASSUMES RESPONSIBILITY FOR ANY DAMAGES OR OTHER LIABILITY WHATSOEVER (INCLUDING ANY CONSEQUENTIAL DAMAGES, EVEN IF EPRI OR ANY EPRI REPRESENTATIVE HAS BEEN ADVISED OF THE POSSIBILITY OF SUCH DAMAGES) RESULTING FROM YOUR SELECTION OR USE OF THIS DOCUMENT OR ANY INFORMATION, APPARATUS, METHOD, PROCESS, OR SIMILAR ITEM DISCLOSED IN THIS DOCUMENT.

ORGANIZATION(S) THAT PREPARED THIS DOCUMENT

EPRI

This is an EPRI Level 2 report. A Level 2 report is intended as an informal report of continuing research, a meeting, or a topical study. It is not a final EPRI technical report.

ORDERING INFORMATION

Requests for copies of this report should be directed to the EPRI Distribution Center, 207 Coggins Drive, P.O. Box 23205, Pleasant Hill, CA 94523, (800) 313-3774.

Electric Power Research Institute and EPRI are registered service marks of the Electric Power Research Institute, Inc. EPRI. ELECTRIFY THE WORLD is a service mark of the Electric Power Research Institute, Inc.

CITATIONS

This document was prepared by

Structural Integrity Associates Inc.
3315 Almaden Expressway, Suite 24
San Jose, CA 95118-1557

Principal Author
D. Rosario

R. Placek
Consultant
75 Birchwood Lane
Schenectady, NY 12309

EPRI
1300 West WT Harris Blvd.
Charlotte, NC 28262

Principal Author
P. Zayicek

This document describes research sponsored by EPRI.

The publication is a corporate document that should be cited in the literature in the following manner:

Technical Approach to Turbine Missile Probability Assessment: EPRI, Palo Alto, CA: 2001. 1006451.

REPORT SUMMARY

The current methodology and basis for assessing the risk of turbine missiles is explored and described. Areas of potential conservatism are identified, which may become the basis for a new analysis process that provides relief to plant operators who are seeking increased time intervals between turbine inspections and turbine control tests.

Background

The licensing basis for all nuclear plants includes the requirement to maintain a low probability of creating damage to safety-related plant equipment due to release of high-energy turbine missiles. The task of providing the technical basis to prove the risk of turbine missile generation does not exceed the required level has rested with the turbine manufacturers for most plants. These manufacturers perform the routine turbine disk inspections, and also maintain a database of turbine control failure rates for their fleets, both of which form the primary basis for assessing risk. Turbine operators are increasingly concerned that a significant level of conservatism exists in the current missile probability evaluation, and as a consequence operators are required to perform frequent turbine inspections and control system tests. Operators are seeking relief from the current test and inspection requirements.

Objective

The objective of the current project is to examine the current methodology for assessing risk of turbine missiles, identify areas of conservatism, and eventually improve or update these portions of the methodology. Ensuring implementation of this improved methodology is also critical, so facilitating the interface between plant operators, regulatory agencies, and the turbine manufacturers is an important aspect of the project objectives.

Approach

A review was performed of relevant regulatory documents, technical papers, and technical reports by experts in turbine component risk assessments. Advanced turbine disk nondestructive examination techniques were also explored. Case histories were identified, involving both turbine failures and instances of operational relief granted by the NRC. An analysis was undertaken of the cost-effectiveness of potential development activity that could achieve the objective of reducing conservatism. This interim report provides the basis for upcoming discussions among the licensees, manufacturers, and regulators.

Results

Based on the results obtained to date, the most promising areas for reducing conservatism in the current risk assessment methodology include a refinement in the probabilistic fracture mechanics analysis of turbine disk stress corrosion cracking. Another area with a high potential for refinement is the assessment of probability of achieving turbine overspeed due to controls or valve failure. A third area of refinement is the application of advanced ultrasonic testing techniques to improve the characterization of stress corrosion cracking in disk bore regions. A case history is presented that demonstrates concurrence by the NRC with improved fracture mechanics analysis methodology.

EPRI Perspective

The assessment of turbine missile probability is one of several turbine-related projects being performed by EPRI that are seeking to reduce plant O&M costs through improved risk assessment methodology. Use of advanced fracture mechanics and NDE techniques have been successfully applied by EPRI in risk assessment of other turbine components. EPRI's perspective is that these advanced techniques are ready for application to the risk assessment of turbine disk failure and when completed, conservatism will be removed from the current risk assessment procedure.

Keywords

Turbine
Missiles
Overspeed
Risk Assessment
Probabilistic
Inspection Interval

ABSTRACT

Evaluating and managing the risk of turbine disk failure and the consequential release of high-energy missiles is a key aspect of the required operations and maintenance practices at U.S. nuclear plants. The primary impact on O&M is the need for frequent testing of turbine controls, and periodic turbine disk nondestructive examination. Plant operators are seeking relief in the form of increased test and inspection intervals, which can be obtained through a refinement in the analysis methodology and technical basis for the current intervals. This interim report contains a description of the technical approach currently used to evaluate risk of missile generation. Areas of potential conservatism are identified and explored, with recommendations for which technical areas to pursue that would have the greatest chance of achieving the objectives of increased test and inspection intervals. The elements of the risk evaluation that appear most promising for a reduction in conservatism are the probabilistic fracture mechanics analysis, evaluation of turbine overspeed probability, and characterization of service-induced stress corrosion cracks in the bore/keyway region.

CONTENTS

LIST OF FIGURES

LIST OF TABLES

1
INTRODUCTION

The turbine-generator is not considered part of a nuclear power plant's safety-related equipment, however a possibility exists that high-energy missiles created by failure of the low-pressure turbine disks could penetrate intervening barriers and damage plant safety-related equipment. Disk and rotor failures have occurred in a number of fossil turbine and generators, and one nuclear turbine located outside the U.S. [1,2]. Two potential missile generation scenarios are relevant; stress corrosion cracking in the disk bore with subsequent brittle fracture at design speed, and destructive overspeed of the turbine-generator due to failure of the turbine controls and/or steam valve failure to close. Appendix A of Section 10 of the Code of Federal Regulations (CFR) Part 50 states that equipment critical to safety of nuclear power plants must be appropriately protected against missiles resulting from equipment failures [3]. Turbine missile protection is addressed during the plant's initial licensing process and is described in either the licensing language or the supporting documents that form the licensing basis. Compliance with regulatory requirements by the plant typically impacts operations and maintenance by mandating intervals for in-service inspections of disks, and testing of plant controls. EPRI members who are operating turbines with built-up rotors are seeking to optimize plant operation and maintenance activities, while staying within approved limits on the risk of damage to safety-related equipment. Operators are requesting that the technical and regulatory issues that govern compliance with the NRC relative to turbine missiles be re-examined. Specifically, plant operators are seeking relief by decreasing the frequency of these disk inspections and control system tests, while still remaining in compliance with the NRC. This interim report provides a status of EPRI project 047015 titled "Re-evaluation of Turbine Missile Probability".

1.1 Background

EPRI report 1001267 issued in December 2000 provides an overview of the technical and regulatory issues associated with the assessment of turbine missile probability [4]. The report recommends a re-examination of the existing techniques for assessing missile probability. These techniques, either directly or indirectly, constitute part of each plant's licensing basis. Potential areas for relief identified in report 1001267 are; improved ultrasonic disk inspection, probabilistic fracture mechanics, and updating the database used for projecting failure rates of turbine controls and valves. Subsequent project activity in 2001 examined these aspects more closely, and the findings are reported in this document.

1.2 Project Objectives

The objectives of this EPRI project are to:

- examine all technical and regulatory factors that influence the current requirement for plants to conduct periodic inspections of turbine disks and regular tests of turbine overspeed protection systems

- develop the technical basis for a re-evaluation of the missile probability to support relief from potentially unnecessary and excessive tests and inspections
- assist EPRI members in their interactions with regulators and with the implementation of new probabilistic assessment procedures.

1.3 Report Scope

This report contains an update on findings relative to:

- Improved NDE techniques for disk bore inspections
- Assessment of probabilistic disk fracture mechanics methodology
- Missile strike probability
- Plant regulatory issues
- Case histories of regulatory relief

References

1. D. Kalderon, "Steam Turbine Failure at Hinkley Point A", Proc. Inst. of Mech. Engrs., Vol. 186, 1972, pp. 341-377.

2. A. Goldberg, R. D. Streit, "Observations and Comments on the Turbine Failure at Yankee Atomic Electric Company, Rowe Massachusetts", NUREG/CR-1884, March, 1981.

3. General Design Criterion 4, "Environmental and Missile Design Bases," of Appendix A, General Design Criterion for Nuclear Power Plants," to 10 CFR 50, "Domestic Licensing of Production and Utilization Facilities".

4. *Assessment of Turbine Missile Probability: Technical and Regulatory Issues,* EPRI, Palo Alto, CA: 2000. 1001267

2
OVERVIEW OF RISK ASSESSMENT PROCESS

Plant licensees who operate with built-up low-pressure turbine rotors consisting of shrunk-on disks or wheels are required to demonstrate an acceptably low risk of missile generation prior to each post-refueling plant startup. Many operators rely on analyses prepared by the turbine original equipment manufacturers (OEMs) for regulatory compliance. OEMs also oversee or perform many of the disk NDE inspections that influence the disk re-inspection interval. This chapter outlines the structure and history of the current risk assessment procedure.

2.1 Definition of Risk Components and Historical Basis

2.1.1 Bush Studies (1973, 1978)

The first study by Bush [1] defined the overall risk of damage to safety-related equipment (P_4) in terms of three components (P_1, P_2, and P3), as shown in Figure 2-1.

Bush evaluated P_1 based on historical failure data obtained from a wide range of turbine sizes (including fossil, nuclear, and industrial units) and conservatively estimated an upper value of 10^{-4} per turbine-year. Bush expected a reduction in failure rate to ~7 x 10^{-5} by the late 1970s due to general improvements in plant equipment and operation.

Regarding the strike probability, P_2, Bush cites results of a detailed analysis by Semanderes [2] that assesses strike probabilities for typical BWR and PWR plant layouts. Probabilities were calculated for individual plant regions that contain safety-related systems. Strike probabilities were estimated to be less than $9x10^{-3}$ for unfavorable turbine orientation, except for a direct strike on the containment wall. Direct strikes on the containment structure by low trajectory missiles (LTMs) are not expected to result in penetration through the reinforced concrete wall based on results of analyses conducted by the Naval Ordnance Lab [3]. Therefore, the upper limit of probability of striking safety-related equipment is effectively 10^{-2} as indicated Figure 2-1.

The damage probability (P_3) is set at a value of 1.0, which is reasonable for unprotected strike locations such as the control room and spent fuel pool. However, P_3 is likely to be less than 1.0 for safety-related systems that are protected by concrete. Using a value of 1.0 provides an additional small margin since P_3 is calculated independent of P_2. Otherwise, the combined probability P_2 x P_3 for each strike location could be calculated, in which location-specific values of P_3 could be used. Bush's approach, still accepted by the NRC, is to de-couple P_2 and P_3. The second study by Bush [4] provided an updated and more detailed historical-based analysis of P1 that determined 3x10-5 < P1< 3x10-4. This finding confirms Bush's earlier projection of P1 being approximately 7x10-5.
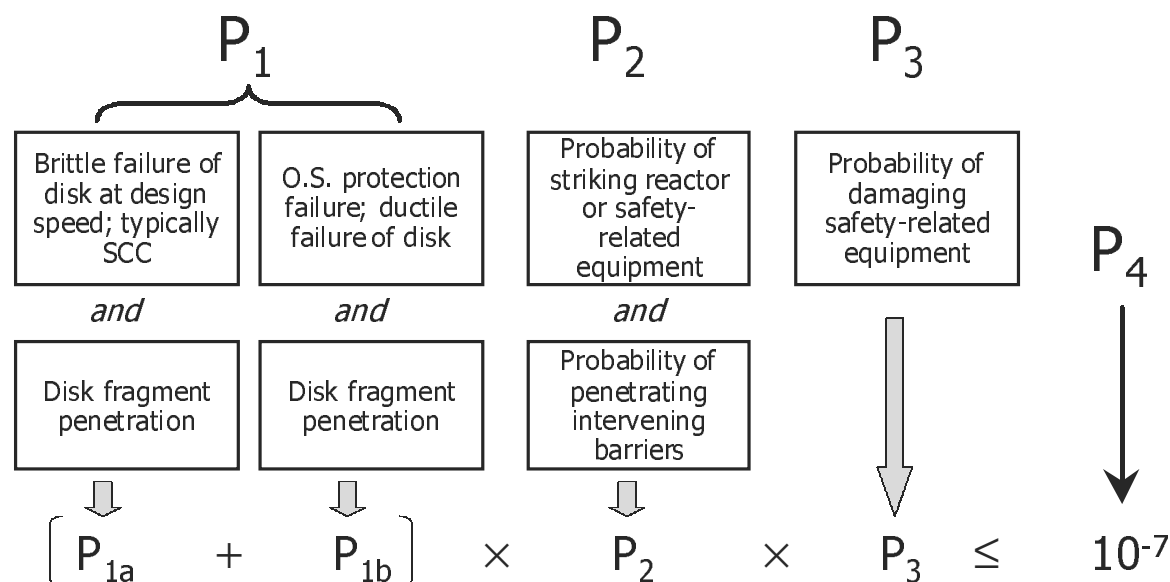
Figure 2-1 Risk Components Relative to Damage of Safety-Related Equipment

2.1.2 USNRC Regulatory Guide 1.115 (1977)

RG 1.115 contains the NRC's statement that 10^{-7} is the upper limit for P_4 probability per turbine-year. The NRC also states that $P_2 \times P_3$ must be less than 10^{-3} for new operating license applications, and recommends that this be achieved by placing safety-related equipment out of the expected path of low-trajectory missiles. Barriers are an alternative method of protecting safety-related equipment according to RG 1.115, however licensees must then prove that the combined probability $P_2 \times P_3$ is less than 10^{-3}.

2.1.3 Hope Creek SER (NUREG-1048 Supplement 6, 1986)

A shift in emphasis within the NRC review process is noted in the Safety Evaluation Report (SER) for Public Service Electric and Gas Hope Creek Generating Station [6]. Following the observation of service-induced stress corrosion cracking in disk bore regions of U.S. nuclear turbines in the early 1980s the NRC outlined an approach for ensuring safe operation of these plants.

The significance of the Hope Creek SER is that the NRC replaced the use of historical-based assessments of P_1 with detailed probabilistic analyses. This change then enabled the benefits of periodic turbine overspeed control tests and disk inspections to be properly accounted for as "plant-specific factors" in the detailed assessment of P_1.

In NUREG-1048, the NRC maintains the position established earlier in RG 1.115 that the combined probability $P_2 \times P_3$ is reasonably estimated at values of 10^{-2} for unfavorable orientation and 10^{-3} for favorable orientation. Many of the licensed plants, and some new plants in the process of licensing at that time were designed with unfavorable orientation of the turbine relative to safety related equipment. It was not practical for these plants to consider

modifications to produce a favorable turbine orientation. The NRC, to simplify the procedure for evaluating turbine missile risk, decided to discourage the submission of detailed evaluations of the product $P_2 \times P_3$, and simply credit licensees with the accepted values of 10^{-2} and 10^{-3} as stated above. The NRC emphasis then shifted toward maintaining an acceptable level for P_1, which when combined with the product of $P_2 \times P_3$ yields the acceptable P_4 value of 10^{-7}.

The NRC cited analyses by Burns [7] and Clark, Seth, and Shaffer [8], in stating that "missile generation can be modeled and the assessed probability can be strongly influenced by in-service testing and inspection frequencies". Essentially, the NRC states that the value and uncertainty of P_1 previously reported by Bush can be maintained at acceptable levels (i.e. less than 10^{-5}) by instituting a program of turbine maintenance that includes periodic testing of the overspeed control system and disk inspections.

2.1.4 Summary

A review of the key technical papers and regulatory documents shows how the current NRC requirements related to the risk components have evolved. The current NRC position can be summarized as follows:

1. The overall probability of damage to safety-related equipment must be maintained at or below 10^{-7}.

2. It is possible to calculate the probability that a turbine missile, once generated, will strike and damage a safety-related system. Such a calculation would take into account the specific layout of each plant, the relation between missile size and its likelihood of penetrating intervening barriers, and the probability of damage to safety-related equipment once struck. However the NRC has elected to discourage licensees from submitting this type of detailed calculation and instead credits licensees with the appropriate 'standard' value for $P_2 \times P_3$ (10^{-2} and 10^{-3} respectively for unfavorable and favorable orientation) [6].

3. The allowable probability for P_1 is either 10^{-5} or 10^{-4} depending on whether the turbine is unfavorably or favorably oriented. A majority of the currently licensed plants are designed with unfavorable orientation and must therefore maintain $P_1 < 10^{-5}$. Many licensees have their periodic disk inspections performed by the turbine OEMs, who submit reports containing P_1 probability projections that are based on results of these inspections and a calculated crack growth in future operation.

2.2 OEM Evaluations of Probability P_1

Although EPRI does not have access to the full set of detailed procedures and technical bases used by suppliers of turbines used in domestic U.S. plants, some information on P_1 evaluation methods is available in the open literature [6,8].

2.2.1 General Electric

The Hope Creek SER [6] provides information on General Electric's approach to calculating P_1. An overview is shown in Figure 2-2.

turbine speed probability
- fault-tree model
- EHC, MHC systems
- valve reliability

disk burst probability integrated over speed range

probability of wheel burst versus speed and wheel temperature
- crack initiation probability
- crack detection and sizing uncertainty
- crack growth rate (field & lab)
- material toughness variations
- deep-seated material properties
- crack geometry variations
  - stress
  - shape factor
  - branching

multiply → missile generation probability

probability of fragment penetration versus speed
- assumed fragment size distribution
- turbine stage

Figure 2-2 Overview of Approach to Turbine Missile Probability Assessment from Hope Creek SER

The General Electric approach is comprehensive, taking into account uncertainty in a number of variables such as turbine speed, SCC crack growth rate, material toughness, and fragment casing penetration. The turbine speed probability calculation is a key element of the overall process affecting not only the likelihood of destructive overspeed (ductile failure), but also the probability of brittle failure due to SCC as well. Brittle failure is more probable if the turbine experiences speed excursions - even if they stay within the design limit of 120 percent of running speed. Therefore, the probability of wheel burst as a function of speed must be integrated over the probability distribution of speed to yield the overall probability of wheel failure. Temperature affects the probability of brittle failure, so this integration must be performed over a range of probable wheel temperatures. Finally, the probability that wheel fragments, once created, will penetrate the turbine casing must be taken into account. The assumption that all wheel fragments will penetrate the turbine is overly conservative and extensive analyses and tests show that many of the lower energy fragments will be contained [10]. The General Electric turbine design features relatively massive interstage diaphragm rings, which together with the inner casing and outer hood structure are predicted to contain all but the most massive or highly energetic wheel fragments. Fragment energy is a function of fragment size and wheel speed at time of failure. The latter stages, particularly the final stage, employ more massive wheel designs and therefore are more likely to produce fragments with sufficient energy to penetrate the intervening structure of the turbine casings. Compounding this situation is that fragments from failure of a final stage wheel are more likely to penetrate the turbine outer casing because the inner casing may not be in the fragment path and thus be unable to absorb energy. The overall missile analysis approach balances the relatively higher probability of wheel failure for upstream stages against the lower probability of fragment penetration if these failures were to

occur. Conversely, the relatively low probability of brittle failure of the final stage wheel is balanced by the greater likelihood that a fragment (if created) would penetrate the turbine casing structure.

The Hope Creek SER does not provide details of General Electric's numerical technique for combining the individual probability elements in Figure 2-2 to evaluate the overall probability. Potential methods include use of a Monte-Carlo technique, closed-form mathematical solution involving combinations of common distribution forms, or a "bounding" approximation based on a select set of deterministic analyses. The Monte-Carlo approach, if used, would be computationally extensive due to the large number of variables involved and the very large number of iterations needed to accurately predict the relatively low probability event of missile generation. A review of the Facility Safety Analysis Report (FSAR) from Duke Energy's Catawba Plant indicates that General Electric establishes 64 different combinations of stage groups, wheel fragment groups, and energy groups. Each group contains four elements, which together creates the total of $4^3 = 64$ combinations. The four stage groups are: Stage 7 (120 and 180 percent speed), Stages 1-3 (180 percent speed), and Stages 4-6 (180 percent speed). The fragment groups assume various portions of the fractured wheel penetrate the casing, ranging from the largest size (120º arc) to the least massive ("extra small"). The energy groups are termed "Low", "Mid-Low", "Mid-High", and "High". More details are needed to fully understand the mathematical approach that General Electric uses to assess missile probabilities.

It is noted that probability distributions for several of the key variables in Figure 2-2 are reportedly based in part on results of laboratory tests, systematic in-service inspections, or destructive tests of cracked wheels, all of which are assumed proprietary to General Electric. The accuracy of the resulting probabilistic analysis likely to be enhanced through General Electric's use of this observed data on initiation rate, crack growth rate, and deep-seated material toughness. Any independent approach to missile probability assessment may require a source of equally reliable data. The important details of the General Electric analysis that are not fully described in [6] relate to the fracture-mechanics model used and the assumed stress distribution in the vicinity of the crack and keyway.

2.2.2 Westinghouse (Siemens-Westinghouse Power Corporation)

The Westinghouse missile analysis process reportedly first used in the early 1980's is described in an ASME technical paper [8]. A brief synopsis is presented below. It is not clear whether the approach described below has changed significantly since the paper was published in 1981.

Critical crack size is estimated using a semi-elliptical surface crack in an infinite plate. The crack length used in the analysis includes the keyway radius. The aspect ratio of the cracks is assumed to be 4:1, based on examination of service-induced keyway cracks. A value of 1.35 is used for the flaw shape parameter. It is not clear whether Westinghouse uses the detailed stress gradient surrounding the keyway, or a uniform stress when evaluating the stress intensity, K_I.

Fracture toughness at room temperature is used as a lower bound in the analysis. Toughness is estimated from Charpy V-notch data supplied by the disk supplier based on an empirical correlation developed by Westinghouse that uses upper-shelf Charpy data and material yield strength [9]. It is not stated in the ASME paper whether Westinghouse uses deep-seated FATT

and fracture toughness properties in their analysis procedure. Use of deep-seated toughness is considered to be a very important aspect of the assessment of brittle failure.

Westinghouse developed an empirical relation for SCC growth rate as a function of disk operating temperature and yield strength. This relation is given in Equation 5-6. The relationship was reportedly developed based on a series of in-service ultrasonic inspection of over 40 disks from operating turbines. Since only a single inspection for each disk was included in the empirical analysis, crack initiation times were effectively assumed to be zero. (This assumption may actually result in non-conservatism in the prediction of future crack growth). Westinghouse reports that following the development of the relation presented in Equation 5-6, it was successfully used to fit several larger datasets, and they have therefore judged it adequate for use in the missile probability calculations.

Westinghouse employs a probabilistic approach to evaluating P_1. Data from field inspections of disks were used to estimate probability of crack initiation. Westinghouse employs the growth rate formula described in the above paragraph and presented in Equation 5-6 with distributions on both yield strength and temperature. The result is reportedly a log normal distribution for crack growth rate variation.

The basic edge-crack model is modified for use in the Westinghouse analysis to incorporate a flaw geometry factor, G, which accounts for both the gross shape of the flaw as well as the beneficial effects of crack branching and irregularities in the shape local to the crack tip. The resulting crack model is given in Equation 2-1 below.

$$a_{cr}^{*} = \frac{1}{1.21\pi}\left(\frac{K_{IC}}{\sigma}\right)^2$$

<div align="right">**Equation 2-1**</div>

where:

> a_{cr}^{*} is the nominal critical crack size accounting for shape parameter or branching factor
> $a_{cr} = G \cdot a_{cr}^{*}$ is a larger, effective critical crack size that includes shape parameter and branching factor
> K_{IC} is the material toughness
> and, σ is the applied stress

Westinghouse reports evaluation of critical crack sizes using samples of actual service induced cracks has indicated a greater effective material toughness compared to laboratory specimens, by as much as 50 percent. This increase in apparent toughness is postulated to be due to the beneficial effects of crack branching and by the actual branched shapes of service-induced cracks. Westinghouse therefore allows the critical crack size to increase by as much as a factor of two to account for this observed increase in apparent toughness. A factor of two on crack size corresponds to a factor of 1.4 on toughness, which is slightly conservative relative to the 50 percent observed increase in toughness. In the probabilistic analysis, Westinghouse imposes a uniform variation in G ranging from 1.0 to 2.0 when evaluating critical crack size. The uniform distribution is considered conservative compared to use of a normal distribution. A distribution

is also assumed on parameter K_{IC} (variation of 15 percent) and a conservative allowance of 10 percent increase in σ is assumed in Equation 2-1 to complete the probabilistic formulation. The resulting distribution of critical crack size, a_{cr}, is presumed random and represented as a truncated normal distribution within the range of two standard deviations. In the calculation process, Westinghouse reduces the critical crack depths by the height of the keyway radius, as well as an assumed value accounting for the depth of any undetected cracks.

Overall turbine missile probability is calculated by summing the probability values obtained for each disk. Each probability is a product of the probability of crack initiation and the probability of the resulting crack reaching critical size. The calculation is performed by representing the equations in integral form and solving using conventional numerical techniques. All calculations for brittle failure are performed at design speed (100 percent running speed). An assumption is made that the relatively greater risk of disk failure at the higher speed is more than offset by the low probability of the turbine achieving design overspeed (typically defined as 120 percent). In analyses of disks with known cracks, the probability of initiation is set at 1.0, and the initial crack size is set at the known size prior to projecting the increase in crack length over time.

Disk fragment penetration of the turbine casing is not discussed by Clark et. al. [8]. The paper refers to a separate analysis, and states that the results of this separate analysis are used to refine the missile probabilities to account for fragments that are contained by the turbine casings.

Overall missile probability results are presented as tables of probability versus time, relative to the last inspection. The plant operator then selects the disk re-inspection interval based on the requirement to maintain the value of P_1 below 10^{-5}.

2.3 Assessment of Current Approach to Analysis of P_1

The summary information presented in the previous section regarding OEM processes for evaluation of P_1 provides the basis for a preliminary assessment of the level of conservatism (or non-conservatism) in these analyses. Until more details are obtained on these OEM analyses, many of the cited areas of conservatism must be considered potential at this time. This discussion will be the basis for going forward toward the overall project goal of providing nuclear plant operators with relief in the area of turbine control system tests and disk inspection. Five points are discussed in the following paragraphs:

2.3.1 Crack Model

Both OEM procedures should be studied to assess the fracture mechanics model used to establish critical crack size. A simple edge-crack model may be employed by the OEM analyses. Cracks that originate at the bore of the disk may be more accuracy characterized using a thick-walled cylinder model, or a model that includes a hole in a large plate. Figure 2-3 shows the differences between the edge-crack model commonly used and a more appropriate cylinder or hole-in-plate model. Depending on the ratio of the hole diameter to the disk outer diameter, the model of a hole in an infinite plate may be less compliant than the corresponding edge-crack model, and will therefore predict a larger critical crack size.

Another consideration in selecting a crack model is its ability to accurately account for the significant local stress gradients near the bore keyway. The assumption of uniform stress, as

shown in the edge-crack model of Figure 2-3, may be overly conservative given the sharp reduction in disk stress at locations away from the keyway. Additional conservatism can therefore be removed from the analysis through use of an appropriate critical crack size model, however the trade-off is that these models must be solved using a numerical process typically found in commercial fracture-mechanics analysis software [15].

The final consideration in selecting a crack model is the ability to employ a realistic crack aspect ratio. The most conservative assumption for crack geometry is a through-crack, which extends the full width of the bore. Semi-elliptic cracks, as shown in Figure 2-4, are reportedly more common and also less conservative.

Chapter 4 of this report discusses the choice of crack model, stress distribution, and aspect ratio in more detail. Examples of the benefits of using these more sophisticated models are given in the case studies presented in Chapter 5.
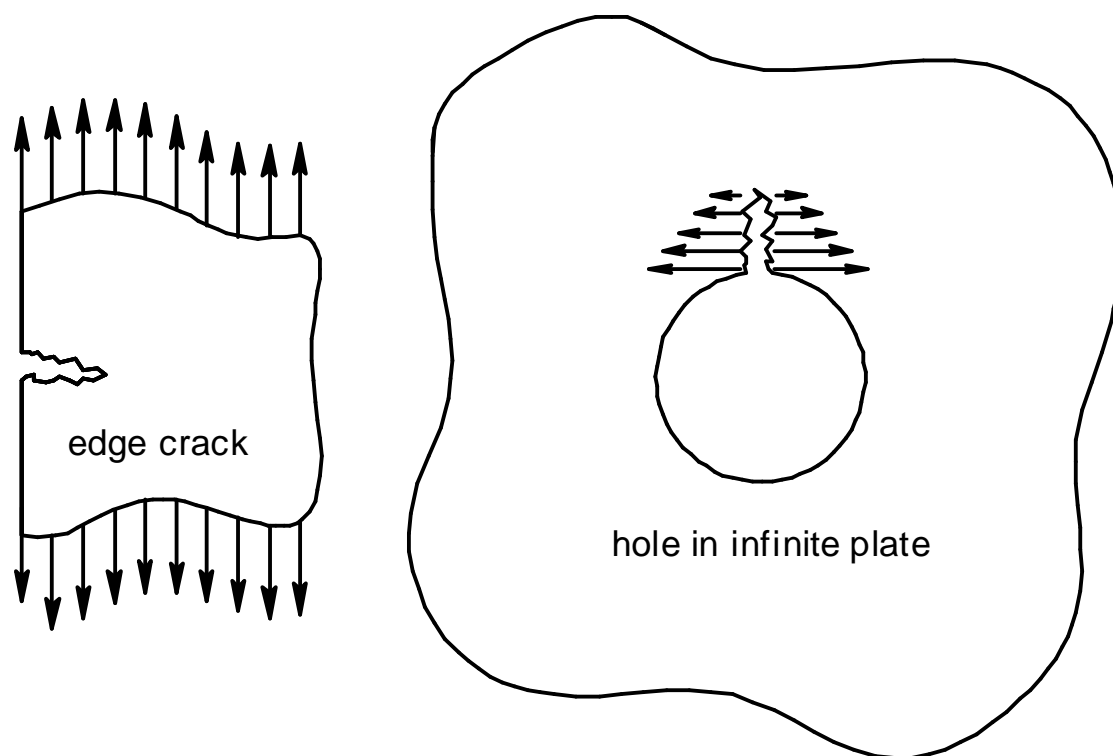
Figure 2-3 Crack models relevant to disk keyway cracking
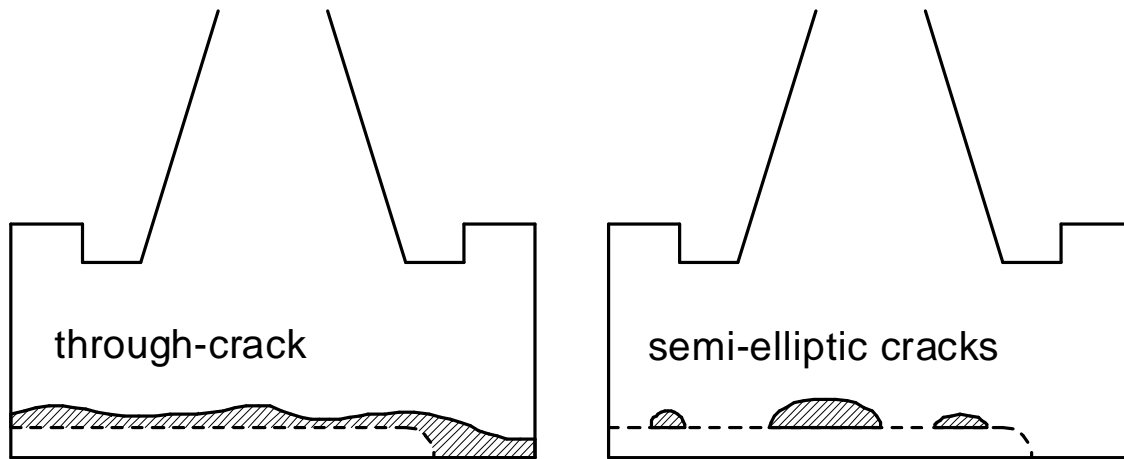
Figure 2-4 Aspect ratios of disk keyway cracks

2.3.2 Process for Combining Uncertainty in Analysis Parameters

An evaluation of P_1 must take into account the variations and uncertainty in values of the key analysis input parameters. Examples of these parameters include material toughness, measured crack size and aspect ratio, crack growth rate, disk temperature, and applied stress. A variety of mathematical approaches can be used to account for these variations. The existing OEM analyses appear to evaluate P_1 using a type of closed-form solution technique that use standard distribution forms to define the range of values for the input variables. An alternative approach is to use a Monte-Carlo (or random-walk) procedure, similar to that employed in EPRI's SAFER program [11] and LPRimLife software [12]. The Monte Carlo approach analyzes thousands of combinations of input parameter values, within the user-defined defined range of each. This is inherently a numerically intensive approach, but has become more practical in recent years as the cost of numerical computation has lowered and computational speed has increased. In this application, the result of a Monte-Carlo simulation is the probability of a crack reaching a specified size over defined time periods. This type of result directly satisfies the analysis objective, which is to estimate the probability of brittle failure prior to the next disk inspection. The lower the probability of an event (such as missile generation), the greater the number of Monte-Carlo iterations required for a reliable probability estimate.

It is not clear how much, if any, conservatism exists in the present OEM process as a result of the probabilistic analysis methodology currently used. It is possible that in adopting a numerical approach such as Monte-Carlo, more accurate probability distributions can be employed to define the key input parameters. A more detailed study, including comparison calculations, is recommended to assess any inherent advantages to replacing the closed-form approach with a numerical procedure such as Monte-Carlo for probabilistic evaluation of brittle failure.

Chapter 4 of this report contains a more detailed discussion of probabilistic assessment methodology as applied to disk failure.

2.3.3 Disk Inspection Techniques

The assessment of P_1 is directly related to the uncertainty in the detection and sizing of service-induced cracks in the bore and keyway region. The current practice for disk inspection utilizes ultrasonic test (UT) methods to detect and size cracks in the bore region [16]. Studies performed by the OEMs have resulted in probability data relative to detection and sizing of bore cracks [13]. The ability of UT systems to detect cracks depends on the crack location. Cracks in the hub area are easier to detect than those located in the web region, and the OEM detection probability data reflects this relative uncertainty. These uncertainties in both detection and sizing of cracks factor directly into the resulting probabilistic calculation of P_1.

Chapter 4 of this report contains a discussion of the application of improved UT techniques to the inspection of disk keyways. A preliminary assessment of the potential benefits of advanced UT technology is presented.

2.3.4 Turbine Control Failure Probability

Assessments of the probability of turbines reaching destructive overspeed due to load interruption has been based on historical analysis of failures of individual components [1,7]. Components include the individual stop and control valves, their respective control systems, the intercept stop/control valves and their control systems, and finally the mechanical and/or electrical sensors designed to detect turbine overspeed. The NRC describes a straightforward methodology for combining the reported failure data from the industry for each subsystem to yield an overall probability of achieving destructive overspeed per turbine-year [7].

In a statistical sense, the accuracy of failure projections improves as the sample size increases (i.e. number of turbine-years of U.S. nuclear operation). The accuracy of P_{1b} defined in Figure 2-1 should improve, therefore, by continually reassessing the probability of turbine overspeed control failures using up-to-date industry data. Evidence suggests that the probability will decrease by accounting for recent event data, since there has been practically no occurrences involving loss of turbine control at nuclear plants. For example, General Electric has released a non-proprietary report that describes a reduction in failure probability of turbine controls and valves as a result of a reassessment of the General Electric nuclear turbine fleet performed in the early 1990s [14]. Compared to the original valve failure-to-close data, General Electric reports a reduction of between 21 to 48 percent in probability of valve failure. The reported range in reduction corresponds to performance of the various systems such as main stop, main control, and intercept valves, etc.

A revised assessment of P_{1a}, including event data reported since the early 1990s, could potentially further reduce the P_{1a} probability. Many of the control system failures are attributed to mechanisms such as EHC fluid contamination. Likewise, valve failure-to-close events are often related to steam chemistry. The increased industry awareness of both EHC fluid contamination and steam chemistry issues may yield improved operating practices that in turn contribute to a future decrease in P_{1a} [17].

2.3.5 Improved P_1 Assessment Process

The technical approach that would be required to develop an independent process for assessment of P_1 is summarized below. This approach should not be interpreted as the final EPRI

recommendation at this time, but rather a technical description of what would constitute the most complete approach in the absence of all other issues such as regulatory or project funding issues. Additional technical details on some of the steps identified below are discussed further in Chapter 4 of this report. Regulatory issues are discussed in Chapter 3.

1. Investigate the current OEM probabilistic analysis process in more detail, to confirm possible areas where conservatism can be removed. This investigation would be contingent on receiving permission from the OEMs, since these procedures are considered proprietary.

2. Identify all input data considered critical to successful use of any proposed new P_1 assessment procedure. This includes, for example, material toughness data, crack growth rate, SCC initiation probability data, component geometry, disk loading and temperature, and failure data on components of the turbine overspeed protection system. Perform an assessment of each parameter to determine the availability of suitable data in the open literature (both mean values and variation). Identify those parameters that are not documented in the open literature that will therefore require additional research to evaluate. Identify potential sources of replacement data, and the effort involved in obtaining this data.

3. Qualify advanced NDE techniques such as phased-array for detection and sizing of bore cracking in shrunk-on disks. This will require a rigorous program of tests on scrap wheels containing service-induced SCC (both General Electric and Westinghouse design). Produce a database that defines uncertainty in both detection and sizing as a function of disk type and axial location (i.e. hub location versus web location).

4. Obtain a complete list of reported events relating to failure of any component of domestic nuclear turbine overspeed protection systems. A potential source for this data could be the Institute of Nuclear Power Operation (INPO). Use this event data as the bases for a revised analysis of the probability of overspeed protection system failure, similar to that proposed by Burns [7]. To the extent possible, categorize the data to reflect OEM, the control system vintage, valve design, etc.

5. Develop technical specifications for the computer program that performs the entire P_1 assessment. This program must include a probabilistic assessment of both brittle failure and the risk of overspeed protection (P_{1a} and P_{1b} respectively).

6. Develop and verify computer code under a Nuclear QA program.

Accomplishing all the above steps will require a significant level of funding. During the past 25 years, the OEMs have expended significant effort in quantifying deep-seated material properties, assessing uncertainty in disk inspections, and obtaining crack growth rates through inservice inspections. Some of this data is not possible to obtain independently without destructively testing a number of turbine disks.

References

1. S. H. Bush, "Probability of Turbine Damage to Nuclear Components Due to Turbine Failure," Nuclear Safety, 14(3): May-June 1973, p.187.
2. S. N. Semanderes, *Methods of Determining the Probability of a Turbine Missile Hitting a Particular Plant Region,* USAEC Report WCAP-7861, Westinghouse Electric Corp., February, 1972.
3. J. E. Proctor, *Effects of Angle of Incidence and Containment Liner on Penetration of Concrete Walls by Hypothetical Turbine Missiles,* Internal Memorandum from Naval Ordnance Laboratory, March 7, 1972.
4. S. H. Bush, "A Reassessment of Turbine-Generator Failure Probability," Nuclear Safety, 19(6): November-December 1978, p. 681.
5. "Protection Against Low-Trajectory Turbine Missiles", U.S. Nuclear Regulatory Commission, Regulatory Guide 1.115, Rev. 1, 1977.
6. "Safety Evaluation Report; related to the operation of Hope Creek Generating Station", Docket No. 50-354, U.S. Nuclear Regulatory Commission, Office of Nuclear Reactor Regulation, NUREG-1048, July 1986.
7. J. J. Burns, "Reliability of Nuclear Power Plant Steam Turbine Overspeed Control System", ASME Failure and Reliability Conference, Chicago, IL (September 1977).
8. W. G. Clark, B. B. Seth, D. M. Shaffer, "Procedures for Estimating the Probability of Steam Turbine Disc Rupture from Stress Corrosion Cracking", presented at Joint ASME/IEEE Power Generating Conference, October, 1981.
9. J. M. Barsom, S. T. Rolfe, "Correlations Between K_{IC} and Charpy V-Notch Test Results in the Transition – Temperature Range – Impact Testing of Metals", ASTM STP 466, 1970.
10. *Full-Scale Turbine Missile Casing Tests*. Electric Power Research Institute, Palo Alto, CA: January 1983. Report NP-2741.
11. *SAFER-PC User's guide and Technical Reference.* Electric Power Research Institute, Palo Alto, CA: March 1995. Report AP-104911.
12. *Development of an LP Rotor Rim Attachment Cracking Life Assessment Code (LPRimLife).* Electric Power Research Institute, Palo Alto, CA: December 1999. Report TR-110407.
13. A. Morson, J. J. Pepe, R. T. Bienvenue, "A Review of G.E. Fossil Steam Turbine Rotors with Shrunk-on Wheels", General Electric Technical Report GER3539A.
14. Probability of Missile Generation in General Electric Turbines, Supplementary Report: "Steam Valve Surveillance Test Interval Extension", General Electric Report GET-8039.1, non-proprietary version, September 1993.
15. Structural Integrity Associates, "pc-CRACK", Version 2.1, 1991.
16. F. V. Ammirato, et. al. Nondestructive Evaluation Sourcebook. Palo Alto, Calif.: Electric Power Research Institute report NP-7466-SL, September 1991.
17. INPO document O&MR 423, "Maintaining Main Turbine Hydraulic Control System Fluid Quality", Institute of Nuclear Power Operations, December, 1996.

3
REGULATORY ISSUES

Implementation of any revised procedure for assessing the risk of damage to plant safety-related equipment by turbine missiles must include consideration of regulatory issues. Each licensee is responsible for determining the specific regulatory path to implement a revised missile analysis procedure. Interface with the regulators must be the responsibility of the licensees, either individually or as an industry group. EPRI's role in this process is primarily to provide technical guidance, manage the development of all analysis procedures and databases that support the individual licensees, and assist in organization of any industry group to interface with regulators.

3.1 Process Overview

Figure 3-1 is a flow diagram that contains a general description of the basic regulatory paths involved in implementing a revised turbine missile probability assessment, or a change to the existing requirements regarding either disk inspection or turbine control test intervals. There is no standard licensing agreement for U.S. nuclear plants, which means that each plant's regulatory path may be different.

Each plant should first examine their operating license to determine whether specific language exists that pertains directly to missile probability assessment methodology, disk inspection frequency, and/or turbine overspeed control testing intervals. If such language exists, processing a licensing change is necessary, and is done according to plant procedures. The proposed change cannot be implemented without appropriate internal/external approvals of this licensing change.

If the license does not contain specific language relating to missile probability assessment methodology, disk inspection frequency, and/or turbine overspeed control testing intervals, then other documents which comprise the current licensing basis (CLB) must be examined. These documents include the updated facility safety analysis report (UFSAR) and the technical specification bases. If the CLB documents do not specifically reference, describe, or mandate aspects of the disk inspection and turbine control test interval, then regulatory action may *not* be required. It is more likely, however, that the CLB does reference the subject of missile probability and the related maintenance requirements, which will mean that changes to these documents are required and must be made in accordance with plant procedure.

```
┌─────────────────────────────┐
│  Modification proposed to    │
│  overspeed protection test   │
│  interval, or disk           │
│  inspection interval         │
└─────────────────────────────┘
              │
              ▼
┌─────────────────────────────┐
│  Does current operating      │
│  license contain specific    │
│  language related to OS      │
│  protection system tests,    │
│  disk inspection, or missile │
│  probability assessment?     │
└─────────────────────────────┘
   │ yes          │ no
   │              ▼
   │   ┌──────────────────────────┐
   │   │ Do any of the current     │
   │   │ licensing basis (CLB)     │
   │   │ documents (UFSAR, Tech    │
   │   │ Spec Bases) reference,    │
   │   │ describe, or mandate      │
   │   │ aspects of turbine        │
   │   │ maintenance or testing as │
   │   │ related to prevention of  │
   │   │ turbine missiles?         │
   │   └──────────────────────────┘
   │      │ yes         │ no
   ▼      ▼             ▼
┌──────────┐ ┌──────────┐
│ Process  │ │ Process  │
│ license  │ │ change   │
│ amendment│ │ in       │
│ in       │ │ accordance│
│ accordance│ │ with plant│
│ with     │ │ procedures│
│ plant    │ └──────────┘
│ procedures│
└──────────┘
   │      │             │
   ▼      ▼             ▼
┌────────────────┐ ┌────────────────┐
│ Need appropriate│ │ CLB contains no │
│ approvals to    │ │ information on  │
│ proceed         │ │ turbine missiles,│
│ (internal/external│ │ proceed         │
└────────────────┘ └────────────────┘
```

Figure 3-1 General Regulatory Process

3.2 Issues Relative to 10 CFR 50.59

10 CFR 50.59 allows the licensee to make changes to the facility or operations as described in the facility safety analysis report (FSAR) without obtaining a licensing amendment *only* if the change meets certain requirements. The turbine missile analysis is described in the FSAR of many plants. Because any change to the turbine inspection/test procedures may "*result in more than a minimal increase in the likelihood of occurrence of a malfunction of a structure, system or*

component (SSC) important to safety previously evaluated in the FSAR as updated," such a change could consequently require a license amendment. An example would be a plant in which the turbine has an unfavorable orientation and the NRC originally accepted the turbine missile analysis based on a six-year inspection interval. This plant would need to file a licensing amendment to go to a ten-year interval.

In the event that the plant wished to extend the interval to ten years, a revised procedure could be used to define the probability of generating a turbine missile. However, because the new evaluation procedure is a departure from the method of evaluation described in the FSAR (as updated), and the analysis would likely be less conservative, the NRC would have to approve the method for determining missile probability. This assumption is based on NEI 96-07, Section 3.4.

Another question used to determine if a change requires an evaluation under 10 CFR 50.59 is "Does the activity result in more than a *minimal increase* in the frequency of occurrence of an accident?" Minimal in this case is defined as ten percent. The minimal increase requirement is constrained by the additional stipulation that the licensee must meet all other requirements or other NRC acceptance criteria to which the licensee is committed. To the extent that a commitment exists in the current licensing basis to follow OEM recommended procedures, a licensing amendment could be required by 10 CFR 50.59. NEI 96-07 does allow for a plant-specific accident frequency analysis to be used to demonstrate meeting the minimal probability change requirement for a license amendment.

3.3 Issues Relative to 10 CFR 50.65 (The Maintenance Rule)

The following paragraphs describing the maintenance rule are excerpted from Regulatory Guide 1.160. NUMARC 93-01 provides guidance for compliance with the Maintenance Rule:

Paragraph (a)(1) of 10 CFR 50.65 requires that power reactor licensees monitor the performance or condition of SSCs (structure, system or component) against licensee-established goals in a manner sufficient to provide reasonable assurance that such SSCs are capable of fulfilling their intended functions. Such goals are to be established commensurate with safety and, where practical, take into account industry-wide operating experience. When the performance or condition of an SSC does not meet established goals, appropriate corrective action must be taken. Paragraph (a)(2) of 10 CFR 50.65 states that monitoring as specified in Paragraph (a)(1) is not required where it has been demonstrated that the performance or condition of an SSC is being effectively controlled through the implementation of appropriate preventive maintenance, such that the SSC remains capable of performing its intended function.

Paragraph (a)(3) of 10 CFR 50.65 requires that performance and condition monitoring activities and associated goals and preventive maintenance activities be evaluated at least every refueling cycle provided the interval between evaluations does not exceed 24 months. The evaluations must be conducted taking into account, where practical, industry-wide operating experience.

Paragraph (b) of 10 CFR 50.65 states that the scope of the monitoring program specified in Paragraph (a)(1) is to include safety-related and non-safety-related SSCs as follows:

> (1) Safety-related structures, systems, or components that are relied upon to remain functional during and following design basis events to ensure the integrity

of the reactor coolant pressure boundary, the capability to shut down the reactor and maintain it in a safe shutdown condition, and the capability to prevent or mitigate the consequences of accidents that could result in potential offsite exposure comparable to the 10 CFR 50.34(a)(1) or § 100.11 of this chapter, as applicable.

(2) Non-safety-related structures, systems, or components

> (i) That are relied upon to mitigate accidents or transients or are used in plant emergency operating procedures (EOPs)

> or

> (ii) Whose failure could prevent safety-related structures, systems, and components from fulfilling their safety-related function

> or

> (iii) Whose failure could cause a reactor scram or actuation of a safety-related system

The turbine-generator is not a system that is relied upon to mitigate an accident or a transient. However, in the case of turbine missiles, the damage resulting from a missile could prevent other systems or components from fulfilling their safety related function. Also, the failure of the turbine generator system would cause a reactor scram. Therefore, the turbine generator system is within the scope of the Maintenance Rule 10 CFR 50.65.

The guidance in NUMARC 93-01 states that normally-running systems that are non-risk significant are addressed under (a)(2) above and their performance is monitored against plant level criteria. If plant level criteria are not met, and a maintenance preventable failure (MPFF) of the non-risk significant system is identified as the root cause, the system may then be moved to category (a)(1) or continue in (a)(2) after corrective action. The turbine generator may also be addressed under category (a)(2) because its performance is being effectively controlled through a preventive maintenance program.

4
DETAILS OF RISK ASSESSMENT APPROACH

Chapter 2 defined the basic elements that comprise the risk of damage to plant safety-related equipment due to turbine missiles. An overview of what is published regarding the current risk assessment procedures developed by the domestic U.S. nuclear turbine suppliers was also presented in Chapter 2. Finally, Chapter 2 proposed potential areas that should be explored for removing conservatism. Chapter 3 briefly discussed the regulatory ramifications of changing either the risk assessment procedure, disk inspection interval, or turbine overspeed control system test frequency. This chapter provides technical discussions on several facets of the revised process for evaluating P1 that may be developed under this program.

Chapter 4 topics include the assessment of turbine overspeed protection system failure risk, application of advanced disk bore/keyway NDE techniques, disk brittle failure probabilistic assessment, disk fragment penetration through casing, and missile strike probability. These areas will be considered in selecting the most cost-effective approach to removing conservatism in development of any future revised missile probability assessment.

4.1 Failure of Overspeed Protection System

It has long been recognized that the steam turbine has the potential to generate energetic missiles if a shrunk-on turbine disk were to fail. The resulting disk fragments, or missiles, could cause damage if they strike other plant safety-related equipment. Generally, turbine manufacturers have considered two failure modes. The first mode postulates failure at running speed (or *controlled* overspeed which is generally considered to be up to approximately 20 percent overspeed). Failure in this first scenario would occur if the disk contained flaws or cracks that initiate rapid brittle crack growth when the material toughness is exceeded. The second failure mode occurs when the overspeed protection system fails, resulting in the turbine potentially attaining speeds as high as 180 to 190 percent of rated speed. At these high rotor speeds, the centrifugal tensile stresses in the disks will eventually exceed the tensile strength of the material and ductile failure will result, even if the disk initially contains no flaws or cracks. This scenario is often termed destructive overspeed.

The reliability of turbine steam valves and related systems must be accounted for in the analysis of overspeed probability. These valves and associated components are identified by Burns in his early analysis of turbine overspeed probability and are itemized below [1]:

- stop valves
- control valves
- intermediate stop valves
- intercept valves
- associated sensors, electronics and hydraulics for control of valve motion

Various manufacturers have compiled event data from surveys relating to failure of valve control components and combined this with reported valve failure-to-close data to evaluate the overall

probability of control system failure and consequential ductile wheel failure [2]. These probabilities will vary depending primarily on the valve design, the model of control system in use, and the interval of surveillance tests performed on the valves and associated valve control components. The EHC/MHC system maintenance practices at individual plants will also affect the probability of overspeed protection system failure, but this is not specifically accounted for in overall industry event analysis.

In general, the calculated probability of losing control of turbine speed is small, with early-published data indicating probabilities on the order of 10^{-7} to 10^{-8} [1]. Therefore, in most situations the overall probability of generating a turbine missile is driven by the likelihood of a brittle failure caused by stress corrosion cracking in the bore/keyway region. The turbine manufacturers have adopted the position taken by Burns [1] and endorsed by the NRC (Hope Creek Safety Evaluation Report, NUREG 1048) that as valve surveillance test intervals are extended, the probability of failure of the overspeed protection system also increases. As this component of failure probability is increased, the corresponding contribution of a destructive overspeed event to the *overall* missile probability (P_1) becomes greater. Manufacturers, in their standard reports to turbine operators containing calculated missile probabilities, give options that offer a trade-off between valve testing intervals and wheel boresonic test intervals. In this way, operators whose turbines have few or no bore indications can increase the intervals between valve surveillance tests, and still stay below the required upper limit of P_1. Burns' analysis presents valve failure data and shows the quantitative effect of changing valve testing intervals from daily, to weekly, monthly and even yearly [1]. Each of these incremental increases in interval increases the estimated control system unreliability by approximately one order of magnitude according to Burns.

In 1991, General Electric initiated a survey on turbine overspeed protection performance on behalf of the BWR Owner's Group [2]. The survey results were used to recalculate the probability of various abnormal control system failures that could cause an overspeed event. The results presented in [2] indicated reduced failure probabilities in general, presumably due to the use of more recent data. This is beneficial to operators, and provided a basis for offering some relief in valve testing intervals. Because ten years has passed since this survey, it would seem desirable to conduct a new survey and recalculate the probabilities with new and more complete industry event data. A further reduction in calculated probability may be justified as a result of this effort, due to the ongoing industry control system retrofits and an increased level of awareness and preventative maintenance activity related to EHC fluid quality.

EPRI could perform an updated survey, or research available industry event data to establish the updated probability of a turbine attaining destructive overspeed. This raw event data could be processed in a manner similar to that used by Burns [1]. However, other statistical approaches to evaluating the effect of varying the valve surveillance test intervals should be researched as well. A key question is this …can the extent to which frequent surveillance testing of the overspeed protection system decreases the probability of attaining destructive turbine overspeed be quantified? Since failure of redundant systems is required for the turbine to reach destructive overspeed, surveillance testing of each individual system will help reduce the probability that both parallel systems will fail simultaneously. The statistical process for evaluating the industry event data should be re-examined to ensure that there is no excessive conservatism, or non-conservatism in the manner that results of surveillance test are used to determine the probability of destructive overspeed.

The maximum interval of surveillance testing currently recommended by the manufacturers, irregardless of the calculated probability, is quarterly/quarterly/quarterly for the stop valves, control valves, and intermediate valves respectively. If there is no operating history in U.S. plants corresponding to intervals greater than quarterly, the desired extension of test intervals beyond quarterly would therefore represent an extrapolation based on the industry's current operating history. Consideration must be made, therefore, of the possibility of new failure mechanisms involving the valves, valve controllers, or sensors that become significant once the test interval extends beyond quarterly. There may be new reliability issues, for example, with the large steam valves for nuclear units or the turbine trip mechanisms that have not yet appeared in the industry because these systems have been tested fairly frequently for the past thirty years.

4.2 Inspection of Shrunk-on Disks

Stress corrosion cracking in shrunk-on turbine disks is a problem that has been experienced globally since the catastrophic failure of the Hinkley Point low-pressure rotor in 1969. Since that event, the industry has implemented improved disk designs for retrofit applications and massive forgings for production of rotors with integral disks to mitigate the problem. For those rotors operating with the original shrunk-on disk design, periodic nondestructive examination (NDE) of the disks is necessary for early detection of stress corrosion cracking and for monitoring crack propagation to ensure that critical crack size is not reached during operation. State-of the-art disk inspections generally use conventional fixed angle ultrasonic technology (UT) for crack detection and sizing. The limitations of this technology contribute to conservative predictions for disk remaining life. Advanced ultrasonic techniques, such as phased array ultrasonics, offer improved detection and sizing performance resulting in more accurate ultrasonic data for remaining life predictions and, ultimately, increased intervals between inspection outages.

Low-pressure rotor shrunk-on disks are keyed to the rotor shaft to maintain relative position during torsional loading. During rotor assembly, a key is inserted between matching keyways machined in the outer diameter of the rotor shaft and the inner diameter of the disk bore. The number of keyways per disk varies in number and shape depending upon the manufacturer. Examples of typical keyway configurations are shown in Figure 4-1 [1]. The disk keyway produces a stress concentration in the nominally highly stressed disk bore area. Additionally the keyway area traps corrosive contaminants that precipitate from the passing steam. These corrosive agents are a factor in the initiation of stress corrosion cracking in the keyway areas and other locations within the disk bore.

Detection and sizing of stress corrosion cracking in the disk bore/keyway area has historically been accomplished with conventional ultrasonic technology. Collectively these inspection techniques have used focused and non-focused, pulse echo and pitch catch, single and tandem, transducers for detection and sizing with success. Implementation of linear phased array transducer technology, as a replacement for conventional NDE technology in other turbine inspection applications, has resulted in improved performance in terms of flaw sizing and flaw characterization. The objective of this effort is to determine whether the keyway/bore inspection may also benefit from application of this advanced NDE technology [2]. A description of the feasibility investigation performed at EPRI's NDE Center in 2001 is presented below.

single rectangular keyway   multiple round keyways
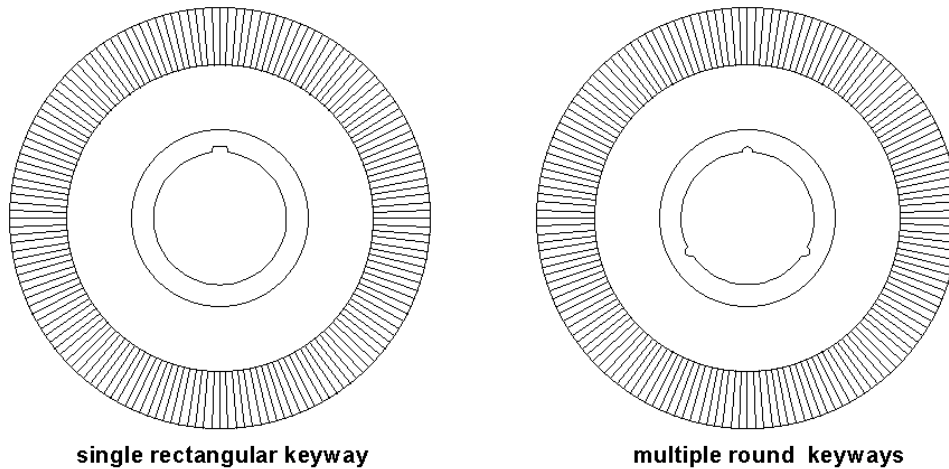
Figure 4-1 Typical keyway configurations

4.2.1 Equipment Description

A linear array UT inspection probe is comprised of a series of individual, small ultrasonic transducers arranged in a row or array. Each transducer element has its own electrical connections and is acoustically isolated from the other elements. Varying the timing pulse and reception for each element controls the angle, mode and focus of the composite ultrasonic beam. The array probes successively generates longitudinal or shear mode beams from 30 to 80 degrees (typically), in one-degree increments [2].

For this investigation, a 32-element phased array transducer was used to transmit and a 24-element phased array transducer was used to receive (pitch-catch configuration). Both longitudinal and shear wave focal laws were designed for beam angles from 64 to 89 degrees in 0.5 degree steps. An R/D Tech Tomoscan data acquisition system, an R/D Tech FOCUS phased array control unit and an R/D Tech Manual Encoder were used for data collection.

4.2.2 Experimental Disks and UT Setup

Two turbine disks were selected for use in this investigation as shown in   Figure 4-2. One disk is retired from service with known service-induced cracking in the disk keyway area. The other disk is a mockup fabricated with multiple keyways featuring EDM notches and implanted cracks.
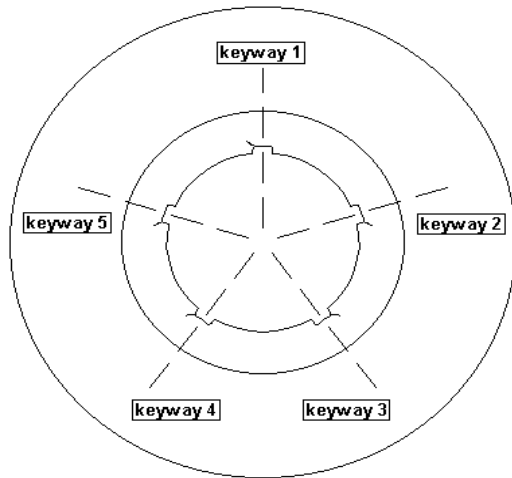
Figure 4-2 Test disks used in investigation

In-service inspection of shrunk-on disks usually requires that the LP rotor be rotated while a fixtured transducer rides the disk surface. In this investigation, the disks were not installed on a rotor, so the phased array transducer was fixtured to a simple scanning arm and manual encoder as shown in Figure 4-3, eliminating the need to rotate the disks.
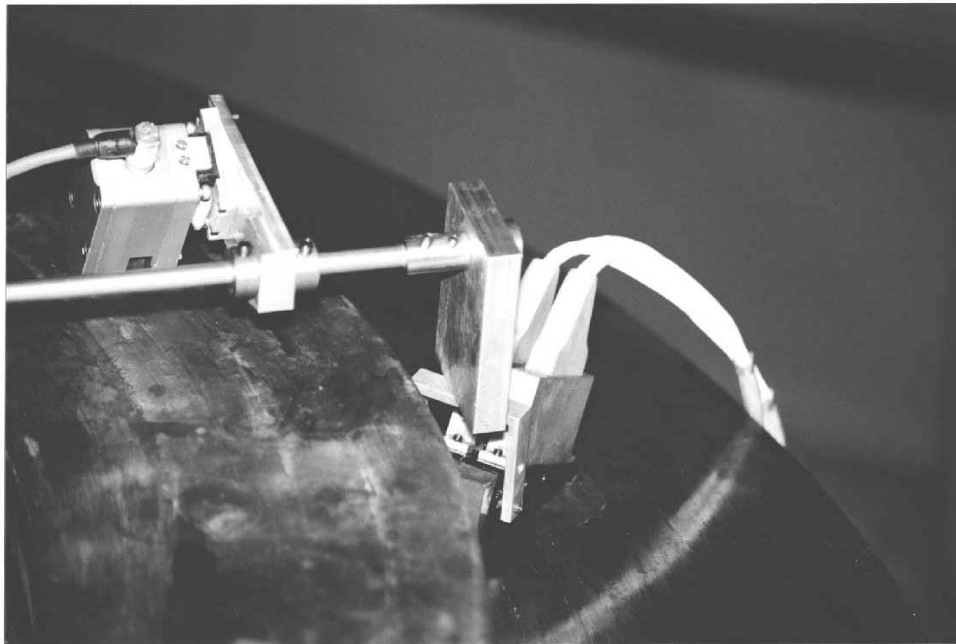
Figure 4-3 Scanner mounted on disk

Typical techniques for inspection of the disk bore/keyway area use a series of individual, conventional, single angle, ultrasonic probes (Figure 4-4). The use of non-focused, fixed angle probes in a long metal path application, limits flaw sizing performance and efficient inspection coverage of the area of interest. Usually, several different transducer inspection angles combined with multiple inspection locations are required to achieve reasonable inspection coverage [1].
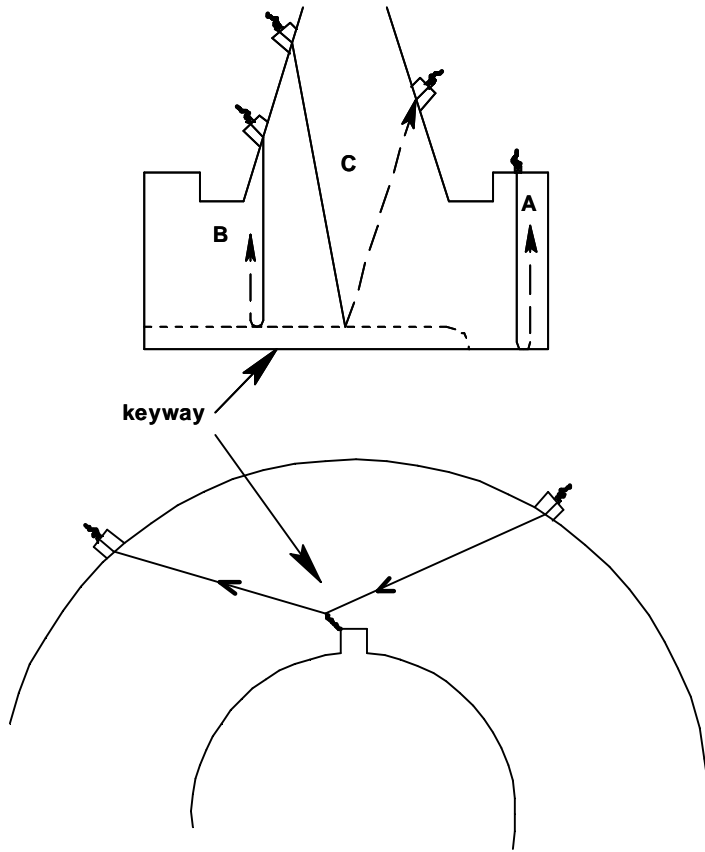
Figure 4-4 Illustration of inspection location on disk [1]

Linear phased array transducers offer improved performance and versatility compared to conventional transducers. The ability to dynamically steer the beam angle of a linear phased array transducer and capabilities for beam focusing, as depicted in Figure 4-5, offer a distinct advantage as compared to a non-focused fixed angle conventional transducer.
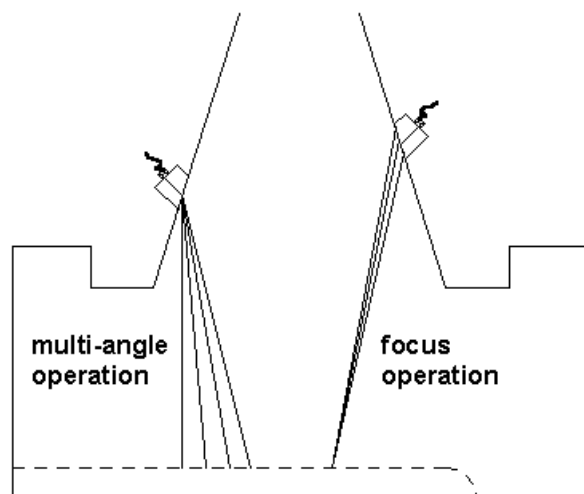
Figure 4-5 Linear phased-array application for disk bore/keyway [1]

4.2.3 Technique Investigation

In preparation for inspection of the two disks, a computer model was used to determine optimum probe position for inspection of the keyway area. Disk geometry and inspection parameters were included in the model. The phased array probe was positioned and scanned based on information from the model.

Data for this experiment was collected from the discharge side of the disks only, using a dual phased array probe in pitch catch mode. For each keyway, scanning was performed with the search unit aimed in both the clockwise and counter clockwise direction for the skew angles, which resulted in obtaining incident angles relative to the side of the keyway of 90 and 50 degrees. Each keyway was also examined with the search unit aimed at the centerline of the disk (zero degrees).

4.2.4 Discussion of Results from EPRI Disk

Table 4-1 contains results from measurements performed on notches and the crack in the EPRI disk and on the inservice crack of the retired disk. Crack locations are identified on the diagram in Table 4-1. EDM notches that were located in the keyways at approximately the same axial position (notches #3 & #6) as the search unit contact surfaces on the disk web section were detected with all techniques. Notches that were located in the keyways at approximately the disk axial mid-position (notches #2, #5 & #8) section were detected with some but not all techniques. None of the notches located below the axial mid-position (#1, #4, & #7) were detected. Notch #9, which is located axially approximately four inches below the contact surface of the search unit, was detected with both modes at the 50 and 90-degree skew angles.
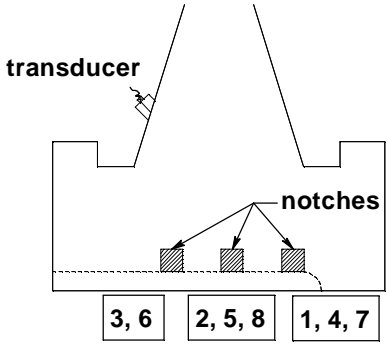
The crack located in keyway number five of the EPRI disk, was detected with all techniques. The crack appears to be at an angle more tangential then radial from the keyway surface. The maximum radial depth measured with this equipment is 0.06 inches. See Figure 4-9 and Figure 4-10 (a view looking down the keyway from the disk face). Figure 4-7 and Figure 4-8 show notch #3 using the same view as the above. Figure 4-6 shows this same view of keyway number

one with no notches present. Figure 4-11 and Figure 4-12 show the "A" scan presentation with the 50 degree incident skew angles for each mode. Note the width of the crack envelope (a characteristic crack signature). The inservice crack in the retired disk appears to run in a radial-axial plane and was detected with both modes using a 45 degree skew and with one mode using a 90 degree skew. No radial depth information was determined.

4.2.5 Conclusions and Recommendations

The observation of the test results in this report clearly demonstrates the potential for phased-array technology to improve over use of the present fixed angle techniques in both crack detection and crack sizing. It is predicted that subsequent inspection from the admission side of the disks would have resulted in detection of the notches located past the axial mid-position (Notches #1, #4, & #7). The ability to inspect the disk bore/keyway area with multiple angles, simultaneously, improves the inherent flaw detection probabilities and provides multiple angle sizing information. These attributes may also reduce the time needed for inservice inspection due to a reduction in the number of setups required (as compared to a conventional fixed angle probe inspection) to inspect the disk bore/keyway area of interest. Pitch-catch array techniques will be required to optimize detection and sizing in the mid-axial sections of a disk. Utilizing single arrays with smaller contact areas and better lateral beam directivity should significantly improve on this technology capability shown in this report [3].

Table 4-1 Turbine disk keyway ultrasonic data

Notch Number	90°LW	90°SW	50°LW	50°SW	0°LW	0°SW
#1	nd	nd	nd	nd	nd	nd
#2	nd	nd	2.0sn	nd	nd	nd
#3	2.5sn	3.0sn	3.0sn	8.0sn	3.8mm	3.9mm
#4	nd	nd	nd	nd	nd	nd
#5	nd	3.0sn	nd	6.0sn	nd	nd
#6	3.0sn	4.0sn	2.5sn	3.0sn	4.2mm	2.6mm
#7	nd	nd	nd	nd	nd	nd
#8	2.0sn	2.0sn	nd	7.0sn	nd	nd
#9	2.5sn	3.0sn	4.0sn	4.0sn	nd	nd
Crack	10.0sn	15.0sn	12.0sn	14.0sn	0.5mm	1.8mm
Inservice Crack	nd	2.5sn	4.0sn (45°LW)	4.0sn (45°SW)	nd	nd

Key: SW= shear wave LW= long wave sn= signal to noise amplitude nd= no detection **Notes:** The 0° detections are given in radial depth (mm). Incident angle and mode at the heading of each column to identify the technique used.	**transducer** **notches** 3, 6 2, 5, 8 1, 4, 7
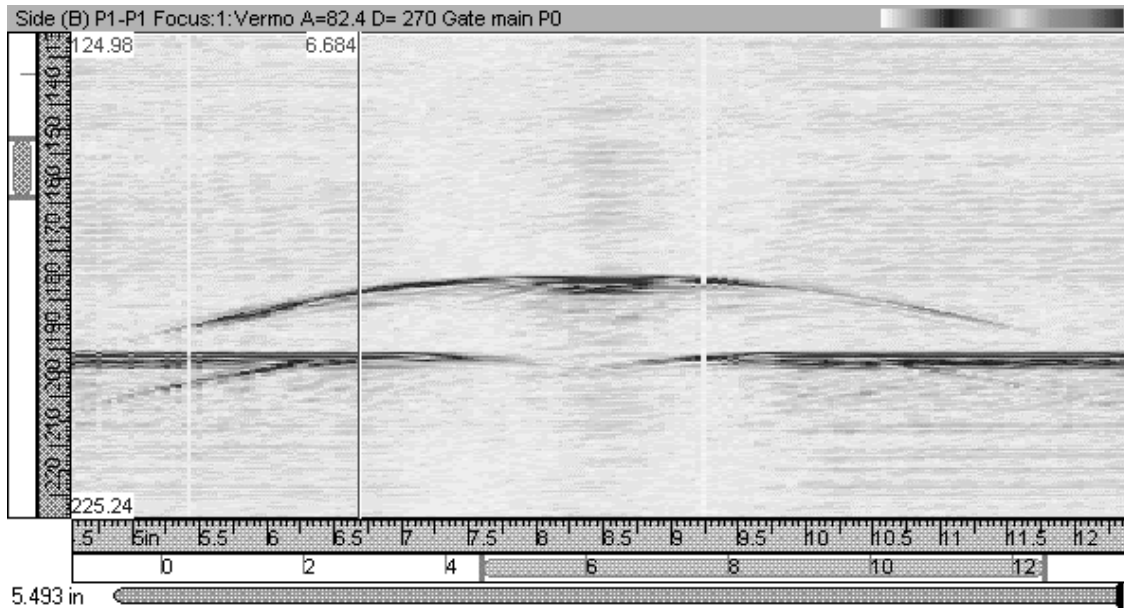
Figure 4-6 Image from keyway #1 of EPRI disk, no notches
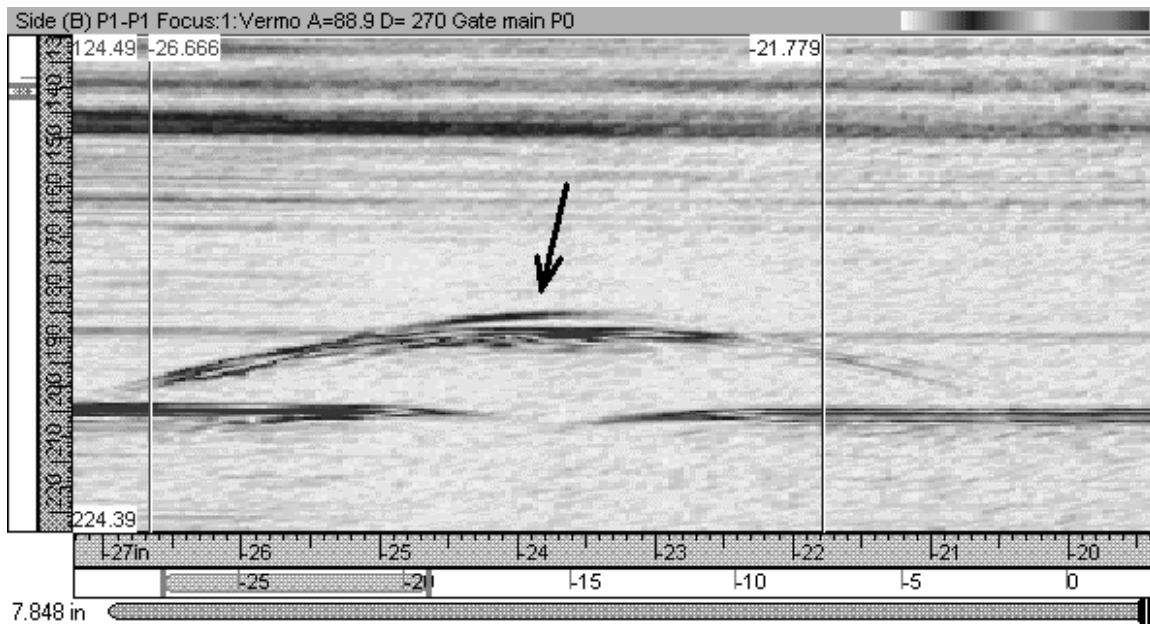
Figure 4-7 Image from Notch #3 of the EPRI disk using long wave, zero-degree skew
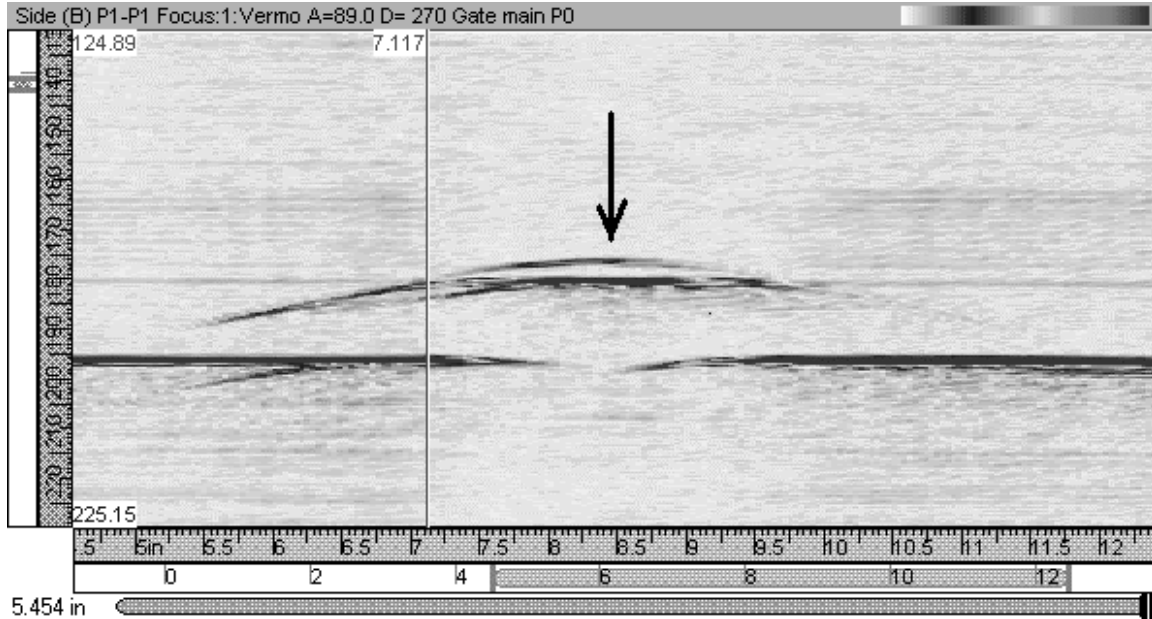
Figure 4-8 Image from notch #3 of EPRI disk using shear wave, zero degree skew
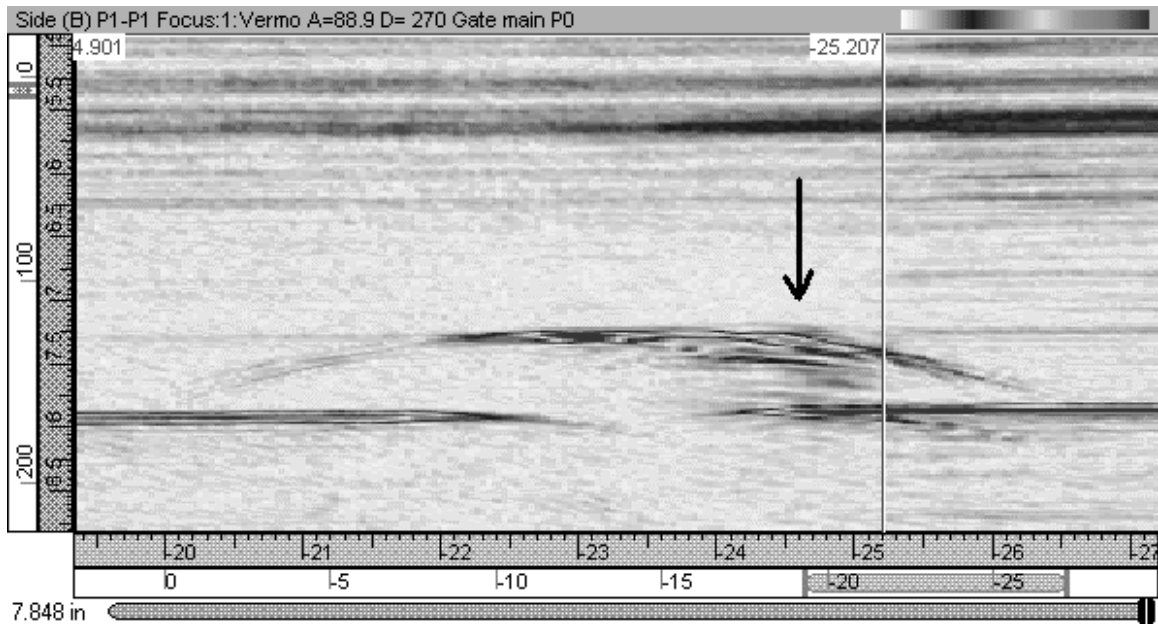
Figure 4-9 Image from crack in EPRI disk using long wave, zero degree skew

Side (B) P1-P1 Focus:1:Vermo A=88.5 D= 270 Gate main P0
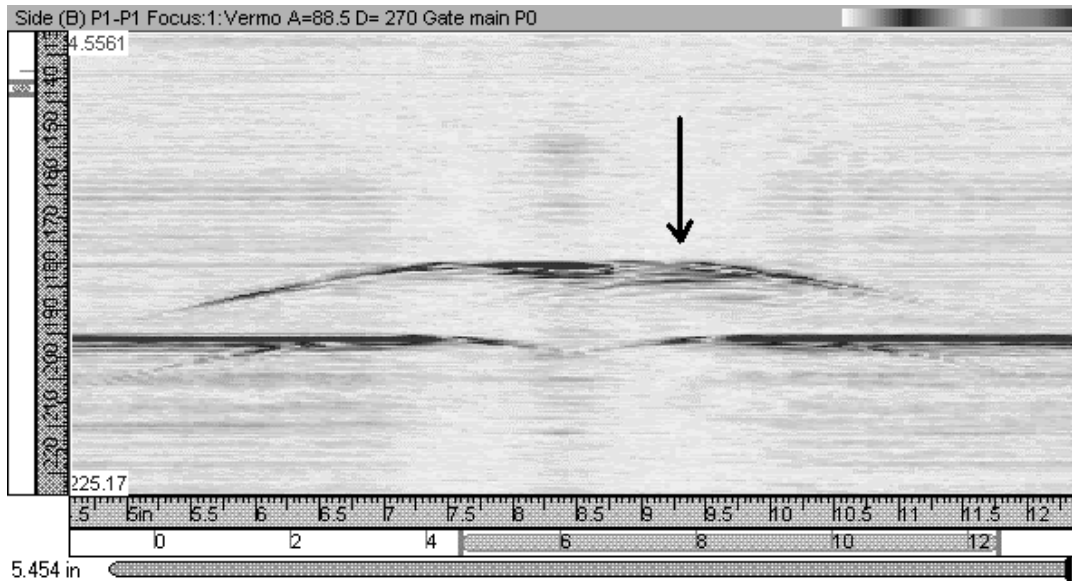
Figure 4-10 Image from crack in EPRI disk using shear wave, zero degree skew

A-Scan P1-P1 Focus:1:Vermo A=63.9 D= 270 Gate main P0
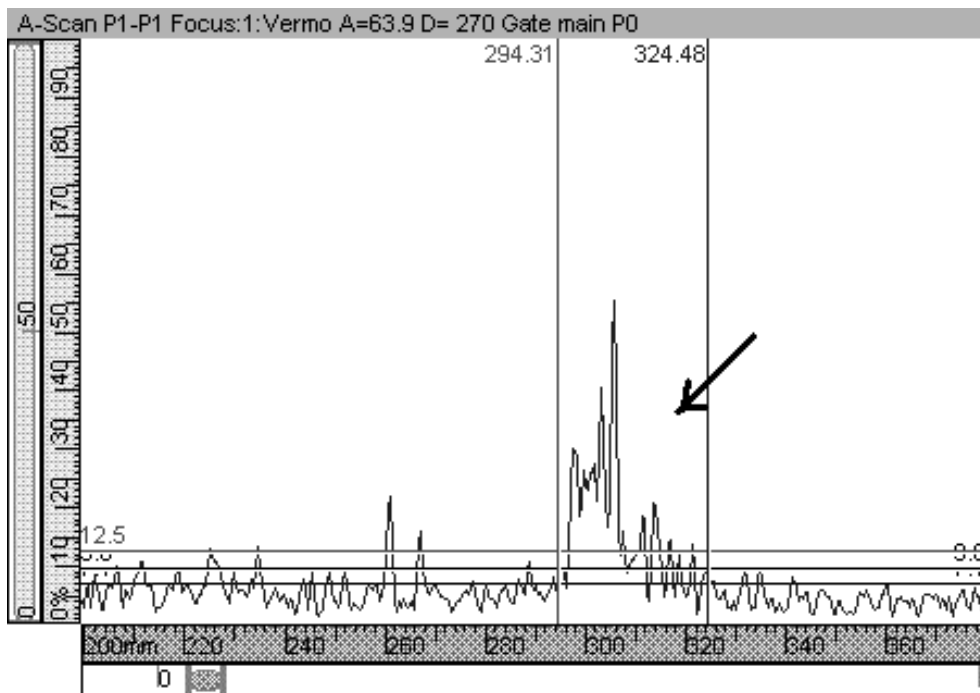
Figure 4-11 Crack "A" scan using long wave, 50 degree incident angle
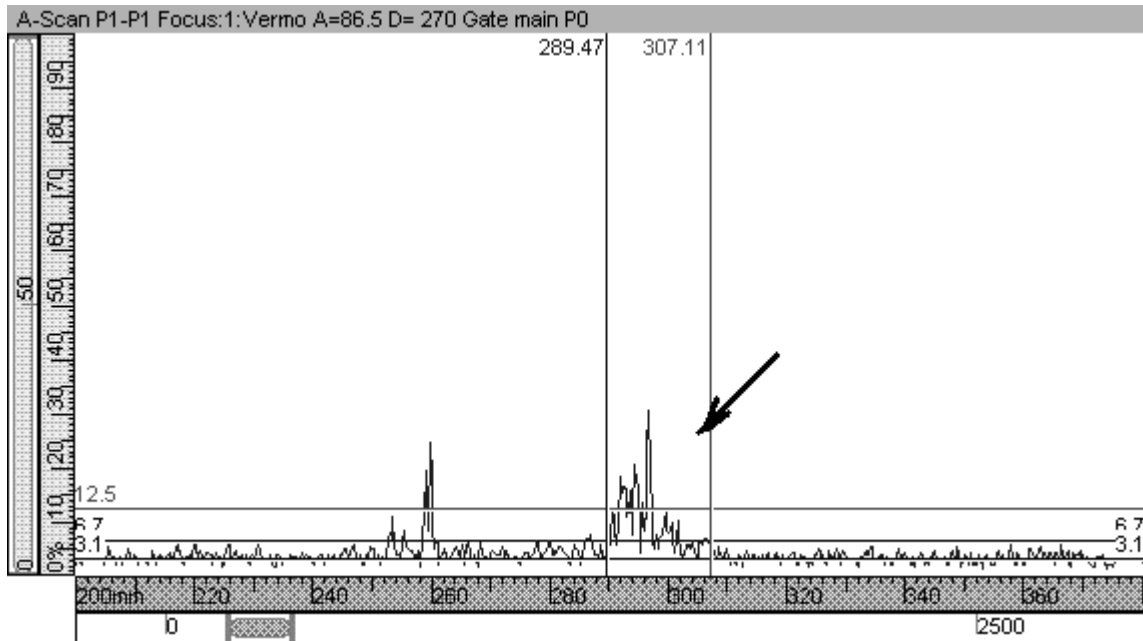
Figure 4-12 Crack "A" scan using shear wave, 50 degree incident angle

4.3 Disk Brittle Failure

Disk brittle failure occurs when the crack tip stress intensity exceeds the disk fracture toughness, and is the principal failure mechanism for LP rotor shrunk-on disks affected by stress corrosion cracking (SCC) at the disk bore and keyway regions. This failure mechanism takes precedence over net-section overload (limit load) failure when cracking is present because disk fracture toughness (K_{Ic}) is finite and flaw instability is predicted to occur before net-section overload in the event of overspeed. This report section focuses on key elements that govern disk brittle failure.

The key elements influencing disk brittle failure can be separated into four principal categories, as illustrated in Figure 4-13:

- Stress – induced by mechanical and thermal effects
- Initial Crack Size – measured using nondestructive examination
- Critical Crack Size – estimated using fracture mechanics
- Crack Initiation and Growth – determined from material tests

Each of these categories is addressed in further detail below.

Disk Stresses

Mechanical
- shrink fit
- RPM

Keyway K$_t$ and gradient

W = 3.0   GE = 2.2

Plasticity

Final Stress

Thermal

startup
radial & axial
gradients

NDE
- location
- depth/length

Operating Data
- temperature
- environment (wetness, chemistry
- overspeed

Material Properties
- yield/ultimate strength
- K$_{IC}$, FATT(deep-seated and rim)

Initial Crack Size/Shape

Crack Growth

Critical Crack Size

Time to Failure
- deterministic
- probabilistic

Figure 4-13 Key elements influencing disk brittle failure

4.3.1 Stress

Applied stresses in the disk due to mechanical and thermal contributions are discussed in the following paragraphs (see Figure 4-13). Mechanical stresses result from two types of mechanical loading, shrink-fit and rotation as described below:

> *Shrink-Fit*: This is the press fit or interference fit between the disk and shaft at assembly to transmit rotational torque from the disk blading to the shaft during normal operation. The magnitude of the shrink fit (radial interference) is typically calculated during rotor design to ensure contact between disk and shaft up to

about 120 percent of rated speed (or 20 percent overspeed). A keyway coupling between the disk bore and shaft provides torsional coupling for rotor speeds beyond the design limit of 120 percent rated speed. Data from a 1984 EPRI study [6] indicates that the magnitude of interference is typically 0.15 percent to 0.18 percent for the GE design and 0.19 percent to 0.30 percent for the Westinghouse design. Stresses due to shrink fit are the highest at zero rotor speed and decrease as a function of the square of rotational speed, typically becoming insignificant at or above 20 percent overspeed. Hoop stresses due to shrink fit are highest at the disk bore and decrease by a factor of about three to four moving radially outward from bore to rim. Sample distributions of radial stress distributions are presented in Chapter 5.

Rotation: Stresses due to rotational inertia of the disk and attached blading increase as a function of the square of rotational speed and are therefore the only primary stresses in the shrunk-on disks that can result in gross overload failure during a run-away overpeed. Hoop stresses due to rotation are highest at the disk bore and decrease radially outward from bore to rim by a factor of about three to four, similar to the shrink-fit stress distribution.

The combined mechanical stresses due to shrink fit and rotation result in a relatively high stress level in the disk over the entire speed range, with the loss of shrink fit stresses being offset by increasing centrifugal stress (see Figure 5-1, Figure 5-11, and Figure 5-22 in Chapter 5). Nominal bore stresses at 1800 rpm, from Reference [6], are in the range of 40 to 55 ksi for a typical GE nuclear LP rotor and 60 to 70 ksi for a typical Westinghouse nuclear LP rotor.

Thermal stresses develop in the disk during startup/shutdown. The stresses arise from both radial and axial temperature gradients that are caused by transient heat transfer. A startup, negative temperature gradients develop radially from the disk rim toward the bore and axially in the direction of steam flow. From the standpoint of disk brittle failure, transient thermal stresses during startup are of concern because this contributes to even higher tensile stresses near the disk bore, which combined with the typically lower metal temperatures at the disk bore location during startup may increase the risk of brittle failure. For typical double-flow LP rotors with five to seven shrunk-on disks per flow (see Figure 5-15), the first few disks are subjected to higher steam temperatures and thus have the potential for developing significant thermal stresses. For typical inlet steam conditions of approximately 200 psig and 500°F [6], the first two or three disks see superheated (dry) steam. Therefore, the potential for higher thermal stresses in the first several disks is offset by the minimal amount of time these disks may be surrounded by wet steam, which is a necessary prerequisite for the onset of stress corrosion cracking (SCC). For the downstream stages, which are in continual contact with wet steam and experience higher disk/blade centrifugal stresses, the level of thermal stresses relative to mechanical stresses is relatively small. For disks with higher FATT values, and therefore lower fracture toughness at these lower startup temperatures, a transient thermal analysis could be performed to identify any susceptibility to brittle fracture during startup.

Keyways provide torsional coupling between the disk and shaft at speeds above approximately 120 percent of rated speed. Axial keys with round or rectangular cross-section are often used. The Westinghouse design uses three round keys, typically 0.75 inch in diameter, spaced equally

at 120° intervals around the disk/shaft interface (see Figure 4-14). The stress concentration factor (K_t) in the disk for this axial semi-circular keyway is 3.0. The GE design typically incorporates a single axial key of rectangular cross-section between the disk and shaft (Figure 4-15). The keyway in the GE disk design is typically 0.625 inch in height by 2.5 inches in width. A stress concentration factor (K_t) of 2.2 is calculated for this keyway design based on finite element analysis [6].

The decay in the peak K_t value (either 3.0 or 2.2) with distance from the keyway surface, from [6], is evaluated by Equation 4-1:

$$K_t(x) = 1 + (K_t - 1)\left[0.25(\frac{R}{R+x})^2 + 0.75(\frac{R}{R+x})^4 \right]$$

Equation 4-1

where:

       R is the keyway depth (0.375 inch for Westinghouse or 0.625 inch for GE)
       x is the radial distance into the disk from the keyway top surface

A typical stress distribution with depth from the surface is presented in the first case history contained in Chapter 5 (Figure 5-2).

Peak elastic surface stress for a typical Westinghouse keyway, from [6], were calculated to be above 160 ksi. An elastic-plastic analysis assuming a disk yield strength 120 ksi predicted a plastic zone depth of approximately 0.1 inch. It was shown that for 20 percent overspeed, the benefit of the localized plastic zone is small from a fracture mechanics standpoint. For the GE design evaluated in [6], the peak keyway surface stress was approximately 100 to 110 ksi. Plasticity was therefore predicted to be highly localized and insignificant. In terms of relative importance of plasticity from an overall evaluation standpoint, the reduction in conservatism by using elastic-plastic stresses instead of elastic stresses is insignificant - provided the critical crack depth is much larger than the depth of the plastic zone.

100 mm
(4 in)

A

STEAM FLOW

SPACER

KEYWAY

A

SHAFT

DIAMETER : 19 mm (0.75 in)
CLEARANCE BETWEEN DISC
AND KEY: 0.050 mm (0.002 in)

DISC
SHAFT
KEY

SECTION A - A
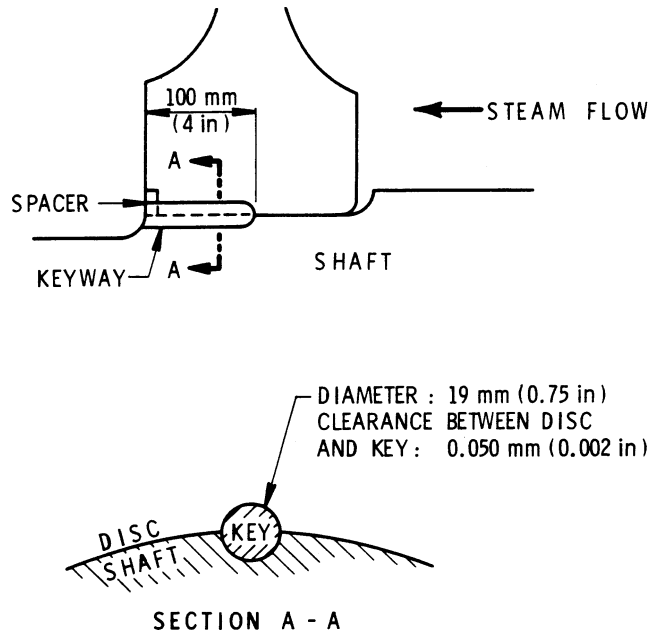
Figure 4-14 Schematic of keyway design used by Westinghouse in shrunk-on disk LP rotors [16]

DISC

STEAM
FLOW

A

KEYWAY

LOCKING RING

SHAFT

A

CLEARANCE AT B : 0.32 mm (0.13 in)
CLEARANCE AT C : 0.79 mm (0.03 in)

B

C

DISC
SHAFT
KEY

64 mm
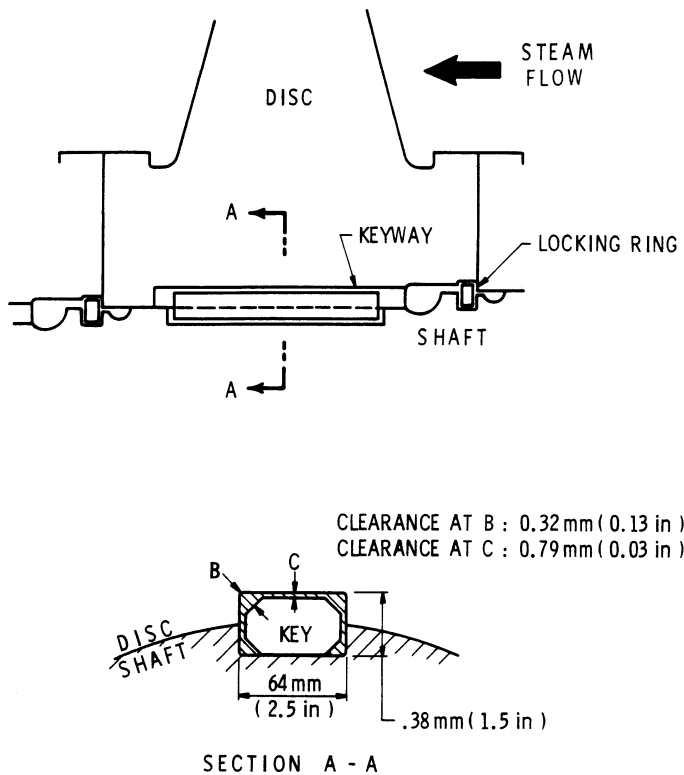(2.5 in)

.38 mm (1.5 in)

SECTION A - A

Figure 4-15 Schematic of keyway design used by GE in shrunk-on disk LP rotors [16]

4.3.2 Initial Crack Location and Size/Shape

The location and size of existing cracks (see Figure 5-9) is another factor influencing the probability of brittle failure. Crack detection and sizing using UT inspection was discussed in the preceding section of this report. From the standpoint of disk brittle fracture analyses, however, the location and size/shape of the crack are important. The location of cracking, particularly in regards to the bore surface versus keyway, determines the global and local stresses applicable for determination of crack tip stress intensity factors.

From an analytical standpoint, two crack parameters are needed to define the basic crack geometry – crack depth, a, and surface length, l. Typical bore or keyway cracks are semi-elliptic in profile with crack aspect ($a: l$) ratios in the range of 1:2 to 1:10. Cracks in the failed Yankee Rowe LP disks [7] were found to be essentially semi-circular in profile ($a: l$ of 1:2, see Figure 5-17). For a given crack depth, cracks with greater surface lengths produce higher stress intensity factors and are therefore nearer to the critical stress intensity value.

4.3.3 Critical Crack Size Calculation

For brittle failure, critical crack size is the crack size beyond which failure due to rapid unstable crack propagation occurs ($K_I > K_{Ic}$). Determination of critical crack size requires calculation of applied stress intensity factor at the crack tip (K_I) and estimation of disk material fracture toughness (K_{Ic}). This process is illustrated in Figure 4-16.

For a given applied stress field and crack shape/size, crack tip stress intensity factors can be calculated using linear elastic fracture mechanics principles with the resulting level of accuracy dependent upon the assumptions and simplifications made. The model types are discussed below.

> *One-Dimensional Crack Models*: Simplified crack models are available which require the assumption of an infinitely long (through-thickness) crack in a body of infinite or finite width. Stress intensity factor solutions are available for these models assuming either a uniform stress field or a stress gradient that can be represented by a cubic polynomial curve-fit (Figure 5-4a, b). Another one-dimensional model features an edge crack at a hole in a plate (Figure 5-4b). This model simulates the central disk bore and can simulate the high disk stiffness due to its large size. The potential for overestimation of disk stiffness is not significant for the relatively small expected critical crack depths relative to disk size. Overall, edge-crack models typically yield very conservative estimates of stress intensity factor because actual crack lengths are finite and small relative to disk features.

> *Two-Dimensional Crack Models*: These models are more advanced than one-dimensional models and typically simulate a crack as a semi-ellipse with semi-major axes of the ellipse representing the crack depth and half-length. Stress intensity factor solutions are typically generated using special-purpose fracture mechanics software, for example pc-CRACK [8] or BIGIF [9]. Applicable crack models for bore/keyway cracking simulate an axially-oriented semi-elliptic surface-connected crack at the bore of a hollow cylinder (Figure 5-6). These models provide reasonably good stress intensity factor results, but do not include

geometric complexities such as branching of SCC cracks or the variation in hub/web axial width versus radial position which affects the overall stiffness of the simulated semi-elliptic crack in the disk.

Geometry-Specific Crack Models: To include the exact stiffness of the shrunk-on disk which is a function of the hub/web axial width versus radial position, advanced three-dimensional (3D) finite element (FE) modeling of the disk and crack are required. This is the most advanced model type, and can be accomplished by the use of finite-element modeling software such as ANSYS [10] and/or 3D fracture mechanics crack front modeling software codes such as ALT3D [11]. The complexity of crack branching, which is applicable and significant to SCC cracks, can also be incorporated by explicit 3D modeling or published research on this subject [12].

4.3.4 Fracture Toughness

Fracture toughness (K_{Ic}) data for disk steels has been compiled by OEMs [13] and EPRI [14], and is typically plotted versus excess temperature, as illustrated in the Figure 4-16 flowchart. Excess temperature is defined as the difference between the disk metal temperature (T) and the Fracture Appearance Transition Temperature (FATT); i.e., $T_{excess} = T - FATT$. A statistical compilation of K_{Ic} versus T_{excess} data from [14] for Ni-Cr-Mo-V rotor steel is shown in Figure 4-17. Corresponding data from manufacturers [13] is shown in Figure 5-12.

4.3.5 Material Toughness Variations from Forging Process

In addition to the variation of K_{Ic} with temperature, K_{Ic} also decreases at locations inside any surface of the disk toward the center. For each shrunk-on disk, the manufacturer usually provides two disk-specific values of FATT, one value *measured* at the surface of the forging (Rim FATT) and the other *estimated* at the center of the forging (Deep-Seated FATT). The reason for the difference in these FATT values is the inherently higher cooling rate experienced by the forging near the outside surface relative to the center, which results in higher toughness (lower FATT) at the outside compared with that at the center of the forging. The gradient of this increase in FATT (decrease in K_{Ic}) with distance from the outside surfaces of the forging is very steep, typically approaching the deep-seated level within the first 4 to 7 inches from the outside surface [15]. Selecting FATT values for bore/keyway cracking analyses must account for material removed from the forging periphery and bore in the final machining process.   In other words, the final location of the disk bore/keyway relative to the forging locations at which rim and deep-seated values were measured/estimated must be accounted for in K_{Ic} calculations. This decrease in fracture toughness away from the disk bore surface (radial gradient) is significant for critical crack depths that fall within the FATT gradient (less than 6 to 7 inches in depth). For larger critical crack depths, the use of deep-seated fracture toughness is appropriate.
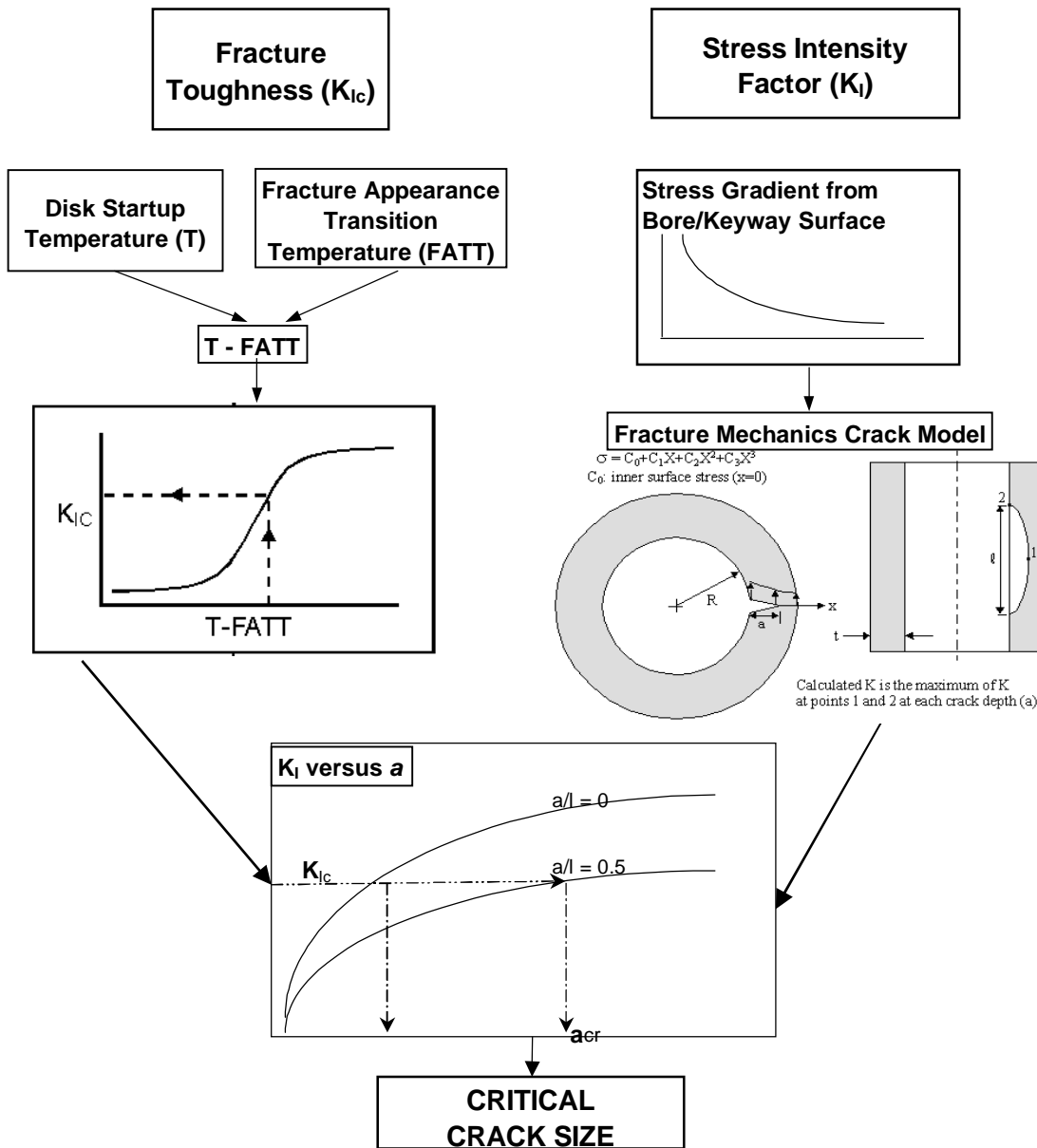
Figure 4-16 Critical crack size flow diagram

SAFER ROTOR TOUGHNESS DATA
MSET = 4, NiCrMoV data
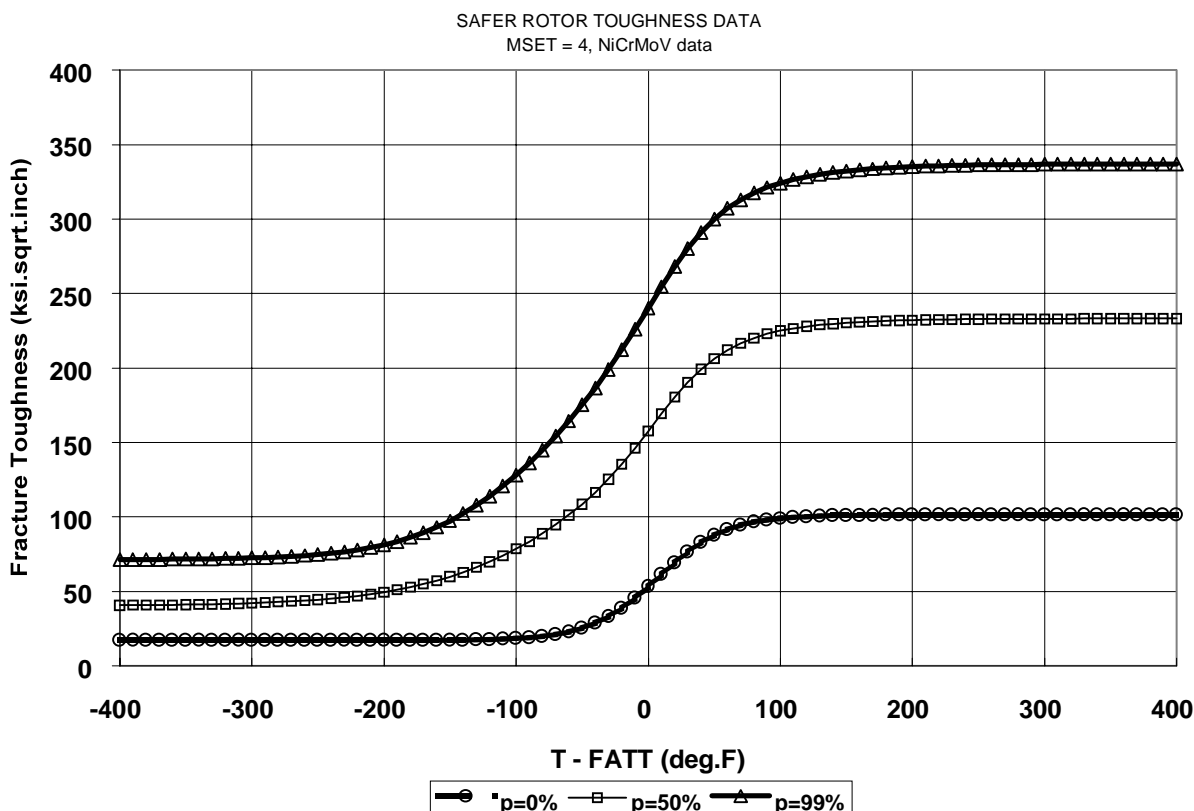
Figure 4-17 Default fracture toughness data for NiCrMoV rotor steels [9]

4.3.6 Crack Initiation and Growth

Extensive research on disk cracking in nuclear LP rotors, initiated in the early 1980s [16, 17], has documented stress corrosion cracking (SCC) as the primary mechanism for initiation and propagation of cracking. The contribution of low-cycle fatigue crack growth is insignificant relative to SCC growth for typical nuclear LP rotors. Refer to Figure 4-13 for key parameters influencing crack growth rate (temperature, environment and yield strength).

While no quantitative model is currently available to predict the time to initiation of cracking, the principal factors governing SCC growth, namely disk operating temperature, yield strength, peak surface stress and local environment (wetness, chemical impurities) are known to influence SCC initiation as well. In 1998, EPRI convened a major workshop on corrosion of steam turbine blading and disks [18], to identify and prioritize future R&D efforts to further understanding of the influence of steam chemistry and environment on environmentally assisted degradation mechanisms. Research is currently underway to provide a mechanistic understanding of the SCC initiation process.

The most widely accepted model for SCC growth rate, published by Westinghouse in 1981 [19], is given by:

$$ln(da/dt) = C_1 - (7302/T) + 0.0278\,\sigma_y$$

Equation 4-2

where,

        da/dt is SCC growth rate, in inches/hour,
        C_1 is a constant with a mean value of –4.968 and standard deviation of 0.587
        T is the local temperature of the disk at the bore/keyway, in °R (°F+460)
        σ_y is the disk yield strength, in ksi.

The scatter in the growth rate data, as illustrated in Figure 4-18, reflects the variability in the coefficient C_1 which yields an SCC rate variation of 5.8 times the mean for three standard deviations above the mean (C_1=-3.207).

For evaluation of bore/keyway cracking, local disk temperature at the disk-shaft interface at steady-state must be estimated for use in Equation 4-2. A first-order estimate would be an average of the disk upstream and downstream steam temperatures. A more accurate local temperature estimate, which accounts for two-dimensional heat transfer, could be obtained through finite-element modeling and heat transfer analysis at steady-state, such as that described in EPRI reference [6].

It should be noted that Equation 4-2 defining SCC growth is applicable only in the presence of wetness; i.e., upstream disks that run dry (i.e. exposed to superheated steam) are not susceptible to SCC. Intermittent wetness, which may occur prior to full-load steady-state operation, should be accounted for in assessing overall risk.

**Mean & Upper Bound SCC Growth Rates
for 8000 operating hours/year**
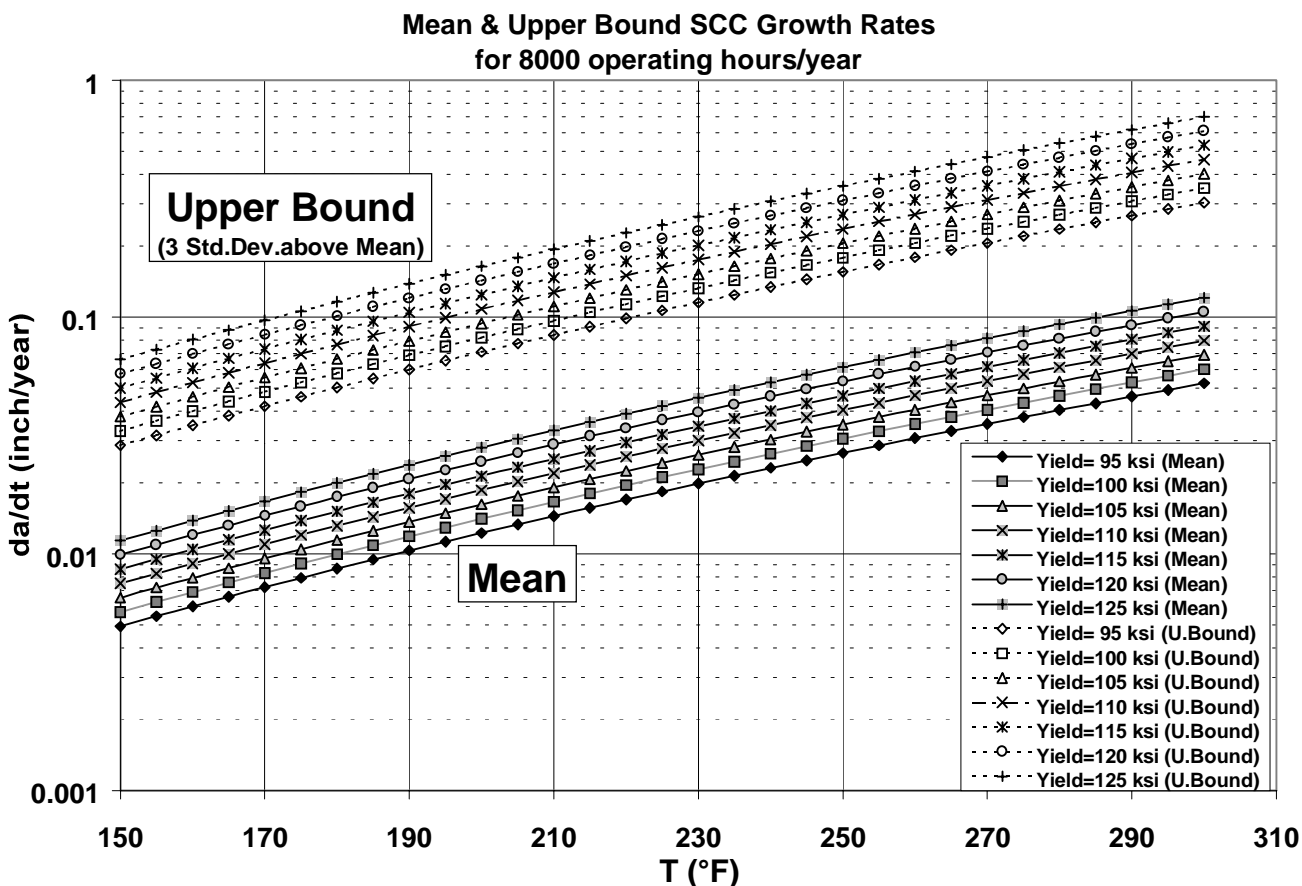
Figure 4-18 SCC growth rates per Clark et. al. of Westinghouse [19]

4.3.7 Summary of Key Variables Influencing Disk Failure

The following is a summary of twelve key variables identified from the preceding discussions that influence disk failure, and are therefore required in a probabilistic evaluation of disk cracking,

Variable #1: Stress and stress intensity (K_I)

The uncertainties associated with the accurate determination of peak stress, stress gradient away from the surface, and the uncertainty associated with calculation of crack tip stress intensity factors can be treated probabilistically. A normal distribution is adequate to model the collective variability in stress or K_I. Use of a single multiplier on stress or K_I with a mean value of 1.0 and an appropriate standard deviation representing the accuracy of the calculation method is considered adequate.

Variable #2: Normal Overspeed (up to trip setting)

This probabilistic variable addresses the possibility of "normal" overspeeds which are typically up to 110 percent of rated speed (1980 rpm), assuming that the overspeed protection system does not fail. Failure of the overspeed protection system would allow the speed to increase beyond the controlled limits and result in a "run-away" destructive overspeed.

Variable #3: Fracture Toughness

The variability in fracture toughness data with excess temperature, shown in Figure 4-17 and 5-12, for typical nuclear Ni-Cr-Mo-V rotor forgings, can be simulated using an appropriate standard deviation about the mean fracture toughness.

Variable #4: Fracture Appearance Transition Temperature (FATT)

The gradient in FATT from bore/keyway surface (forging periphery) to the center of the forging can be modeled using "Rim" and "Deep-Seated" measurements and/or estimates of FATT [10], with the variability modeled using an appropriate standard deviation value.

Variables #5, 6: Disk Temperature at Keyway without/with Prewarming

Local bore/keyway temperature, without and with prewarming, is needed to determine local fracture toughness of the disk material. This data can be obtained from OEM design calculations or from finite-element transient heat transfer calculations. This temperature typically varies between room temperature (70°F) and the running temperature of the disk. For disk brittle failure, OEMs typically use a lower bound value of 70°F, without prewarming. The highest risk of disk brittle failure occurs during startup when the bore of the disk has not warmed completely due to heat transfer from the rim, and the rotor is rolled off turning gear and ramped up to near-operational speed.

Variables #7, 8: Initial Crack Size & Shape (Aspect Ratios)

Variability in initial crack size and shape from NDE are included in this category. Uncertainty in reported crack size is dependent on the characteristics of the inspection system and flaw sizing process used. For example, GE reportedly uses crack depth "adders" of 0.080 and 0.070 inch for non-measurable and sized indications respectively, detected from the hub (see Chapter 5 case history). For web indications GE reportedly uses crack depth "adders" of 0.2 and 0.1 inch for non-measurable and sized indications, respectively; no specific estimates of crack length are provided. These uncertainties can be modeled by applying estimated mean and standard deviation values for initial crack depth, aspect ratio, and length.

Variable #9: Effect of Crack Branching

It has been documented that crack branching effectively lowers the stress intensity of a growing crack thereby increasing critical crack size [12]. Reduction in crack tip stress intensity factor due to crack branching can be simulated using appropriate mean and standard deviation values for the stress intensity reduction factor.

Variables #10, 11, 12: SCC Growth Rate - Coefficient, Temperature and Yield Strength

Coefficient C_1 - Per reference [14], the first term in the SCC growth Equation 4-2, was reported to have a mean value of -4.968 and a standard deviation of 0.587. Some judgement, which must be exercised regarding unit-specific applicability of this large standard deviation, can be based on available repeat inspection results from which an expected/actual growth rate can be inferred. *Temperature* - The variability in steady-state keyway temperature used to calculate SCC growth rate (Equation 4-2), can be modeled as a normal distribution with mean and standard deviation values estimated from upstream and downstream steam temperatures or directly from the results of a steady-state FE heat transfer analysis (if available). *Yield Strength* - The variability in disk yield strength values used to calculate SCC growth rate (Equation 4-2), can be modeled as normal distribution with mean and standard deviation values estimated from disk-specific material property test data.

4.3.8 Probabilistic Evaluation of Key Variables

Deterministic calculations using mean versus worst-case assumptions for key variables identified in the preceding discussion typically produce large differences in predicted remaining lives, suggesting that variability in modeled data cannot be adequately characterized deterministically. Therefore, a probabilistic evaluation that simulates the reduced likelihood of worst-case conditions occurring simultaneously can provide a more realistic assessment of remaining life and the likelihood of missile generation. The large number and complexity of the key variables influencing disk failure do not easily permit simplified closed-form analytical approximations. Numerical simulation techniques such as Monte Carlo, which uses a random sampling technique for input variables, or other more efficient sampling techniques such as stratified sampling, importance sampling or Latin hypercube sampling, to name a few, are recommended for this analysis [20].

In the Monte Carlo technique, a large number of deterministic simulations are performed, each for a randomly generated set of input variables. The basic building block of the random sampling technique used in the Monte Carlo method is the ability to generate random numbers from a uniform distribution between 0 and 1. Numerical schemes used to generate random numbers [20, 21] are actually deterministic but the numbers generated have the appearance of an arbitrary value and are therefore called "pseudo-random" numbers. References [20] and [21] provide additional details on numerical sampling techniques. The recommended number of

simulations is at least two orders of magnitude above the inverse of the desired probability result; i.e., for a failure probability of 10^{-4}, at least 10^6 simulations are needed. Therefore, the Monte Carlo technique may require a large amount of computational time depending on factors such as the time required each deterministic calculation, the total number of calculations needed and the computational speed. This traditional disadvantage to the use of Monte Carlo has been offset by the dramatic increase in the speed of microprocessors used in personal computers over the last ten years. New computational hardware has made it possible to perform all but the most complex probabilistic simulations today on a personal computer, using the Monte Carlo method.

Monte Carlo simulation offers many advantages over other techniques [22]:

- The distributions for input variables do not have to be approximated in any way.
- Correlations and other inter-dependencies can be modeled.
- The level of mathematical complexity is fairly basic with the computer doing all of the work in determining the probabilistic outcome.
- Higher levels of precision can be achieved by simply increasing the number of iterations.
- Complex mathematical functions can be included without difficulty.
- Changes to the model and interrogation of results can be performed with great ease, producing a more flexible approach that can be modified as a greater understanding of the risk parameters is achieved
- Monte Carlo simulation is a widely recognized and valid technique, it has been successfully implemented to address several other nuclear plant component risk assessment problems involving regulatory issues (e.g. BWR Vessel Inspection code [23])

The case histories presented in Chapter 5 of this report further illustrates the success of the Monte Carlo technique in calculating disk failure probabilities of the order of 10^{-4} to 10^{-5}, per the NRC requirement.

4.4 Fragment Penetration through Turbine Casing

If a turbine disk were to fail, it is possible that large fragments weighing thousands of pounds could penetrate the turbine casing. General Electric assumes that wheels could burst at both low speed (up to 120 percent operating speed) and at high speed (between 120 percent and 190 percent of operating speed). Wheels are postulated to burst into fragments that vary in weight from small (approximately 100 pounds) to very large and energetic fragments (up to 8,000 pounds) [24]. The evidence from the failed wheel at the Yankee Rowe plant confirms this large range of fragment sizes.

When a wheel fails, the massive rings and webs of the adjacent diaphragms are severely distorted and displaced by the wheel fragments as they attempt to penetrate the inner casing. During the impact, the wheel fragments dissipate significant energy to the diaphragm rings when moving and distorting them. Penetration of both the inner casing *and* exhaust hood must then take place in order for the fragment to become a missile outside the turbine. The exception to this is the final (L-0) stage wheel, which has fewer barriers to absorb the kinetic energy, as well as a greater wheel mass. Because of the position of the L-0 stage relative to the inner casing, the fragment

trajectory could possibly avoid hitting the diaphragm and may then only need to penetrate the relatively thin outer flow guide prior to impacting the outer casing. In all cases, there is a loss of fragment energy associated with the process of penetrating the turbine stationary components. To avoid being overly conservative in the overall assessment of P_4, this energy loss should be accounted for in calculating the range of initial missile velocities in the subsequent analysis of probabilities P_2 and P_3.

General Electric states that disk burst tests were conducted to clarify the assumptions used in their analysis of fragment penetration probability [24]. The General Electric P_1 probability assessment then integrates the wheel fragment penetration with the individual probabilities of wheel burst to obtain a probability of missile generation. A description of the Westinghouse approach to analysis of casing penetration does not appear in the open literature.

EPRI performed a series of tests to study energy absorption by a simulated turbine casing in the process of stopping or slowing down postulated missiles created by a burst disk. In 1978, two full-scale rocket sled tests were conducted at Sandia Laboratory to simulate the energy absorbing capability of a typical inner casing and turbine shell [25]. Two possible orientations of a turbine wheel fragment were considered: a) blunt orientation, and b) piercing orientation. In blunt orientation, the fragment contacts a large surface area of the casing during impact and consequently forces a large area of the casing to deform in order for penetration to occur. A piercing orientation occurs when the wheel fragment impacts at a sharp edge or other pointed feature. The turbine casing is relatively less able to contain a piercing fragment because the impact energy is concentrated over a much smaller area and the material deforms more easily or fails completely. Depending on the orientation of the missile at impact, the simulated turbine casing either slowed the missile to 60 percent of its initial velocity or essentially brought it to rest. The sled test parameters were established in order to represent the energy of a 120° segment of a turbine wheel leaving a spinning shaft at 120 percent of operating speed.

Additional tests sponsored by EPRI were performed using one-fifth scale models of the original test [26]. These tests successfully demonstrated the feasibility of using subscale models to reduce the cost relative to full-scale tests. Based on these results, a series of additional subscale spin tests were conducted [27].

Approximately one-third of the kinetic energy of a turbine missile is accounted for in its rotation. In the second set of EPRI subscale experiments, ten model tests were conducted using spinning missiles, both with and without blades. It was found that the positive effects of the blades in absorbing fragment energy more than compensated for the detrimental increase in mass and inertia provided by the blades. Further, for an unbladed fragment, the energy absorbing capacity of the shells was lower. From a casing penetration perspective, energy absorbed by the shell due to impact by a rotating fragment with blades is similar to that of a non-rotating fragment with the total energy of the spinning fragment. The observations indicated that the blades have a beneficial effect in reducing the peak impact force and lowering the effective linear energy.

4.5 Missile Strike and Damage to Safety-Related Equipment

In summary, these extensive tests conducted by EPRI provide data that could serve as important input to a detailed study of disk fragment penetration through low-pressure turbine casing structure. Development of a new analysis tool for assessing probability P_1 would necessarily

include these calculations of fragment penetration, most likely in an integrated manner with wheel burst and rotor speed similar to the General Electric approach.

If a disk bursts and fragments penetrate the casing producing missiles, NUREG-1048 assigns standard values for the combined strike and damage probabilities $(P_2 \times P_3)$. These values are 10^{-2} for unfavorable, and 10^{-3} for favorable turbine orientation relative to the reactor. As discussed in Chapter 3, the NRC discourages detailed calculations for $P_2 \times P_3$, most likely because of the large effort needed to perform an adequate review of the different and complex analyses of $P_2 \times P_3$ that would likely be submitted by licensees [28]. There was no standard process or computer program in place for analysis of $P_2 \times P_3$ prior to issuance of NUREG 1048.

Bush, in his first paper, describes the approach taken by Semanderes to calculate strike probability, P_2 [29]. The analysis starts with an assumption regarding the range of angles that low-trajectory missiles may exhibit upon exiting the turbine casing. The accepted value of the maximum missile deflection angle relative to the final stage is 25 degrees, as shown in Figure 4-19.

A Monte Carlo technique was reportedly used to evaluate strike probability for specific areas of the plant. For both low and high trajectory missiles, the analysis uses an assumed range of initial missile velocities and angles, and combined this with the physical layout of the plant (both PWR and BWR layouts are described by Bush). Exposed buildings or structures housing plant safety-related equipment are then identified and the corresponding strike probabilities are calculated based essentially on a ratio of the total of these exposed areas to the total possible area over which the missiles could fall. According to [28], the critical strike targets for PWR plants are the reactor containment (wall and dome), fuel storage, primary auxiliary building, and diesel building. For a BWR plant, the critical strike targets are identified as the fuel pool, radwaste building, control room, reactor heat removal equipment, and diesel building. In both plant types, a direct hit on the containment wall by a low trajectory missile is not expected to penetrate containment due to the strength of the reinforced concrete protection. The specific event that most influences the combined strike probability for the PWR is that of a high trajectory missile impacting the reactor dome. For the BWR, the highest probability event is a strike on the control room. Bush states that the analyses consider a strike on *any* portion of the critical buildings cited above as equally damaging. In reality, only a portion of each building is significant relative to safety-related systems. Thus, a more refined analysis might reduce conservatism by including a ratio of safety significant area to total area. According to Bush, a revised analysis of this sort is expected to reduce the calculated probability of a potentially damaging strike by a factor of between 2-10 [28].
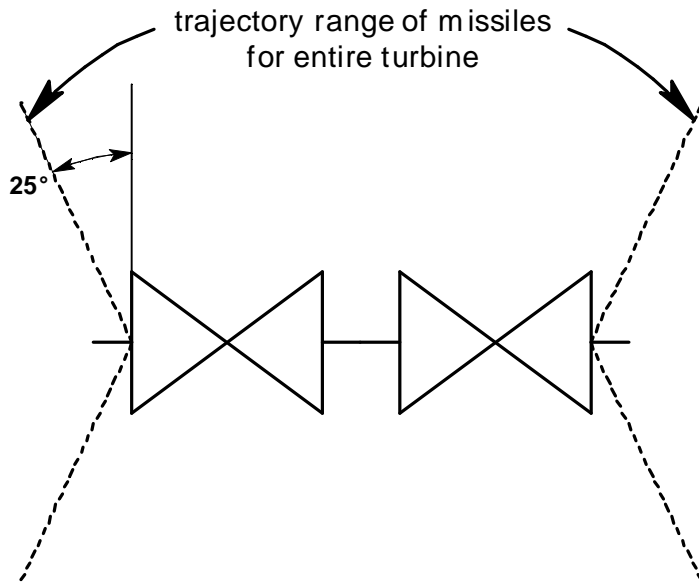
Figure 4-19 Range of assumed angles for low-trajectory turbine missiles

Bush states that a wide range of potential values for damage probability, P_3, exists. The range is bounded by the following extremes:

- no damage is expected to the protected portion of any safety-related system that is protected by at least six feet of reinforced concrete, $(P_3 = 0)$

- targets protected only by thin steel siding or roofs, or by less than three feet of concrete, are assumed to be essentially unprotected, $(P_3 = 1)$

Any remaining safety-related systems will have a P_3 value of between zero and one, and includes mainly those systems protected by concrete having a thickness ranging between three and six feet. The actual P_3 for each potential strike in these cases will depend largely on missile energy, so in these analyses, the calculation of P_3 should ideally be performed in a more integrated manner with the calculation of P_2. This integrated approach was not taken in the analysis presented by Bush, which still forms the basis for the current NRC recommended values for P_2 x P_3. Missile penetration characteristics in concrete were researched by EPRI, however these were performed after the studies cited by Bush [ ]. The EPRI results could help establish a set of guidelines for assigning damage probabilities for strikes on concrete of thickness less than six feet.

In summary, there are three potential tasks within the subject of missile strike/damage that may provide a basis for achieving reduced conservatism. Implementing improvements to the probability analysis scheme based on these issues would best be accomplished using a computer code.

- Implement results of EPRI studies on penetration of turbine missiles in reinforced concrete
- Reduce the conservatism inherent in assuming that a strike on *any* part of a building

containing a safety-related system means a strike on the actual equipment. A reduction in strike probability could be assessed that is consistent with the extent of area actually occupied by the system.

- An integrated calculation of P_2 and P_3 would more accurately account for the range of missile energy in potential strikes on plant safety-related systems with moderate protection (reinforced concrete 3-6 feet thick).

The above three tasks are technically possible, however the decision regarding whether to pursue them in subsequent phases of this project will also depend on regulatory issues and prioritization of project resources. The NRC may wish to maintain their current position that P_2 x P_3 are assigned values of 10^{-2} and 10^{-3}. Also, it may be determined that obtaining the desired relief on P_4 by focusing on P_1 alone is more cost-effective.

References

1. J. J. Burns, "Reliability of Nuclear Power Plant Steam Turbine Overspeed Control System", ASME Failure and Reliability Conference, Chicago, IL (September 1977).
2. Probability of Missile Generation in General Electric Turbines, Supplementary Report: "Steam Valve Surveillance Test Interval Extension", General Electric Report GET-8039.1, non-proprietary version, September 1993.
3. *Assessment of Turbine Missile Probability: Technical and Regulatory Issues* , EPRI, Palo Alto, CA: 2000. 1001267.
4. G. Selby, "Application of the Phased Array UT for Nuclear Plant Nondestructive Examination", Proceedings of the Twenty-Seventh Water Reactor Safety Information Meeting, Bethesda, MD. NUREG/CP-0169, October, 1999.
5. D. Lessard, "Steam Turbine Disk Keyway Inspection Using Phased Array Ultrasonic Technology", Preliminary Report to EPRI, November, 2001.
6. EPRI Report, NP-3340, "Stress and Fracture Analysis of Shrunk-on Steam Turbine Disks", 1984.
7. EPRI Report, NP-2738, "Metallurgical Evaluation of a Failed LP Turbine Disc", Research Project 1398-6, December 1982.
8. Structural Integrity Associates, "pc-CRACK", Version 2.1, 1991.
9. P. M. Besuner, et. al., "BIGIF – Fracture Mechanics Code for Structures," EPRI Report NP-1830-CCM, 1981.
10. ANSYS/Mechanical, Revision 5.7, ANSYS, Inc., December, 2000.
11. **ALT3D** Version 2.1, Copyright 1989-1995, Computational Mechanics, Inc.
12. McMinn et al, "A Review of Stress Corrosion Cracking of Low-Pressure Turbine Discs in the Nuclear Industry," EPRI Research Project 1929-14, December 1989.
13. R. C. Schwant and D. P. Timo, "Life Assessment of General Electric Large Steam Turbine Rotors," EPRI CS-4160, Proceedings of the Seminar on Life Assessment and Improvement of Turbo-Generator Rotors for Fossil Plants, September 12-14, 1984, Raleigh, North Carolina.
14. "SAFER-PC User's Guide & Technical Reference," Version 1.0, EPRI Research Project 2481-6, December 1996.
15. EPRI Report WS-79-235, "Workshop Proceedings: Rotor Forgings for Turbines and Generators," Proceedings, September 1981 (Palo Alto, California, September 14-17, 1980).
16. EPRI Report NP-2429, "Steam Turbine Disk Cracking Experience," Volumes 1 through 7, Research Project 1398-5, June 1982.
17. EPRI Report NP-6444, "Guidelines for Predicting the Life of Steam Turbine Disk Exhibiting Stress Corrosion Cracking," Volumes 1 and 2, Research Project 1929-16, 2518-1, 1929-4, July, 1989.
18. C. Wells, D. Rosario and B. Dooley, "Proceedings: Workshop on Corrosion of Steam Turbine Blading and Disks in the Phase Transition Zone," EPRI, Palo Alto, CA: 1998. TR-111340.
19. W. G. Clark, B. B. Seth, and D. M. Shaffer, "Procedures for Estimating the Probability of Steam Turbine Disc Rupture from Stress Corrosion Cracking", presented at Joint ASME/IEEE Power Generation Conference, October 1981.

20. *Reliability-Based Mechanical Design*, Edited by Thomas A. Cruse, Copyright 1997 by Marcel Dekker, Inc.

21. W. H. Press, S. A. Teukolsky, W. T. Vetterling, and B. P. Flannery, *Numerical Recipes in Fortran: The Art of Scientific Computing*, Second Edition, Cambridge University Press, Cambridge, UK, 1992.

22. David Vose, *Quantitative Risk Analysis*, Copyright 1996 by John Wiley and Sons, New York.

23. EPRI Report No. TR-105697, September 1995, "BWR Vessel and Internals Project, BWR Reactor Pressure Vessel Shell Weld Inspection Recommendations (BWRVIP-05)".

24. D.C. Gonyea,"An Analysis of the Energy of Hypothetical Wheel Missiles Escaping from Turbine Casings", GE Technical Information Series DF73SL12 Class 1, Feb. 1973.

25. Full Scale Turbine Casing Tests, 1983. EPRI, Palo Alto, CA: 1983. NP2741

26. Scale Model Turbine Missile Casing Impact Tests, EPRI, Palo Alto, CA: NP2742.

27. *Spinning Turbine Fragment Impact on Casing Models*, EPRI, Palo Alto, CA: 1983. NP2743.

28. "Safety Evaluation Report; related to the operation of Hope Creek Generating Station", Docket No. 50-354, U.S. Nuclear Regulatory Commission, Office of Nuclear Reactor Regulation, NUREG-1048, July 1986.

29. S. H. Bush, "Probability of Turbine Damage to Nuclear Components Due to Turbine Failure," Nuclear Safety, 14(3): May-June 1973, p.187.

5
CASE HISTORIES

Two types of case histories are included in this section of the report:

Regulatory Relief: These cases histories describe relief obtained by nuclear turbine operators from inspection frequencies and/or repairs recommended by the OEM for continued operation of LP turbines with shrunk-on disk bore/keyway cracks. Two cases are presented below, describing analyses and subsequent relief obtained by the Pilgrim and Clinton generating plants.

Relevant Nuclear Industry Failure: This is an analysis of specific factors that contributed to a documented disk failure in the U.S. nuclear industry. This case provides a basis for benchmarking current analysis techniques against an actual failure. This chapter includes a description of the 1980 failure of a disk on the low-pressure rotor in operation at the former Yankee Rowe generating plant (now decommissioned).

In each of the three case studies, supporting analyses were performed at the time by Structural Integrity Associates (SI) of San Jose California to estimate stress, crack tip stress intensity factor, critical crack size, and crack growth rate. A summary of these analyses is included within the write-up of each case history in this chapter.

5.1 Pilgrim Nuclear Station LP Turbine Cracking

This case history describes the 1993 decision by the NRC to permit the Pilgrim nuclear plant to continue operation with cracked LP turbine disks until 1995, at which time the rotors were scheduled to be replaced. The case shows some evidence of conservatism in the OEM-supplied analysis that recommended against operating the turbine without at least pre-warming the rotor to reduce the risk of brittle disk failure. Most important, this case demonstrates that the NRC is open to the possibility of examining risk assessments submitted by non-OEM's that are intended to provide relief for licensees.

5.1.1 Plant Description and History

The Pilgrim nuclear plant started commercial operation in l972, and has a turbine-generator rated at 670 MW. The reactor is a BWR design. The low-pressure (LP) turbine manufactured by General Electric is a four-flow tandem-compound design, with 43-inch last stage blades. Each LP rotor contains eight shrunk-on disks within each flow. During the April 1993 refueling outage, General Electric performed an ultrasonic inspection of the LPA turbine and reported bore cracking indications in disk numbers 4 through 7 (note that the 7th stage contains the second-to-last row, or L-1 row buckets). Based on results of the inspection and subsequent analysis of P_1 probability, General Electric recommended two options: either remove the 7th stage disk on the generator side (7GA) or pre-warm the LPA rotor before startup to satisfy NRC turbine missile probability limits for continued operation. These recommendations were made to Boston Edison, the operator of the Pilgrim Plant at the time. The details of General Electric's recommendations are contained in a proprietary report issued to Boston Edison. They essentially

provide specific options including the removal of one or both to the 7th stage disk, and/or rotor pre-warming. Doing either of these actions was shown to justify an increase in time prior to the next LP turbine inspection. Pre-warming was the most effective at increasing the inspection interval, and General Electric's results indicate that 90°F was sufficient to allow operation with the existing rotors until at least the scheduled rotor replacement.

To assess whether removal of the 7GA or rotor pre-warming was warranted, Boston Edison engaged the services of Structural Integrity Associates (SI), to perform an independent fracture mechanics evaluation of the 7th stage disk. A review/summary of the SI evaluation [1], which was reviewed and approved by the NRC [2, 3], and served as the basis for relief from removal of the 7GA disk, is the basis for this case history.

The stress and fracture mechanics evaluation performed by Structural Integrity [1] primarily included a study of the parametric effect of several key variables on the predicted remaining life of the 7GA disk. The 7GA disk was identified to be the most limiting because of a combination of factors which included flaw depth, lower operating temperature, higher fracture appearance transition temperature (FATT) and therefore lower fracture toughness, and potential consequences of disk failure. The following sections describe details of the individual aspects of the fracture mechanics and risk assessment analysis.

5.1.2 Disk Stresses

Detailed blade centrifugal rim loading for the 7GA disk were not available. Based on limited data provided by the turbine OEM to Boston Edison, the centrifugal hoop stress at the disk bore due to rotation at 1800 rpm was 42.4 ksi. The OEM also reported that the disk bore and outside radii were measured to be 16.5 and 43.5 inches, respectively. The stress level decreases from the maximum level at the bore location to locations outward from the bore surface. This stress distribution was estimated using the classical solution from D'Isa [4] for a rotating cylinder with the bore surface stress at 1800 rpm scaled to match the known value of 42.4 ksi. Disk stresses due to the shrink-fit radial interference (0.0345 inch, provided by Boston Edison) were calculated using the classical solution from Shigley [5] for press-fit members. The disk bore stress due to shrink-fit was calculated to be 35.9 ksi. Disk stress due to shrink-fit varies with rotor speed-squared, and was assumed to be completely relieved (zero) when the rotor attained 120 percent of rated speed (2160 rpm). Resulting disk stress distributions due to the combined effects of rotation and shrink-fit at various speeds, are shown in Figure 5-1. The combined disk bore stress at 1800 rpm was determined to be 53.4 ksi, which is comprised of a centrifugal stress of 42.4 ksi and a shrink-fit stress of 11.0 ksi.

COMBINED (SHRINK-FIT + RPM) HOOP STRESS GRADIENTS from 0 RPM to 2160 RPM (20% Overspeed)
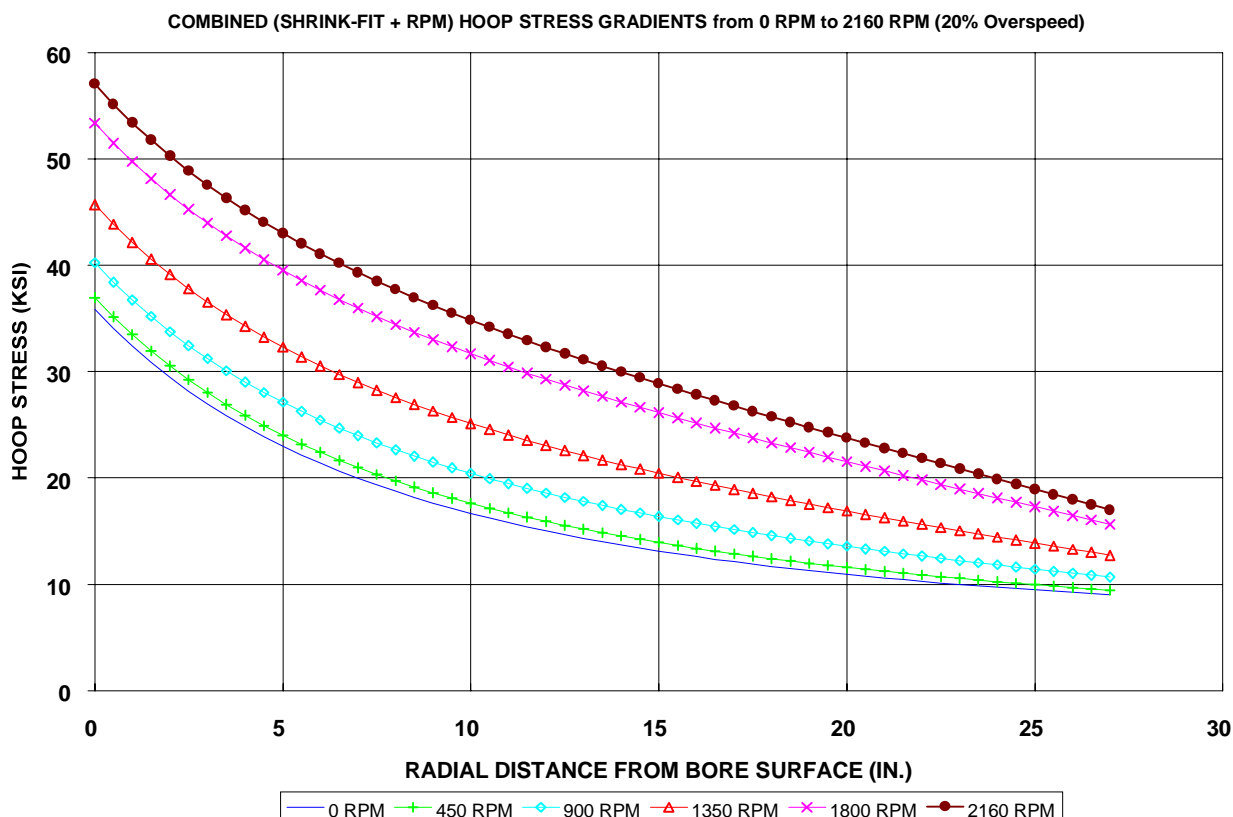

Figure 5-1 Hoop stress as a function of radial distance from the Pilgrim Disk 7G bore, due to the combined effects of rotation and shrink fit at speeds of 0, 450, 900, 1350, 1800 and 2160 rpm (without the keyway stress concentration effect)

5.1.3 Stress Concentrating Effect of Keyway

Boston Edison reported a stress concentration factor (Kt) of 2.2 for use with the General Electric keyway design. This K_t value was consistent with analyses performed under EPRI project NP-3340 [6]. The decay in the peak K_t value of 2.2 with distance from the keyway surface, from [6], is given by:

$$K_t(x) = 1 + (K_t - 1)\left[0.25(\frac{R}{R+x})^2 + 0.75(\frac{R}{R+x})^4 \right]$$

Equation 5-1

where,

R is the keyway depth (⅝-inch), and,
x is the radial distance from the keyway surface.

As illustrated in Figure 5-2, this K_t effect highly localized, reaching a value of only 1.06 at 1 inch away from the keyway surface. Combined centrifugal and shrink-fit stresses with the K_t effect superimposed are shown in Figure 5-3.
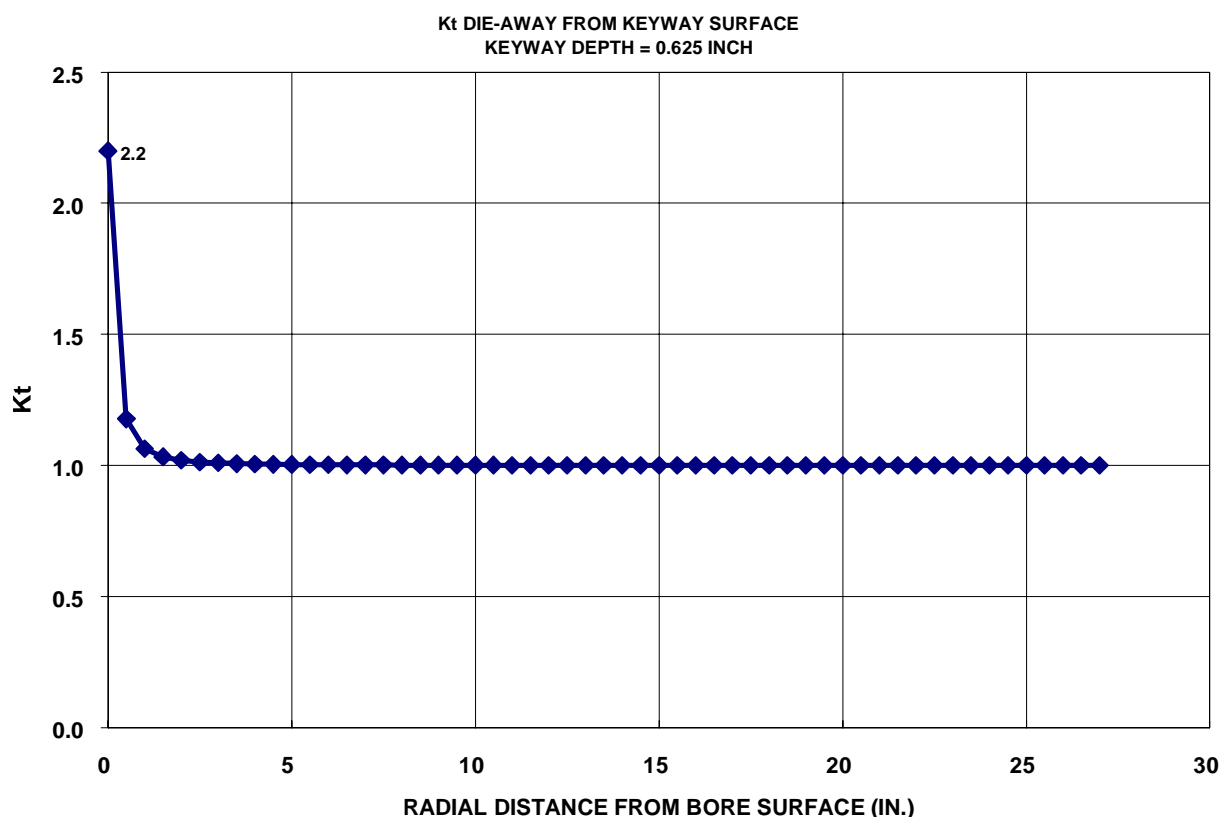
Kt DIE-AWAY FROM KEYWAY SURFACE
KEYWAY DEPTH = 0.625 INCH

Figure 5-2 Decay of peak keyway stress concentration factor, Kt, of 2.2 with increasing radial distance from the keyway surface

5.1.4 Fracture Mechanics Analysis

The primary objective of the fracture mechanics analysis was to compute stress intensity factors (K_I) as a function of crack size (a), which then permit determination of a critical crack size (a $_{cr}$) for a given fracture toughness (K_{Ic}). Structural Intregity compared the equation used by the OEM to compute KI with alternative solutions using their fracture mechanics code pc-CRACKTM [7]. The **pc-CRACK**^{TM} computer program was developed under the Structural Integrity QA program and meets the NRC code of federal regulations 10-CFR-50, Appendix B, ANSI/ASME NQA-1-1986, and NUREG-4640 (for computer software). The following is a discussion of potential areas of conservatism in the OEM solution for stress intensity factor, K_I, and the alternative K_I solution technique used in this case study.

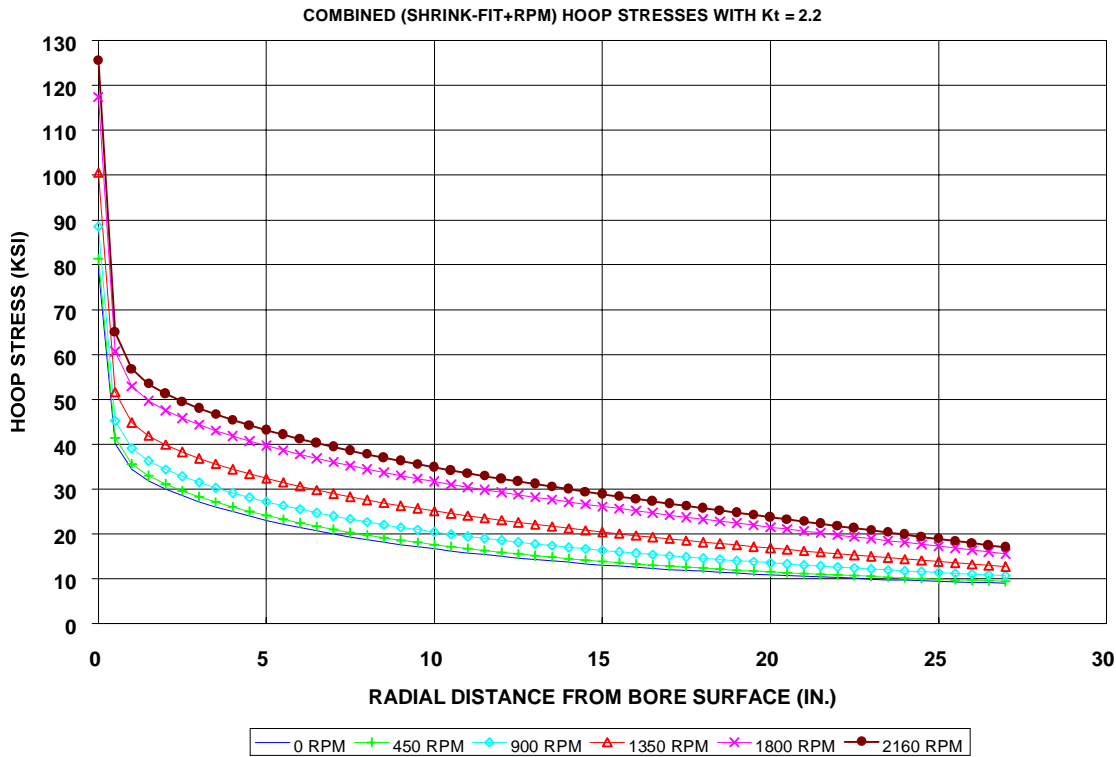**COMBINED (SHRINK-FIT+RPM) HOOP STRESSES WITH Kt = 2.2**

Figure 5-3 Hoop stress as a function of radial distance from the Pilgrim Disk 7G bore, due to the combined effects of rotation and shrink fit at speeds of 0, 450, 900, 1350, 1800 and 2160 rpm, including a peak keyway stress concentration factor, Kt, of 2.2

The K_I solution used in the OEM calculations is given by Equation 5-2:

$$K_I = 2\sigma\sqrt{5/8'' + a}$$

Equation 5-2

where:

σ is a uniform stress normal to the crack face,
⅝-inch is the keyway radial depth, and,
a is the radial extent of the crack measure from the keyway surface.

Equation 5-2 can be expressed in the following form for an edge-crack in a uniform stress field (Figure 5-4a):

$$K_I = 1.12\sigma\sqrt{\pi\, a_{eff}}$$

Equation 5-3

where:

a_{eff} is the effective crack depth = ($\frac{5}{8}$ + a) as given above.

The OEM crack model (Equation 5-3) is perceived as being conservative for the following reasons:

(a) The edge-crack model represents an upper bound computation for K_I because this model (Figure 5-4a) is far more compliant than the actual geometry which can be approximated as a radial crack emanating from the inner diameter of a thick hollow cylinder or a hole in a plate (Figure 5-4a)

(b) The uniform stress field used in the OEM equation is over-conservative because it does not incorporate the significant radial decrease in hoop stress with increasing distance from the bore, as shown in Figure 5-3.

(c) The use of a through-thickness crack (infinitely wide) does not include the beneficial effect of crack aspect ratios that are typically semi-elliptic in turbine disks [8].
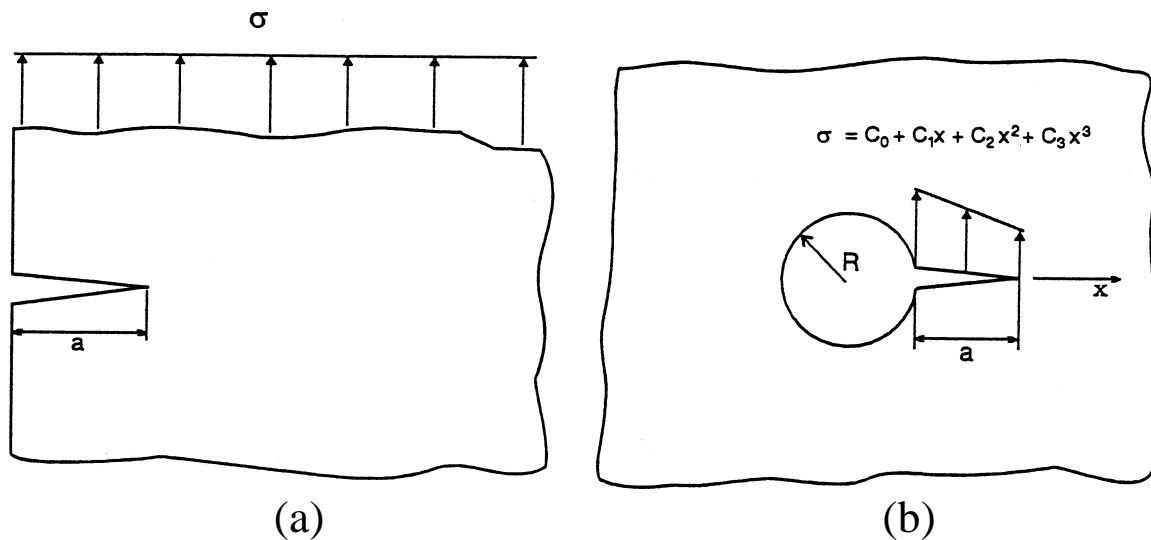
Figure 5-4 Through-thickness crack models used to perform the first set of "K_I versus a" calculations: (a) OEM model and (b) crack at a hole in a plate

To investigate the above-mentioned conservatism associated with the OEM solution for stress intensity factor, K_I, two sets of crack models were used in this case history investigation. The first set of models included improvements in the overall geometric stiffness representation and incorporation of the decreasing stress field (these models are designated Models A and B as shown in Figure 5-4b and Figure 5-5). This first set of models retained the conservatism of assuming that the crack extended the entire axial length of the hub or keyway (through-thickness). The second model included the additional effect of a finite length crack; i.e. the crack is assumed to be a semi-elliptic/semi-circular surface-connected crack with depth-to-length ratios of 1:5 (Model C) and 1:2 (Model D) as shown in Figure 5-6.
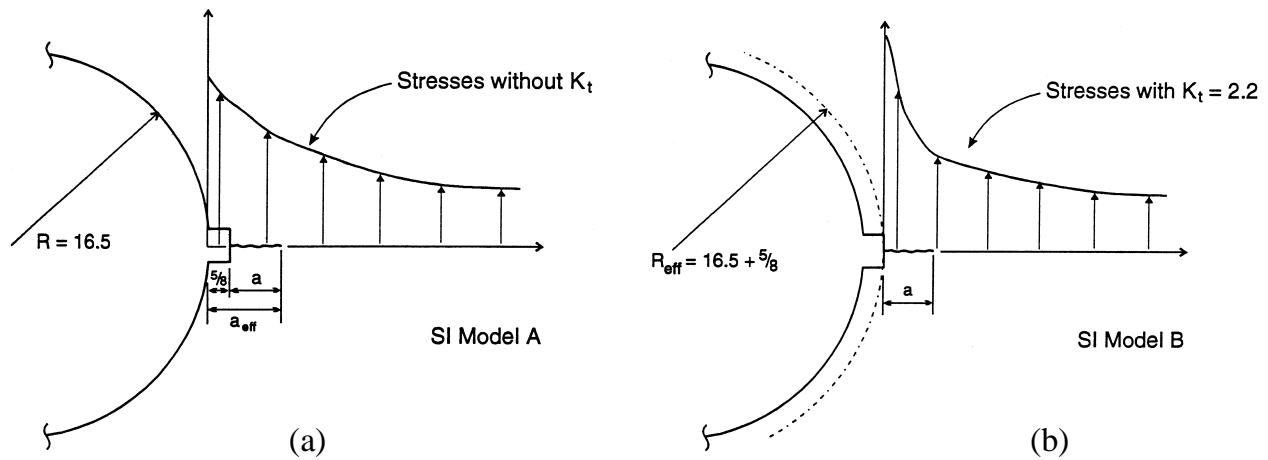
(a)

(b)

Figure 5-5 Schematics of the crack models used to illustrate the measurement of crack size versus hole size and stress distributions; (a) crack at a hole in a plate without keyway K$_t$ effect (Model A), and (b) crack at a hole in a plate with keyway K$_t$ of 2.2 (Model B)
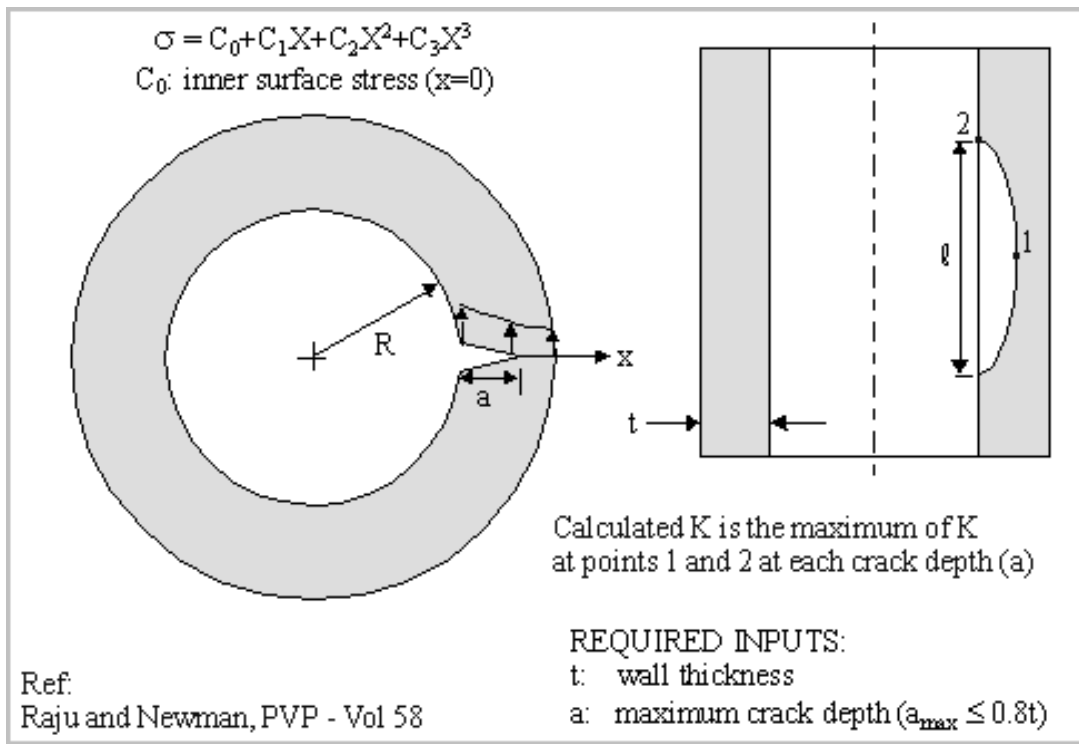

Figure 5-6 Schematic of a finite-length crack illustrating the crack depth (*a*) and length (*l*) parameters used in Model C (semi-elliptic crack with a depth-to-length ratio of 1:5) and Model D (semi-circular crack, i.e. depth-to-length ratio of 1:2)

5.1.5 Analyses Performed with Models A and B (Through-Thickness Cracks)

Models A and B account for the reduced compliance associated with the relatively large size of the shrunk-on disk (outer diameter of 87 inches). The crack model for a hole in an infinite plate shown in Figure 5-4b was used in the first set of K_I calculations. This model is identified as 'Model 1' in the pc-CRACK^{TM} program [7]. The stress concentrating effect of the keyway (K_t) was incorporated using two approaches:

(a) Model A: As shown in Figure 5-5a, for a hole in a plate, the K_t effect was implicitly accounted for by using the unconcentrated stresses (Figure 5-1) and an effective crack length of (5/8+a); the hole radius used corresponded to the inside radius of the disk (16.5 inches).

(b) Model B: As shown in Figure 5-5b for a hole in a plate, the K_t effect was explicitly accounted for by using the concentrated stresses, shown in Figure 5-3, and a crack length measured from the surface of the keyway; the hole radius used was the inside radius of the disk plus the keyway depth (17.125 inches).

Plots of "K_I versus a" solutions for the OEM and Structural Integrity through-thickness crack models are compared in Figure 5-7. The Structural Integrity crack models are considered to more accurately represent the disk stiffness for a "non-measurable" indication located under the web region, and show a significant reduction in estimated K_I values. For a fracture toughness of 105 ksi√inch, the critical crack size predicted by the OEM model was 0.34 inch compared with 0.54 inch for Model A and 0.56 inch for Model B.

5.1.6 Analyses Performed with Models C and D (Finite-Thickness Cracks)

To illustrate the conservatism of using through-thickness crack models to simulate disk cracking, Models C and D with semi-elliptic/semi-circular surface-connected cracks in a cylinder (Figure 5-6) were used in the second set of K_I calculations. The stress concentrating effect of the keyway (K_t) was implicitly accounted for, as described previously for Model A, by using the nominal stresses with an effective crack length of (5/8+a). Models C and D are described as follows:

(a) Model C: A semi-elliptic surface-connected crack in a cylinder with a depth-to-length ratio of 1:5 as shown in Figure 5-6.

(b) Model D: A semi-circular surface-connected crack in a cylinder with a depth-to-length ratio of 1:2 as shown in Figure 5-6.

These finite-length crack models are believed to encompass the range of geometry observed for most of the actual cracks in shrunk-on disks. For example, the cracks observed in post-failure inspection of the failed Yankee Rowe LP turbine disks described later in this chapter were approximately semi-circular in shape [8]. The cylinder thickness-to-inside radius ratio of 0.1, used for Models A-D, is believed to be less stiff (conservative) than ratios obtained from the actual Pilgrim disk geometry which are 0.52 for the hub region and 1.64 for the web region respectively.

Results of "K_I versus a" calculations for Models C and D are shown in Figure 5-8. For the lower bound fracture toughness of 105 ksi√inch the critical crack sizes predicted were 1.02 inch for the

semi-elliptic crack (Model C) and 3.30 inches for the semi-circular crack (Model D). These critical crack size estimates are two and six-times larger than that indicated by the through-thickness models.
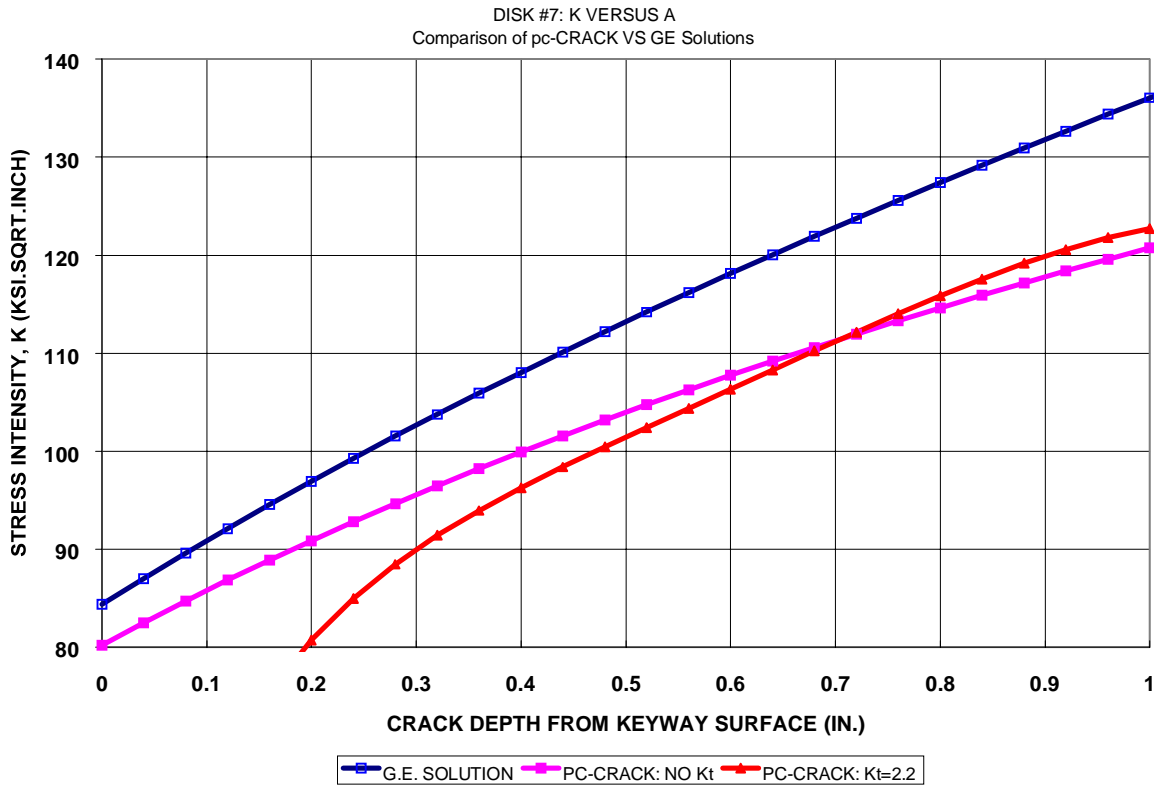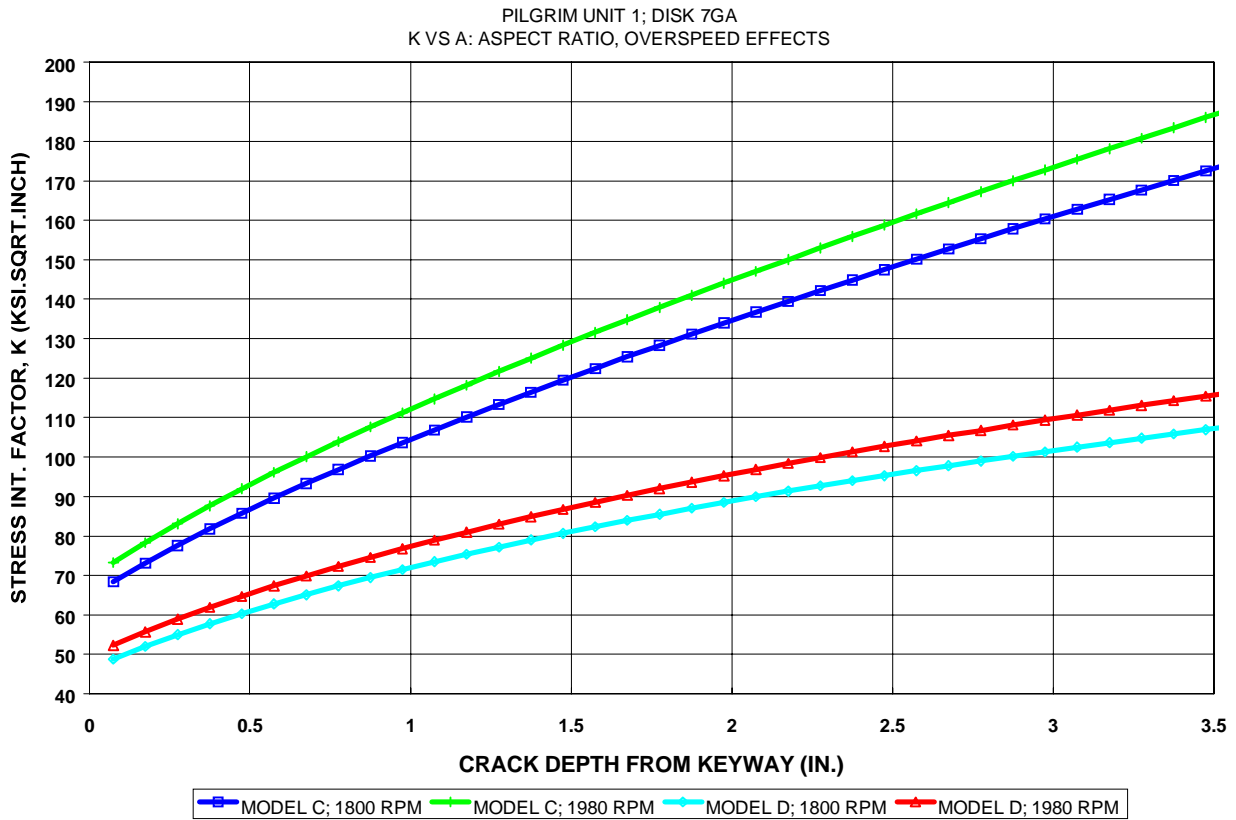

Figure 5-7 Stress intensity factor, K_I, versus crack size, a, for the following through-thickness crack models: (i) edge-crack in a semi-infinite plate with uniform stress (OEM), (ii) crack at a hole in a plate without keyway K_t effect (Model A), and, (iii) crack at a hole in a plate with keyway K_t of 2.2 (Model B)

PILGRIM UNIT 1; DISK 7GA
K VS A: ASPECT RATIO, OVERSPEED EFFECTS

Figure 5-8 Stress intensity factor, K_I, versus crack size, a, for the following finite-length crack models: (i) semi-elliptic crack with a depth-to-length ratio of 1:5 (Model C), and, (ii) semi-circular crack (Model D), at 1800 rpm and at 1980 rpm (10% rotor overspeed)

5.1.7 Parametric Fracture Mechanics Study (Effect of Key Variables)

In this study, the effect of several key variables, which govern the basis for determining remaining life and therefore in-service inspection interval, were examined. Calculations were performed for the 7th stage (specifically disk 7GA), which is the critical disk controlling the recommended in-service inspection interval. A summary of the results of the entire parametric study is presented in Table 5-1.

An in-service inspection interval (t_{insp}) can be computed based on the time-to-failure (t_{fail}) for the subject disk using Equation 5-4:

$$t_{insp} = t_{fail} /SF$$

Equation 5-4

where:

SF is a safety factor

The term t_{fail} is given by Equation 5-5 below:

$$t_{fail} = \frac{(a_{cr} - a_i)}{(da/dt)}$$

Equation 5-5

where:

a_{cr} is the critical crack size,
a_i is the initial crack size, and,
da/dt is the crack growth rate.

"Non-measurable" indications were identified during General Electric's inspection of wheel 7GA. Based on characteristics of their wheel inspection system, General Electric estimated an average initial crack depth (a_I) of 0.25 inch for these indications.

For the estimated initial crack depth of 0.25 inch, the time-to-failure (Equation 5-5) is dependent on two variables: critical crack size and the crack growth rate. Growth rate is primarily governed by stress corrosion cracking (SCC). Items (a) through (h) below identify the effects studied as part of the parametric fracture mechanics study performed by Structural Integrity:

(a) Effect of 35°F Adjustment in Deep-Seated FATT
(b) Effect of Fracture Toughness Variability
(c) Effect of Prewarming
(d) Effect of Crack Growth Rate
(e) Crack Tip Stress Intensity Factor Models (Through-thickness vs. Finite length)
(f) Effect of startup temperatures
(g) Effect of assumed initial crack size
(h) Effect of rotor overspeed during startup

The effect of each of the above variables was studied individually, and the results are described in the following paragraphs, and summarized in Table 5-1.

(A)   Effect of 35°F adjustment in deep-seated FATT

From Reference [9], the best estimate of deep-seated FATT values for Disk 7TA and Disk 7GA are 9°F and 12°F respectively. These values were further adjusted for safety by adding another 35°F to the result, yielding FATT values of 44°F for disk 7TA and 47°F for disk 7GA. For the base case shown in Table 5-1, a lower bound fracture toughness (K_{Ic}) of 105 ksi√inch was estimated from the OEM proprietary data [9], which corresponded to a FATT value of 47°F for disk 7GA. This base case yielded a critical crack size of 0.34 inch and a time-to-failure of 1.5 years. If the 35°F margin were not included, the lower bound K_{Ic} estimate increases to 128 ksi√inch, with a corresponding increase in critical crack size to 0.82 inch and a time-to-failure in excess of nine years.

(B)   Effect of Fracture Toughness Variability

If the mean value of K_{Ic} of 145 ksi√inch were used [9], instead of the lower bound value of 105 ksi√inch at the same FATT of 47°F, the critical crack depth and corresponding time-to-failure become 1.22 inches and 16.2 years (see Table 5-1). Therefore an inspection interval of 4 years with a safety factor of 4.05 would be justifiable, based solely on mean versus lower bound fracture toughness data.

(C)   Effect of Rotor Pre-warming

The inspection interval recommendations supplied by the OEM contained results of nominal startup temperatures of 75°F, 80°F, 90°F and 100°F to demonstrate the effect of metal temperature on risk of brittle failure. Pre-warming of the rotor during startup results in significantly higher disk toughness and critical crack sizes, as indicated in Table 5-1. At 80°F the lower bound K_{Ic} estimate is 110 ksi√inch and the critical crack size increases to 0.46 inch, with a time-to-failure of 3.5 years. At 90°F the lower bound K_{Ic} estimate is 115 ksi√inch and the critical crack size increases to 0.54 inch, with a time-to-failure of 4.8 years.

(D)   Crack Growth Rate

The primary crack growth mechanism in low-pressure rotor shrunk-on disks is stress corrosion cracking (SCC). Based on information provided in Reference [9], a crack growth rate of 0.06 inch/year was used for the base case analysis (Table 5-1), for a reported steady-state operating temperature of 172°F at the 7th stage. This crack growth rate represents two standard deviations above the mean, based on General Electric inspection results, which included non-measurable indications. For comparison, two alternate sources of crack growth data were used:

(a) Laboratory crack growth data representing a compilation of General Electric, Westinghouse and CEGB data [10] (proprietary)

(b) The SCC crack growth equation used in the analysis of cracking in bores and keyways of LP turbines in nuclear plants (References [11, 12]), is given below:

$$\ln(da/dt) = -\ 4.968 - (7302/T) + 0.0278\ \sigma_y$$

Equation 5-6

where:

T is the operating temperature of the disk in °R (°F+460),
σ_y is the yield strength in ksi, and,
da/dt is the growth rate in inches/hour.

An upper bound crack growth rate of 0.02 inches/year at 172°F was estimated from [10] yielding a time-to-failure of 4.5 years as shown Table 5-1. For a

reported disk yield strength of approximately 120 ksi, the crack growth rate predicted using Equation 5-6 at 172°F was 0.0164 inch/year, resulting in a time-to-failure of 5.5 years as shown in Table 5-1.

(E)   Alternate Models for Stress Intensity Factor Estimates (through-crack)

As discussed earlier in this case history, the first set of alternate models used to calculate stress intensity factors retained the conservative assumption of a through-thickness crack. "K_I versus a" results shown in Figure 5-7, yielded a 60 percent increase in critical crack size using Models A and B as compared to the baseline estimate by the OEM. The "crack at a hole in a plate" model used by Structural Integrity is predicted to provide an even closer representation of the "non-measurable" keyway crack under the web region by incorporating the added constraint imposed by the large disk size (87-inch diameter) relative to the small critical crack size. Results using Model A and Model B are summarized as:

Model A: For the crack model shown in Figure 5-5a (without the K_t effect), the critical crack size predicted for a lower bound toughness of 105 ksi√inch was 0.54 inch, with a time-to-failure of 4.8 years; i.e., a critical crack size increase by a factor of 1.6 over the OEM K_I solution.
Model B: For the crack model shown in Figure 5-5b, incorporating the keyway stress concentrating effect, K_t, the critical crack size predicted for a lower bound toughness of 105 ksi√inch was 0.56 inch, with a time-to-failure of 5.2 years.

The above calculations using Model A and Model B removes some conservatism relative to the OEM estimate, while retaining the conservative assumption that the crack extends the entire length of the keyway. The effect of using crack models with a finite aspect ratio is discussed in the following section (f).

(F)   Alternate Stress Intensity Factor Models (finite-length crack)

The second set of stress intensity factor models was developed to address the conservative assumption of a through-thickness crack. "K_I versus a" calculations were performed for a semi-elliptic surface-connected crack with depth-to-length ratio of 1:5 (Model C) and a semi-circular crack (depth-to-length ratio of 1:2, Model D). Based on observed crack geometry documented in cracked turbine disks [8].

Results, summarized in Table 5-1, predict critical crack sizes of 1.02 inch and 3.30 inches for the semi-elliptic and semi-circular cracks respectively. These correspond to failure times of 12.8 years and 50.8 years, respectively. These critical crack size values exceed the results of calculations performed with through-cracks in Model A by factors of approximately two and six. This increase in critical crack size results in increases in remaining life factors by of 2.7 and 10.6.

(G)   Effect of Colder Startup Temperatures

The base-line evaluation performed by the OEM assumed a metal temperature of 75°F at unit startup. To investigate the effect of unit startup with disk temperatures below 75°F, a parametric study using 65°F and 55°F were included in the evaluation.   This study was performed using Models C and D that incorporated finite-length cracks. The results are summarized in Table 5-1 and indicate reduced toughness values of 102 ksi√inch and 98 ksi√inch at 65°F and 55°F respectively. These toughness values correspond to critical crack sizes of 0.92 inch and 0.82 inch for the semi-elliptic crack (Model C) and 3.04 inches and 2.68 inches for the semi-circular crack (Model D), respectively. The shortest time-to-failure of 9.5 years was predicted for the semi-elliptic crack at a 55 °F startup temperature; i.e., a 26 percent reduction in life compared with the baseline 75°F startup temperature.

(H)   Effect of Assumed Initial Crack Size

The initial crack size of 0.25 inch, assumed by the OEM, was also used in the calculations performed with Models A-D. The GE value of 0.25 inch was based on an average of available data for "non-measurable" indications under the web region [9]. To address concerns that the largest of these "non-measurable" indications could be present in the Pilgrim LP rotor, an initial crack size of 0.67 inch was included in evaluation of finite-length surface cracks (Models C and D). As shown in Table 5-1, the time-to-failure for the semi-elliptic crack reduced to 5.8 years with 43.8 years for the semi-circular crack. It should be noted that this 0.67-inch initial crack size clearly represents the worst case for a "non-measurable" indication given recent advances in ultrasonic inspection technology, yielding a very conservative remaining life estimate. Independent assessment of the UT of the Pilgrim disks by experts from the EPRI NDE center concluded that the indications were very small, and that the OEM estimate of 0.25 inch was conservative.

(I)   Effect of rotor overspeed during startup

All "K_I versus a" calculations presented thus far correspond to the rated turbine speed of 1800 rpm. This assumption is considered reasonable because of the minimal possibility of rotor overspeed occurring at 75°F (cold condition). Information on overspeed testing procedures at Pilgrim provided by Boston Edison personnel [13] indicate that the unit must be held at 25 percent load for a minimum of four hours before any overspeed tests are performed. After four hours of operation, the temperature of the limiting wheel, 7GA, is estimated to be 172°F.   At this metal temperature, the lower bound rotor toughness is predicted to be greater than 165 ksi√inch [9], greatly reducing the possibility of brittle fracture due to overspeed.

To address the remote possibility of rotor overspeed occurring in the cold condition, additional calculations were performed at 110 percent of rated speed

(or 1980 rpm) for the finite-length crack models. The results (Figure 5-8, Table 5-1) predict reduced critical crack sizes of 0.81 inch for the semi-elliptic crack and 2.64 inches for the semi-circular crack with remaining lives of 9.3 years and 39.8 years, respectively.

Table 5-1 Summary of Results: Pilgrim Unit 1 Shrunk-on Disk 7GA Keyway Cracking Evaluation

Case Analyzed	$T_{startup}$ (°F)	FATT (°F)	K_{Ic} (ksi√inch)	Crack Model	a_i (inches)	a_{crit} (inches)	da/dt (inch/yr)	t_{fail} (years)
Base Case →	75	12+35	105	GE	0.25	0.34	0.060	1.5
Parametric study results below (effect of key variables in left column)								
(a) FATT without 35°F margin	75	12	128	GE	0.25	0.82	0.060	9.5
(b) Mean K_{Ic}	|	12+35	145	GE	|	1.22	|	16.2
(c) Prewarming								
80°F	80	12+35	110	GE	|	0.46	|	3.5
90°F	90	12+35	115	GE	|	0.54	|	4.8
(d) da/dt @ 172°F								
lab data	75	12+35	105	GE	|	0.34	0.020	4.5
NRC eqn.	75	12+35	105	GE	|	0.34	0.0164	5.5
(e) SI crack models								
Model A	75	12+35	105	SI Model A	|	0.54	0.060	4.8
Model B	75	12+35	105	SI Model B	|	0.56	0.060	5.2
(d) + (e)	75	12+35	105	SI Model A	|	0.54	0.020	14.5
	75	12+35	105	SI Model B	|	0.56	0.020	15.5
(f) Aspect ratio								
Model C (1:5)	75	12+35	105	SI Model C	|	1.02	0.060	12.8
Model D (1:2)	75	12+35	105	SI Model D	|	3.30	0.060	50.8
(f) + $T_{startup}$ = 65°F	65	12+35	102	SI Model C	|	0.92	0.060	11.2
	|	|	|	SI Model D	|	3.04	0.060	46.5
(f) + $T_{startup}$ = 55°F	55	|	98	SI Model C	|	0.82	0.060	9.5
	|	|	|	SI Model D	|	2.68	0.060	40.5
(f) + a_i = 0.67 inch	75	12+35	105	SI Model C	0.67	1.02	0.060	5.8
	75	12+35	105	SI Model D	0.67	3.30	0.060	43.8
(f) + 10% rotor overspeed (1980 rpm)	75	12+35	105	SI Model C	0.25	0.81	0.060	9.3
	75	12+35	105	SI Model D	0.25	2.64	0.060	39.8

5.1.8 Evaluation Summary and Conclusions; Pilgrim Investigation

An independent stress and fracture mechanics analysis of the 7th stage shrunk-on disk 7GA was performed by Structural Integrity Associates, which included a parametric study of the influence of several key variables on the recommended re-inspection interval for this disk.

This study revealed that an increase in inspection interval could be achieved by consideration of several areas of conservatism believed to be present in the baseline OEM analysis. In particular, more accurate modeling of the stress intensity factor for a finite length crack originating in the bore region is recommended. One aspect of this reduced conservatism is the change from use of a simple edge-crack model to a hole-in-plate model. The second change, which is more influential, involves the use of finite-length cracks rather than through-cracks. Finite length semi-elliptic cracks, with depth-length ratios approaching 1:2 (semi-circular) are justified based on post-failure examination of actual SCC disk cracks. The effect on stress intensity factor of changing the crack aspect ratio is very significant. In this parametric study performed for the Pilgrim 7GA disk, use of this less-conservative model yields an estimated time-to-failure of 12.8 years and 50.8 years for semi-elliptic cracks with depth-to-length ratios of 1:5 and 1:2 respectively. This corresponds to an increase in inspection interval by factors of 8.5 and 33.9 over the base case.

It is also noted that use of more representative material toughness properties (FATT, K_{Ic}), rather than conservative lower bound values, result in a significant increase in inspection interval. For example, use of mean fracture toughness alone results in the increase in inspection interval by a factor of eleven.

The preceding analysis was deterministic, however every effort was made to utilize conservative assumptions on distributed variables (i.e., two standard deviations). It is believed that the calculations performed bounded the effects of initial crack size, colder startup temperatures and the possibility of rotor overspeed in the cold condition. A conservative remaining life estimate of 5.8 years for the semi-elliptic crack was obtained by assuming an initial crack size of 0.67 inch corresponding to the largest historical "non-measurable" indication reported by the OEM.

Based on the results of the evaluation performed for Boston Edison by Structural Integrity Associates, it is concluded that the use of a more accurate crack model alone appears to be adequate to justify an inspection interval of four years. This interval includes a safety factor of 3.2 based on an initial crack size of 0.25 inch and a safety factor of 1.5 based on an upper bound initial crack size of 0.67 inch.

5.1.9 NRC Review of Parametric Fracture Mechanics Analysis

The parametric fracture mechanics analysis report [1], prepared by Structural Integrity Associates on behalf of Boston Edison was submitted to the NRC for review. The NRC's interest was to ensure that there was no gross error in the analysis, and to assess the potential impact to plant safety. The chief of the Materials and Chemical Engineering Branch conducted the NRC review.

The NRC review indicated their agreement with the assumptions used by Structural Integrity Associates to reduce conservatism in the OEM analysis, in particular the stress gradient and formulation of the fracture mechanics model [2]. NRC calculations yielded a time-to-failure of 4-12 years corresponding to upper bound and mean SCC growth rates of 0.06 and 0.02 inch/year respectively, which was in close agreement with the time-to-failure range of 4.8 to 14.5 years predicted by Structural Integrity Associates.

The following is an excerpt from the NRC memorandum containing the conclusions of their review of the analysis submitted by Boston Edison [2]:

> "The NRC requires that the turbine missile failure probability be 1E-5 per year or lower for an unfavorably oriented turbine. GE's analysis is based on a turbine missile generation probability of 1E-5 failure per year. SIA did not perform a probabilistic fracture mechanics analysis. Based on engineering judgement, the staff estimated that the missile failure probability for the LPA turbine is between 1E-5 and 1E-4 per year. For this condition, the NRC permits the turbine to be kept in service until the next scheduled outage, at which time the licensee should take action to reduce the failure probability to the 1E-5 per year criterion (Reference: NUREG-1048, Safety Evaluation Report related to the Operation of Hope Creek Generating Station, Supplement No. 6, July, 1986). The licensee has indicated that they are considering the replacement of both LPA and LPB rotors during the next scheduled refueling outage, which is expected to be April 1995. Based on an assessment of the information available, the staff concludes that there is no safety concern for normal operation of the LPA turbine to the end of the current fuel cycle. The SIA analysis appears to reduce some of the obvious conservatisms used in the GE analysis."

A summary of the NRC review was published in the June 28, 1993 issue of INSIDE N.R.C. in an article entitled "Pilgrim Critics Claim Danger from Cracked Low-Pressure Turbine Disks" [3].

5.1.10 Licensee Relief and Successful Continued Operation

Based on results of the evaluation described above, and the subsequent NRC review, Boston Edison successfully operated the LPA turbine to the next refueling outage in 1995, at which time both original rotors were replaced by new low-pressure turbine rotors. The new rotors employed a monoblock design in which the rotor shaft and disks are integral in a single forging. This design eliminates the disk keyway and shrink-fit thereby eliminating any risk associated with keyway cracking.

5.2 Clinton Nuclear Station LP Turbine Cracking

This case history summarizes the evaluation and dispositioning of inspection findings in the Clinton Nuclear Station LPB rotor bore/keyway region in 1996 [14]. The Clinton plant is currently operated by Amergen, but was previously operated by Illinois Power at the time the investigation described below was performed.

5.2.1 Plant Description and History

The Clinton Nuclear Station turbine-generator is rated at 930 MW and the reactor is a BWR-style manufactured by General Electric. The main steam turbine, also manufactured by GE, includes one high-pressure (HP) rotor and two tandem-compound low-pressure (LP) rotors with 43-inch last stage blades. Each LP rotor has a double-flow design with seven shrunk-on disks in each flow path. Commercial operation began in 1987, and through 1996 the unit had accumulated approximately 80,000 operating hours. With the exception of the last stage shrunk-on disks, which have a radial key, all the other shrunk-on disks are keyed to the shaft with an axial key. The disk bore, axial keyways and dovetail regions of the latter stage shrunk-on disks (stages 4-7) which are highly stressed and exposed to wet steam during operation, are therefore potentially subject to stress corrosion cracking (SCC).

An inspection and assessment of the Clinton LPB rotor disks by the turbine OEM in 1990 concluded that the NRC limit on probability P_1 was barely satisfied for future operation over the a six-year period. Following the 1990 report, the Clinton plant was operated for the six years without a disk-related incident, and re-inspected in 1996. This case history describes a comprehensive evaluation of the 1996 Clinton Station bore/keyway re-inspection results performed by Structural Integrity Associates (SI). The evaluation was requested by Illinois Power Company to justify turbine operation for the following six years. The SI evaluation consisted of a critical review of the disk inspection methodology and results, and the subsequent stress and fracture mechanics calculations for critical disks to provide deterministic and probabilistic estimates of remaining life.

5.2.2 1996 Disk Inspection Results

The turbine OEM, General Electric, performed the LPB rotor wheel keyway and bore surface ultrasonic inspections. A tangential pitch-catch technique from the web faces and a shear wave pulse-echo technique from the hub outer diameter were used as illustrated in Figure 5-9. Maximum crack indication depths reported for 1996 inspection of disks 4G, 5G, 5T, 6G and 6T are provided in Table 5-2, along with the 1990 inspection results, for comparison. These depths include the corrections ("adders") applied by the OEM (0.070 inch for cracks detected under the hub and 0.100 inch for cracks sized from the web, per Reference [15]). For "non-measurable" indications under the hub, a minimum depth of 0.080 inch is assigned and for indications located under the web, a minimum depth of 0.200 inch is assigned. No indications were reported on the hub face.

Table 5-2 Summary of Clinton LPB Rotor Ultrasonic Inspection Results

Summary of Worst Keyway Indications: Oct. '96				November 1990 Results
Row #	Stage	Location	Maximum Depth (inch)	
L-3	4G	Keyway	0.27	0.25
L-2	5G	Keyway	0.21	none
	5T	Keyway	0.23	none
L-1	6G	Keyway	0.2	none
	6T	Keyway	0.2	none

5.2.3 Stress Analysis

Stress analyses of the LP rotor L-1, L-2 and L-3 disks were performed using two-dimensional axisymmetric finite element (FE) models of the rotor shaft and disk. A typical half-symmetry FE model used to simulate the rotor shaft and shrunk-on disk is shown in Figure 5-10. Loading included centrifugal effects and the shrink-fit between the disk and shaft, which was simulated using gap elements. These FE stress results do not include the local effect of the keyway stress concentration. This effect was separately accounted for by applying a stress concentration factor (K_t) of 2.2 for the General Electric axial keyway design and a gradient as evaluated by Equation 5-1, presented in the preceding case history for the Pilgrim rotor. Typical hoop stress gradients from the surface of the keyway crown are shown in Figure 5-11 for L-3 disk.
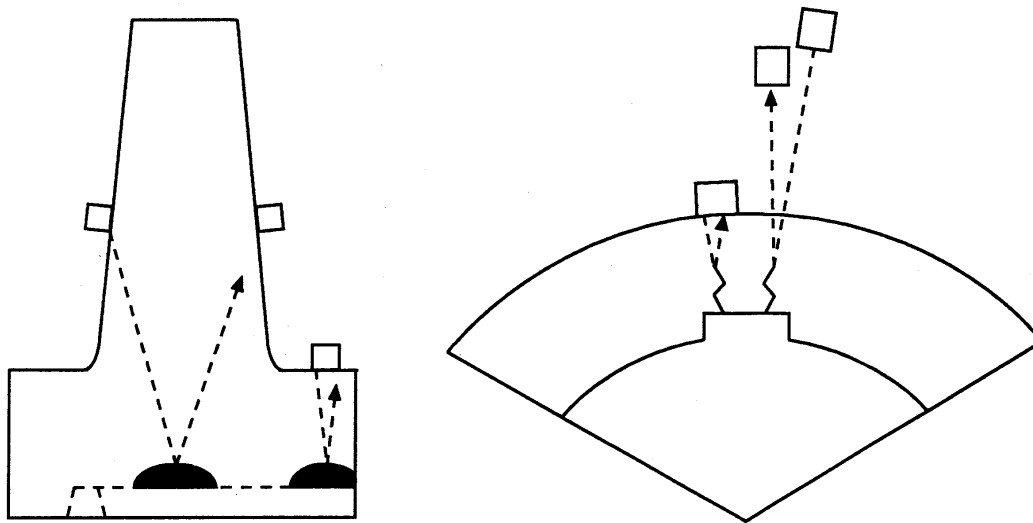
Figure 5-9 Placement of ultrasonic transducers for bore/keyway cracking sizing scans, Clinton Station [14]

5.2.4 Critical Crack Size

Linear elastic fracture mechanics principles were employed to compute stress intensity factors (K_I) as a function of various crack sizes (a) and geometries, which then permit determination of a critical crack size (a_{cr}) for a given fracture toughness (K_{Ic}). Effects of yielding or plasticity, if present, were predicted to be highly localized and, therefore, use of linear elastic principles is predicted to yield slightly conservative results.
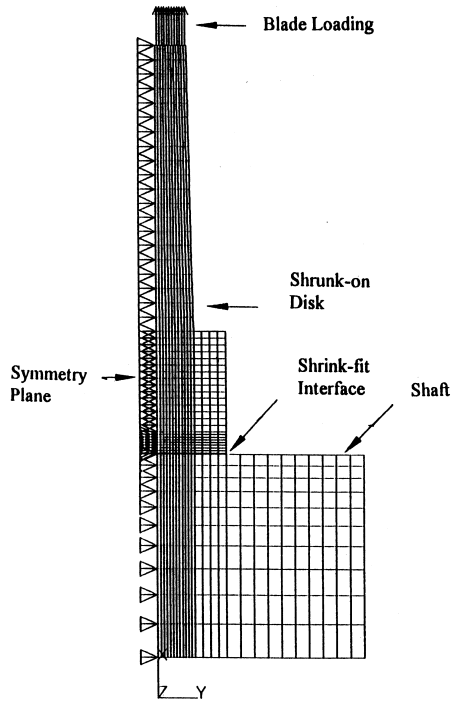
Figure 5-10 Two-dimensional finite-element model of the Clinton LP rotor 4th stage (L-3) shrunk-on disk [14]
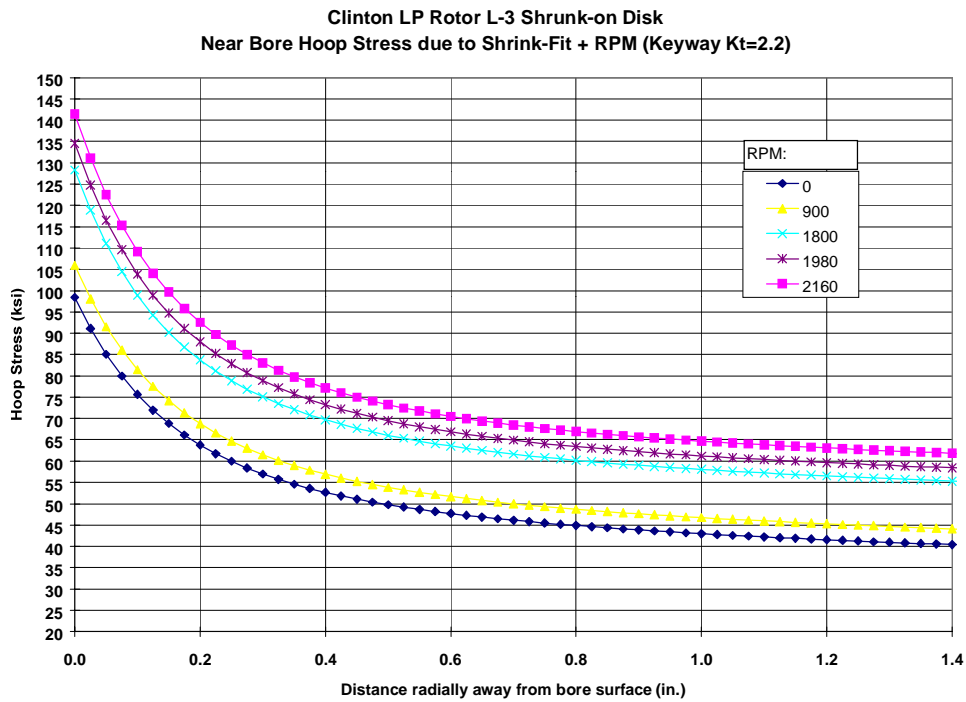
Figure 5-11 Hoop Stresses in the Clinton LP Rotor 4th Stage (L-3) Disk at the keyway [14]

5.2.5 *Fracture Toughness*

Disk-specific fracture toughness (K_{Ic}) data was not available, but deep-seated and rim FATT values (*proprietary*) were available for each disk. Therefore, generic wheel toughness data for GE rotors, shown in Figure 5-12, was used to estimate K_{Ic} [16]. Disk temperatures without prewarming (70°F) and with prewarming to achieve a minimum temperature of 100°F, were used to estimate fracture toughness. Deterministic remaining life calculations included lower-bound and mean estimates for K_{Ic}. The statistical variation in toughness data was incorporated in the probabilistic evaluation for bore/keyway cracking.

NiCrMoV ROTOR TOUGHNESS DATA
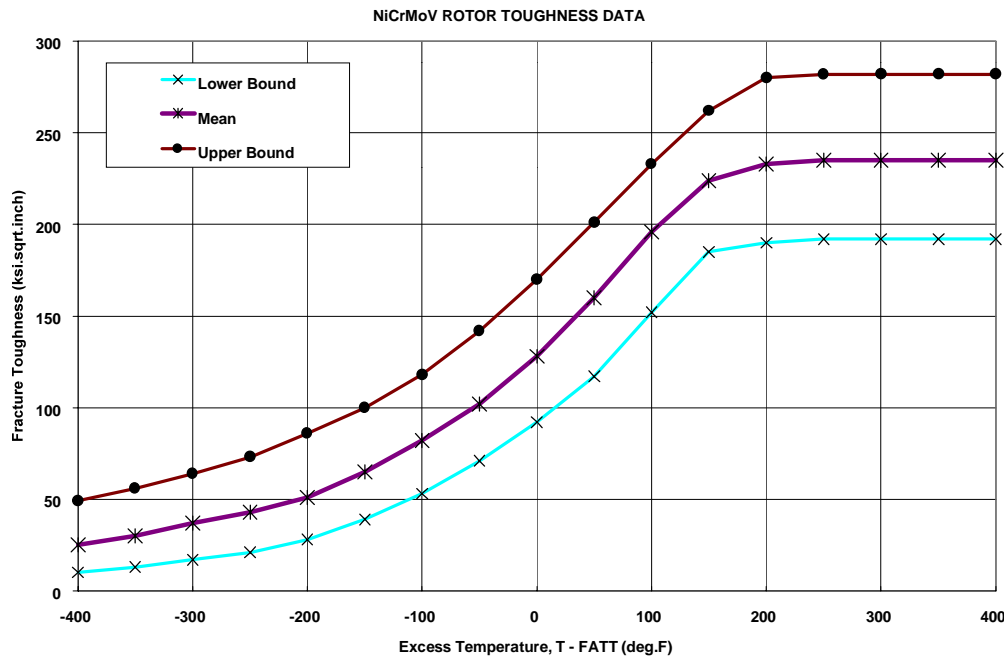
Figure 5-12 Wheel toughness versus excess temperature [16]

5.2.6 *Crack Tip Stress Intensity Factor Solutions*

Stress intensity factor solutions for bore/keyway cracks were generated assuming a semi-elliptic crack at the ID of a hollow cylinder (Figure 5-6) using Structural Integrity Associates' fracture mechanics code pc-CRACK™ [7]. Four crack aspect ratios were considered, a) planar (a/l=0), b) 10:1 (a/l=0.1), c) 5:1 (a/l=0.2), and d) 2:1 (a/l=0.5). The planar crack represents a worst-case scenario and the semi-circular crack (2:1) represents the most favorable crack geometry. The evidence suggests that finite-length crack models rather than conservative planar models are more representative of the actual bore/keyway cracks observed in shrunk-on disks. For example, most of the cracks documented in the failed Yankee Rowe LP turbine disks (described in the next case history) were approximately semi-circular in shape [8]. From a practical standpoint, therefore, a 10-to-1 aspect ratio was considered to be an upper bound for typical bore/keyway cracks simulations. Typical stress intensity factor (K_I) versus crack size (a) results for the L-3

disk are shown in Figure 5-13. Assuming the rotor is not prewarmed, that lower bound toughness values apply, and a crack aspect ratio of 10-to-1, deterministic estimates of critical crack size for keyway cracks ranged from 0.8 inch to 2.01 inch. Using mean values for toughness, the critical crack sizes increase to 1.77 inch to 2.72 inch for the disks evaluated. Because disk-specific material property data is proprietary, the detailed data used in this calculation is not provided here.

Clinton LP Rotor L-3 Shrunk-on Disk (4G,4T)
K vs a: 1980 rpm (10% Overspeed)
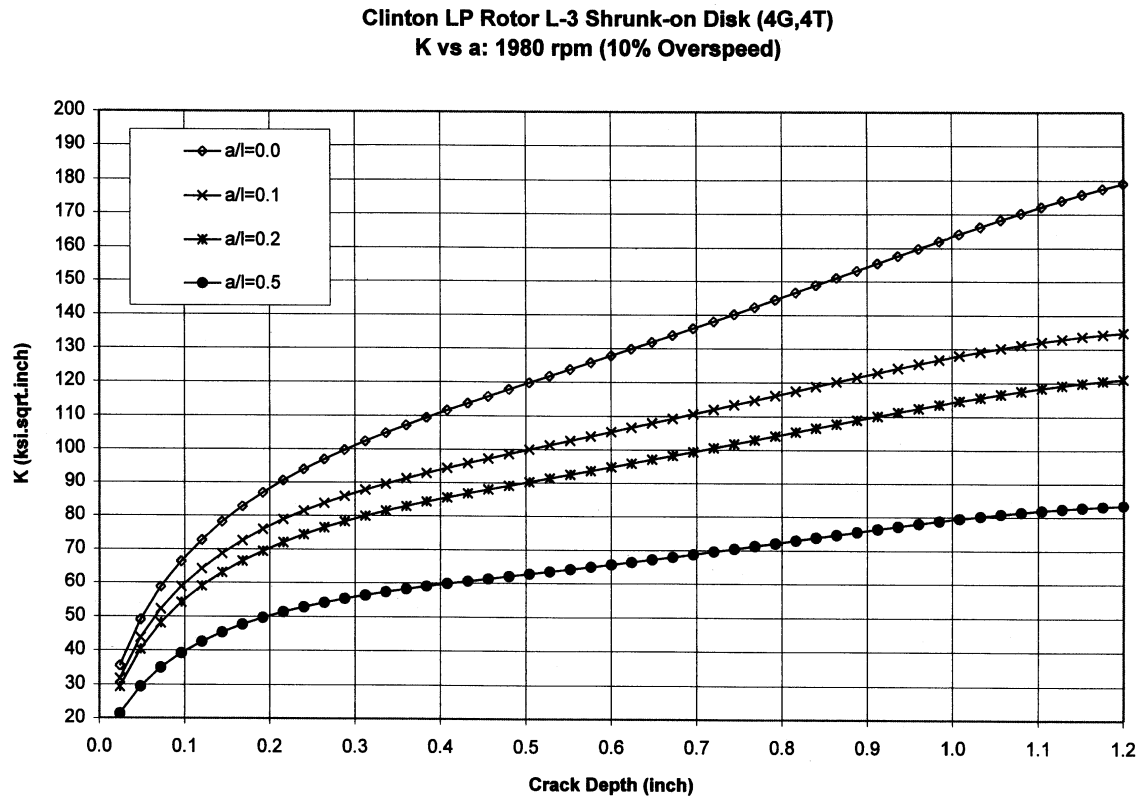
Figure 5-13 Stress intensity factor (K$_I$) versus crack size (a) results for the Clinton LP rotor disk 4 (L-3) bore/keyway at 1980 rpm [14]

5.2.7 Deterministic Assessment of Disk Remaining Life

The disk remaining life was calculated using Equation 5-5, with stress corrosion crack (SCC) growth rates simulated using Equation 5-6, as described in the prior case history. Based on the 1990 and 1996 inspection results for the LPB rotor (Table 5-2) a maximum bore/keyway crack growth rate of 0.038 inch/year was inferred, which is consistent with mean values calculated using Equation 5-6. Deterministic remaining life estimates using the 0.038 inch/year SCC growth rate, were in excess of 15 years for all disks with reported cracks.

5.2.8 Probabilistic Assessment Of Disk Burst

The NRC probability limit of 10^{-4} for generating a turbine missile external to the casing (P_1) is applicable to the Clinton rotor, which is oriented favorably; i.e., the rotor centerline is in line with reactor. The probability P_1 of generating an external missile due to brittle failure is the combination of the probability of disk burst (P_B) and the probability of containment of the disk fragments (P_C) expressed by:

$$\boldsymbol{P_1 = P_B \times (1 - P_C)}$$
  Equation 5-7

The evaluation performed by Structural Integrity focused on a determination of the disk burst probability P_B which changes with operating time and inspection results. An assessment of the containment probability (P_C) which does not change with operating time or inspection results, was inferred from the probabilities P_1 and P_B provided by the turbine OEM [17]; this data is proprietary and is therefore not reproduced in this report. The objective of the Structural Integrity evaluation was to focus on a reassessment of burst probabilities for disks 4, 5 and 6 with keyway indications and demonstrate that the NRC limit on P_1 stated above would not be exceeded even with the new crack indications reported in 1996.

A probabilistic analysis, which incorporates the statistical distributions of key input variables with random sampling, provides a more realistic assessment of failure. The first step in a probabilistic evaluation requires identification of appropriate random variables and determination of a statistical distribution associated with each variable. The generation of probabilistic results can then be accomplished using a technique such as Monte Carlo, which is essentially a series of many deterministic remaining life calculations using randomly selected values for the key input variables.

The selection and distribution of random variables for disks 4, 5 and 6 with keyway indications is summarized in the following paragraphs below:

Variable #1: Stress or K_I uncertainty

The FEM analyses were assumed to provide accurate results with a maximum uncertainty of 5 percent due to errors in either geometric information or applied loads. A normal distribution was assumed.

Variable #2: Probability of Ten Percent Overspeed

The possibility of a 10 percent overspeed event (1980 rpm) was assessed to be no more than two percent of the total number of startups based on actual operating history for the Clinton LP rotors.

Variable #3: Fracture Toughness

The variability in fracture toughness data for General Electric LP rotors was simulated using a standard deviation in fracture toughness of 16.7 ksi√inch above and below the mean with a normal distribution.

Variable #4: Fracture Appearance Transition Temperature (FATT)

To determine fracture toughness, the variability in disk FATT was modeled as a normal distribution. Mean and standard deviation values were determined from proprietary disk-specific data.

Variables #5 and 6: Disk Temperature at Keyway without/with Pre-warming

Without pre-warming the local keyway temperature was assumed to have a mean value of 70°F. The mean disk temperature achievable with pre-warming on turning gear was estimated to be 100°F. No variability in these values was simulated.

Variable #7: Crack Aspect Ratios

To remove the conservatism associated with a planar crack, various probabilities of occurrence were assigned to specific crack aspect ratios as follows: 65% for a 10:1 elliptic crack, 25% for a 5:1 crack and 10% for a semi-circular crack (2:1). This distribution was considered to conservatively represent the non-planar configuration of documented disk cracks.

Variable #8: Effect of Crack Branching

The results of crack branching studies have been summarized under EPRI project RP 1929-14 [18]. It has been documented that crack branching lowers the stress intensity of a growing crack thereby increasing critical crack size. Based on the data presented in [18], a mean stress intensity reduction factor of 0.75 with a standard deviation of 0.1 was used in the probabilistic model.

Variable #9: Initial Crack Size

For hub crack indications General Electric reported using "adders" of 0.080 and 0.070 inch for non-measurable and sized indications, respectively. For web indications General Electric reported using "adders" of 0.2 and 0.1 inch for non-measurable and sized indications, respectively. Therefore, a standard deviation of only 5% of reported size was applied to the keyway indications for SI's probabilistic evaluation. A range of mean initial crack sizes was investigated for each disk to obtain finite disk failure probabilities after 10^7 iterations.

Variable #10: SCC Growth Rate Coefficient, C_1

The first term in Equation 5-6, was assumed to be distributed normally with a mean of -4.968 and a standard deviation of 0.587 [11]. Based on a maximum growth rate of 0.038 inch/year inferred from inspection results, the maximum rate simulated in the probabilistic evaluation was limited to 2.5 standard deviations above the mean representing 99.4 percent of the database values.

Variable #11: SCC Growth Rate Temperature

The keyway temperature in the SCC growth rate Equation 5-6, was assumed to be distributed normally with a mean equal to the stage operating temperature reported by GE and a standard deviation estimated from upstream/downstream temperatures.

Variable #12: SCC Growth Rate - Yield Strength

Disk yield strength values for use in the SCC growth rate Equation 5-6, were assumed to be distributed normally with mean and standard deviation values inferred from proprietary material property data.

5.2.9 Probabilistic Analysis Results

Using the Monte Carlo technique, ten million (10^7) iterations (lifetime calculations) representing a minimum disk burst probability level of 1×10^{-7} were performed for each disk. Reproducibility and consistency of results was tested using various random number generators and random number seeds. Disk burst probabilities after six years of operation are plotted in Figure 5-14 for initial crack sizes ranging from 0.2 to 1.1 inch, without and with rotor pre-warming. The Structural Integrity probabilistic results indicated a reduction in the burst probabilities relative to that computed by the OEM.

The following observations were made based on these results:

(a) Even without rotor pre-warming, the disk burst probabilities predicted based on the 1996 inspection results are sufficiently low to satisfy the NRC limit of 5×10^{-6} per rotor for *unfavorable* orientation. These results indicate a higher margin relative to the 1990 OEM probabilistic analysis results, which indicated that the NRC limit was barely satisfied using the 1990 inspection findings.

(b) Without pre-warming, the L-1 disks are most life-limiting because of high FATT values relative to the other disks, which results in smaller critical crack sizes and therefore a shorter anticipated remaining life.

(c) Pre-warming of the rotor results in a significant reduction in L-1 disk burst probability, and was therefore recommended to reduce the overall probability of disk burst for the LPB rotor. With rotor pre-warming, the L-3 disks became the most probable failure location.

(d) Most of the failures in the 10^7 Monte-Carlo iterations performed were caused by a combination of low material toughness and high SCC growth rate. It was therefore judged that the simulation of a 120 percent overspeed event (2160 rpm) with a low probability of occurrence (less than 1×10^{-4}) would not appreciably change the burst probabilities.

Clinton LPB Rotor L-3, L-2 and L-1 Row Disks: Keyway Cracking
Probability of Failure after 6 years of operation
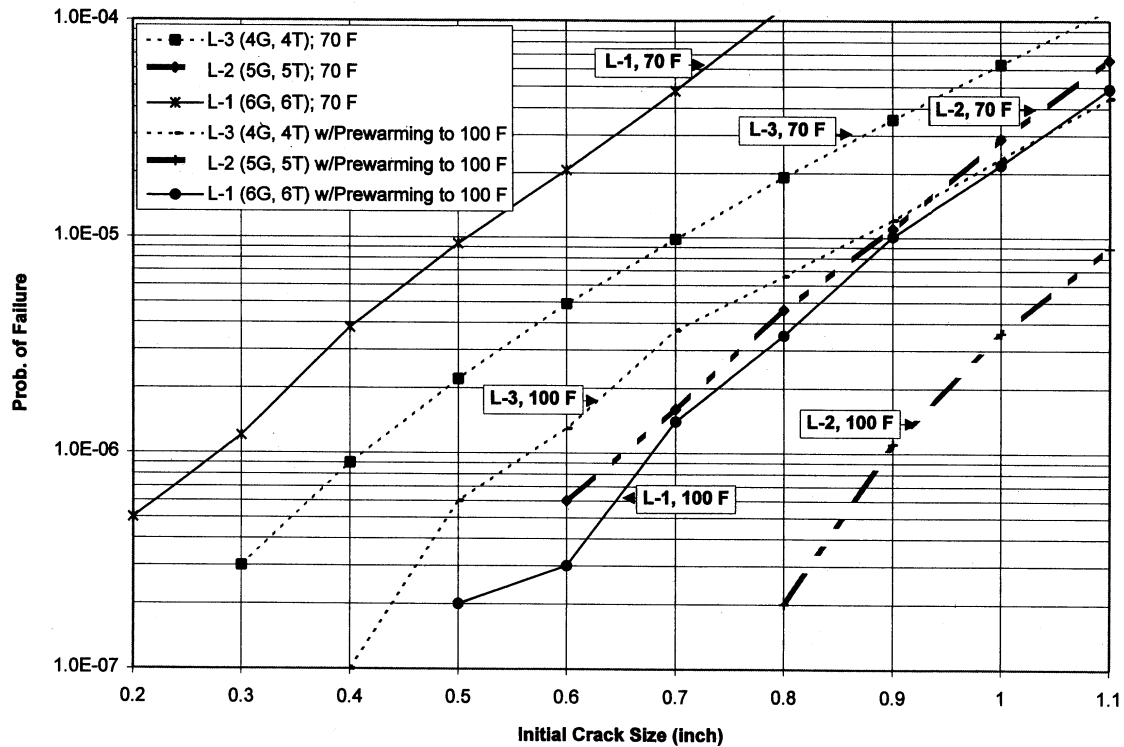
Figure 5-14 Disk burst probabilistic results for the Clinton LPB rotor without (70°F) and with (100°F) pre-warming

5.2.10 Conclusions; Clinton Investigation

Based on the results of both the deterministic and probabilistic analyses, continued operation for another six-year period without repair or removal of the keyway indications reported in disks 4, 5 and 6 was justified. The limiting NRC missile probability of $5x10^{-5}$ per rotor for favorable orientation can be satisfied, even without rotor pre-warming. To provide an additional margin of safety, however, pre-warming to increase the minimum disk temperature to 100°F was recommended. Re-inspection of the disks for keyway cracks at some future date is expected to provide a third data point, which would represent an important benchmark for determining actual SCC growth rates in the LPB rotor. Future inspections may indicate that actual crack growth rates have not changed appreciably and continue to be consistent with "mean" SCC growth rates. This observation could then justify a further reduction in the conservative distribution for SCC growth rate values used in this analysis and be the basis for a future revised probabilistic analysis to justify continued operation of the LPB rotor without repair or removal.

The differences noted in the above calculated probabilities compared to the OEM data is significant, and points out the need for further detailed comparisons to determine specific contributing factors.

5.3 Yankee Rowe LP Turbine Shrunk-on Disk Failure

This case history summarizes the results of a metallurgical evaluation of a failed turbine disk from the Yankee Rowe LP turbine [8, 19], supplemented by stress and fracture mechanics calculations performed by Structural Integrity to better understand the failure. This case history provides a valuable comparison of the fracture mechanics calculation results and actual failure of an operating disk and thus provides some verification of the type of numerical calculations described previously in this report in Chapter 4.

5.3.1 Plant Description and History

The Yankee Rowe turbine-generator is rated at 185 MW and the reactor is a PWR-style manufactured by Westinghouse. The turbines, also manufactured by Westinghouse, include one high-pressure (HP) turbine and one double-flow low-pressure (LP) turbine. Commercial operation of the plant began in July 1961. Through 1980, the plant had accumulated approximately 134,000 operating hours. The Yankee Rowe plant was retired in 1992.

The LP rotor was configured with six shrunk-on disks in each of the opposed flow paths, with two rows of blades carried by each of the first three disks and a single row of blades on each of the final three disks as shown in Figure 5-15. Inlet steam conditions to the LP turbine were; 40 psig pressure, and 265°F temperature. The Yankee Rowe unit employed a non-reheat turbine, i.e. steam conditions are saturated at the LP turbine. The design point LP turbine exhaust pressure was 1.5"Hg absolute (0.74 psia), which corresponds to a saturated steam temperature of 90°F. The disk material was reported to be a proprietary 2.5NiCrMoV alloy steel similar to A294 Class 5 and was specified to be in the normalized and tempered condition.

5.3.2 Failure Description and Examination of Components

On February 14, 1980 two disks in the LP turbine failed catastrophically. The failures occurred during a unit startup while the turbine was being stabilized at operating speed (1800 rpm). Both number-one disks (generator end and governor end of LP rotor) burst into several segments and caused severe internal damage to the turbine. None of the fragments penetrated the outer turbine casing. A schematic illustrating the fractured segments of the No. 1 generator-end disk, which is believed to have failed first, is shown in Figure 5-16 [8]. It was noted that none of the five major fracture paths that extend from the bore to the rim coincided with the keyways at the shaft-disk interface. Segment number 1 was provided to EPRI for the metallurgical investigation that is described in Reference [8].
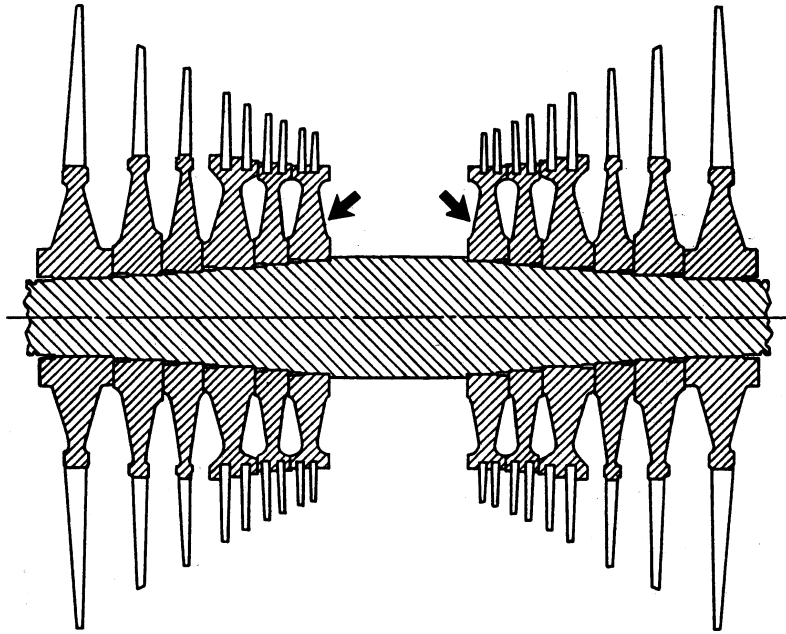
Figure 5-15 Schematic of Yankee Rowe LP rotor; arrows point out failed No.1 disks [8]
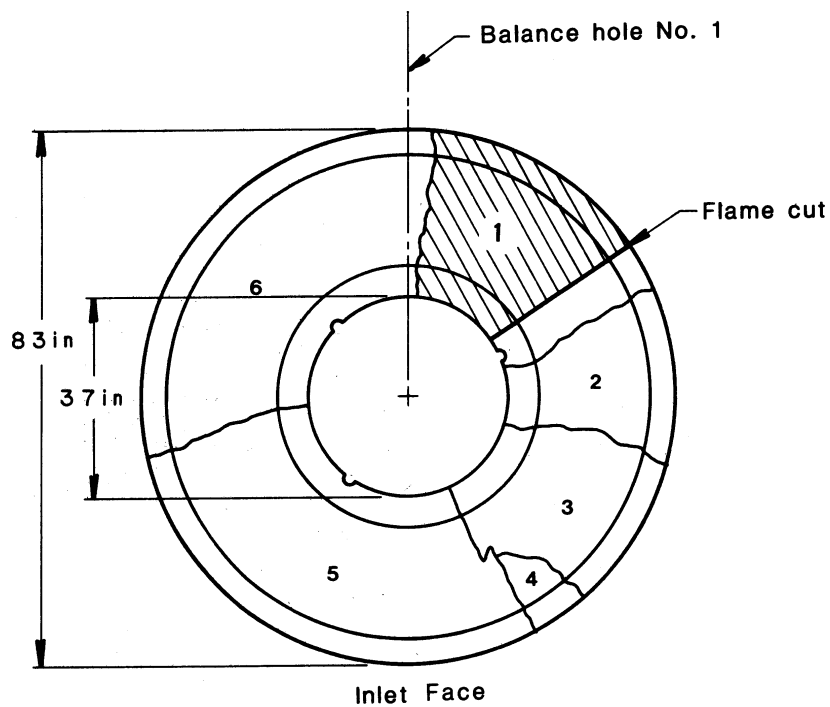
Figure 5-16 Diagram of Yankee Rowe failed generator-end no.1 disk (largest bore crack, 1.94" deep x 1.62" long, is at segments 5/6) [8]

Significant findings and conclusions from the initial NRC site investigation [19] and the EPRI failure investigation [8] were as follows:

(a) The major radial fracture in Segment No. 1 exhibited generally brittle features and contained four separate bore-connected cracks (see Figure 5-17). The largest crack in this segment was 1.04-inch deep and 2.04 inches in axial length. Fast fracture initiated from this crack and propagated in a radial direction from bore to rim. Another larger crack was evident, which is believed to have initiated the failure of the No.1 disk. This second crack measured 1.94 inches deep by 1.62 inches in axial length. This crack was located at the bore between segments No.5 and 6, and was not part of the EPRI investigation.

(b) All cracks were predominantly intergranular, with fractographic features indicating significant corrosive attack of the crack surfaces, but there was no evidence of pitting or general corrosive attack of the bore surface. A large number of crack initiation sites on the bore surface (several hundred) were documented by magnetic particle inspection, with crack lengths ranging from 0.1 to 0.7 inch; several cracks extended almost entirely across the axial width of the disk, which measures 10 inches [19]. The evidence suggested the most likely mechanism for in-service crack initiation and growth was stress corrosion cracking (SCC). Evidence included the intergranular, branched nature of the cracking, the wet steam environment and high tensile stresses in the disk bore. Air leakage may have also contributed to SCC initiation and crack growth.

(c) The tensile properties of the disk material are presented in Table 5-3. The disk was forged in 1958, and conformed to the requirements of ASTM A294 Class 5. This specification implies that no abnormalities in material properties or in microstructure were observed in manufacturing.

(d) Charpy V-Notch (CVN) impact test result and fracture toughness test results are presented in Figure 5-18 and Figure 5-19 respectively. The data indicated a low room temperature (70ºF) toughness in the range of 51-58 ksi√inch near the bore and 72-73 ksi√inch near the rim, with FATT values of 190ºF at the bore and 165ºF at the rim. Upper shelf toughness values of 139 and 166 ksi√inch, at the bore and rim, respectively, were estimated from CVN impact values at the approximate disk temperature of 300ºF.

(e) Significant residual tensile stresses at the bore surface were measured in a separate investigation. The observed levels were 10-25 ksi in the circumferential direction, and may have further contributed to SCC initiation and growth.

(f) Catastrophic rupture of the No. 1 disk occurred when the one or more bore cracks reached critical size for unstable fast fracture (fracture toughness was exceeded) due to an unfavorable combination of centrifugal stress and bore temperature during startup. Turbine startups, especially without pre-warming the rotor, increase the risk of disk brittle failure.
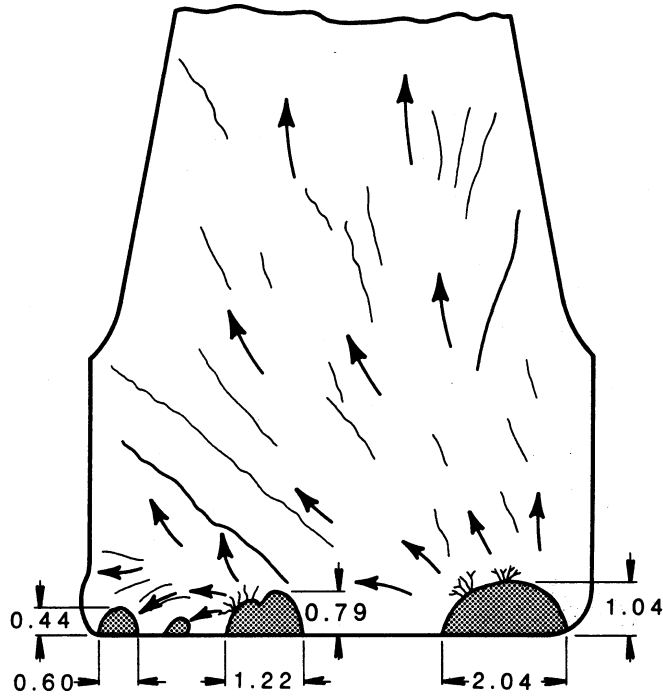
Figure 5-17 Diagram of Yankee Rowe failed generator-end No.1 disk [8]

Table 5-3 Tensile Properties for Yankee Rowe Failed Generator-End No.1 Disk Segment #1 [8]

Location	Ultimate Strength		Yield Strength		Reduction of Area %	Elongation in 2 in. %
	MPa	(ksi)	MPa	(ksi)		
Bore	928.1	(134.6)	768.8	(111.5)	47.0	17.3
	938.4	(136.1)	779.1	(113.0)	50.1	17.9
	950.1	(137.9)	784.6	(113.8)	49.1	17.5
Near Bore	932.9	(135.3)	772.9	(112.1)	47.7	16.1
	937.0	(135.9)	777.1	(112.7)	49.9	16.7
	943.9	(136.9)	780.5	(113.2)	49.6	17.5
Hub Average	938.4	(136.1)	777.1	(112.7)	48.9	17.6
Standard Deviation	± 8.2	(± 1.2)	± 5.5	(± 0.8)	±1.3	±0.6
Rim	891.5	(129.3)	742.6	(107.7)	50.1	18.2
	898.4	(130.3)	748.1	(108.5)	48.9	17.2
	903.9	(131.1)	751.6	(109.0)	46.7	17.6
Average	897.7	130.2	747.4	(108.4)	48.6	17.7
Standard Deviation	± 6.2	± 0.9	± 4.8	(± 0.7)	±1.7	±0.5
ASTM A 294-52 Class B3	827 min.	(120) min.	725 min.	(105) min.	-- --	18.0 min.
ASTM A 294-79 Class 5	860-1000	(125-145)	725 min.	(105) min.	45.0 min.	18.0 min.
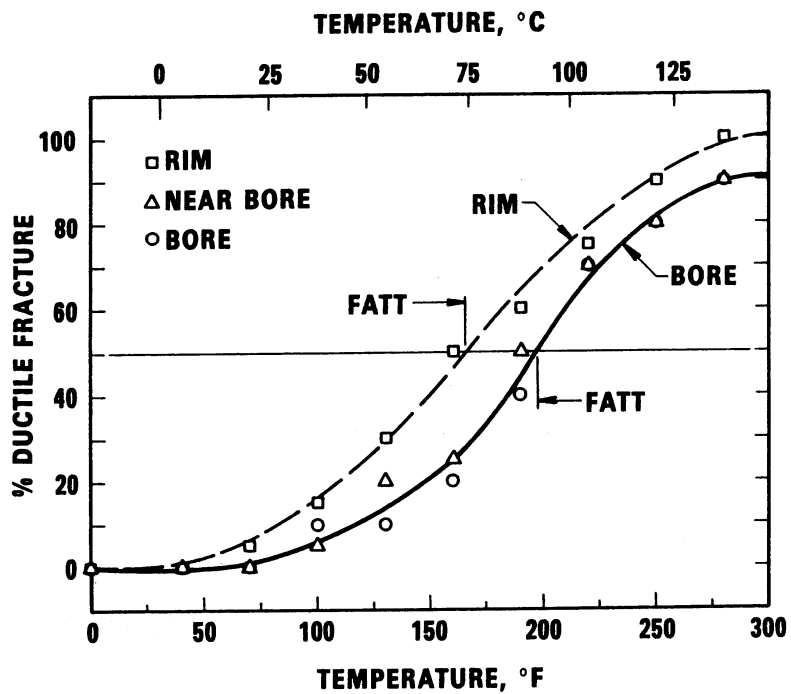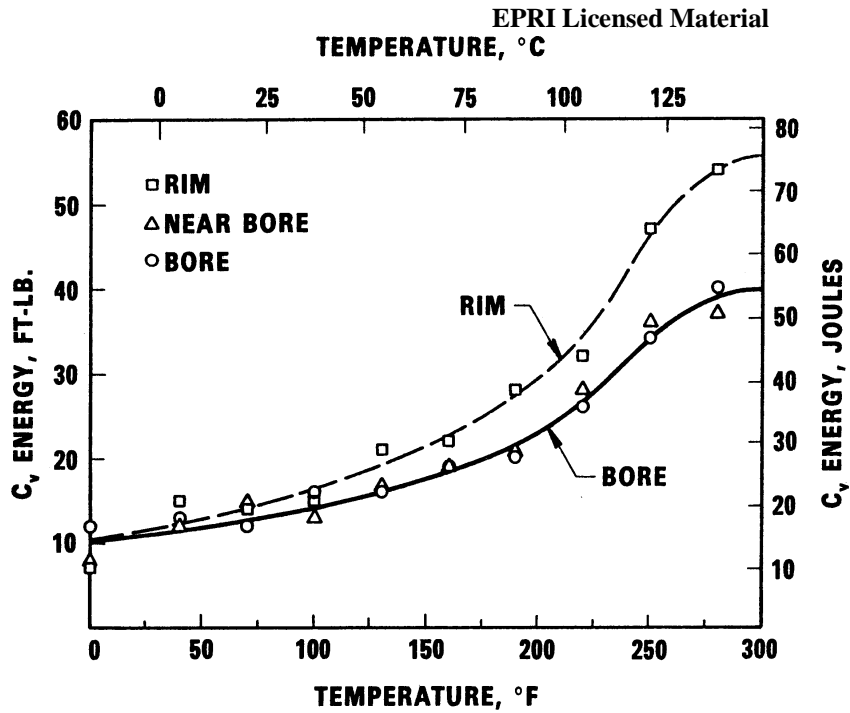
Figure 5-18 Charpy V-notch impact energies for Yankee Rowe failed generator-end no.1, disk segment #1(Bore FATT=190°F, Rim FATT=165°F) [8]
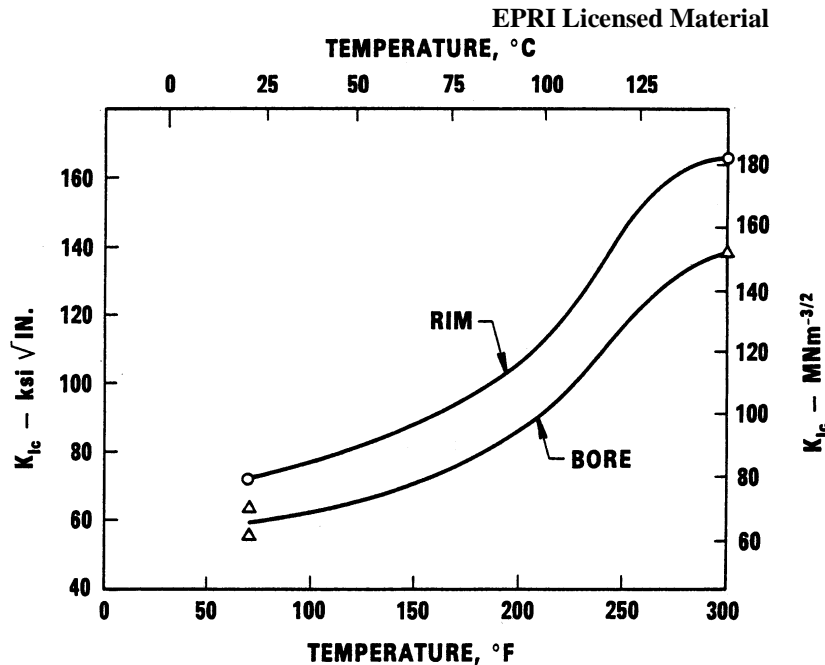
Figure 5-19 Plane strain fracture toughness for Yankee Rowe failed generator-end No.1 disk segment #1 (bore FATT=190°F, rim FATT=165°F) [8]

5.3.3 Stress and Fracture Mechanics Calculations

Structural Integrity Associates (SI) performed stress and fracture mechanics analyses to provide additional insight into the brittle failure of disk 1. Disk stresses were estimated using classical solutions for a rotating cylinder [4] and press-fit of two cylinders [5]. Two methods were used to estimate of stress:

1. The first estimate was based on design criteria contained in References [8] and [19]. This criteria states that the shrink-fit stresses are 65 percent of minimum specified yield strength (105 ksi) or 68.3 ksi, and that these stresses remain approximately constant at operating speed.   As a shrunk-on disk increases rotational speed, the initially high shrink-fit stress is reduced, but the inertial hoop stresses increases. The nominal net result is an approximately constant bore stress, until a speed is reached that removes the shrink-fit. The stress data is plotted versus speed and radial location in Figure 5-20.

2. The second stress estimate was based on a generally accepted design rule for shrunk-on disks fitted with keyways, which states that the level of shrink-fit during assembly is selected such that loss of shrink-fit occurs at 120 percent of rated speed. Hoop stress distributions from the second estimate are plotted in Figure 5-21. There is good agreement shown with the results of the first method presented in Figure 5-20.
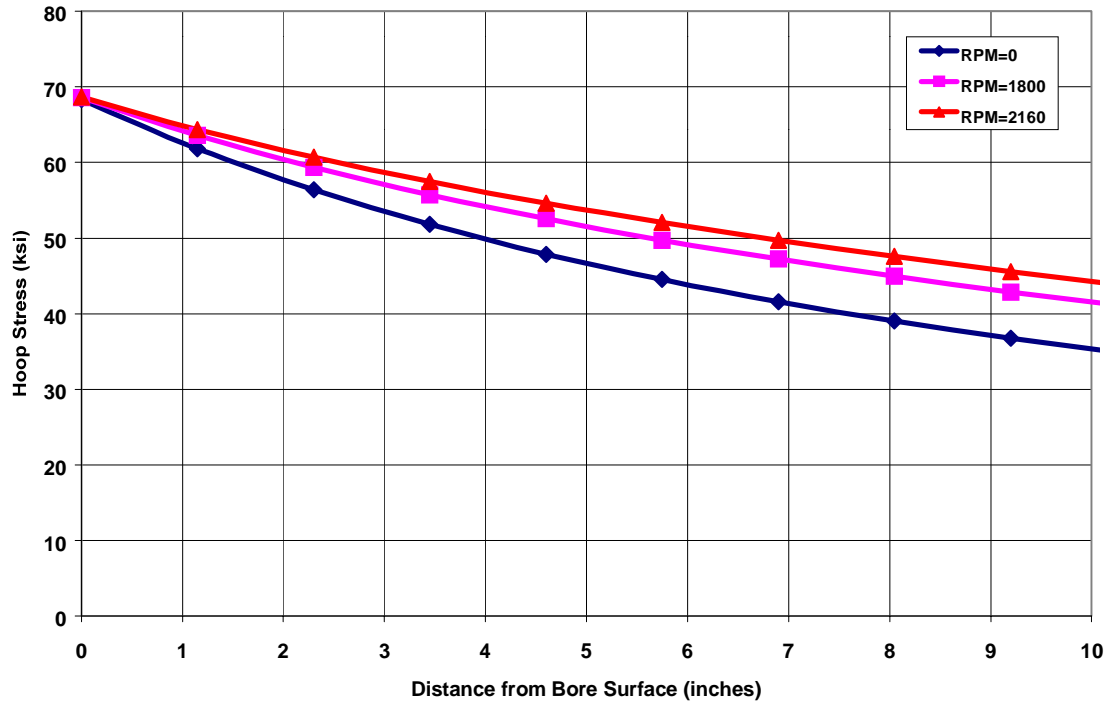
Figure 5-20 Hoop stress gradient from the bore of the failed Yankee Rowe no.1 disk (estimated using 65% of minimum yield or 68.3 ksi)
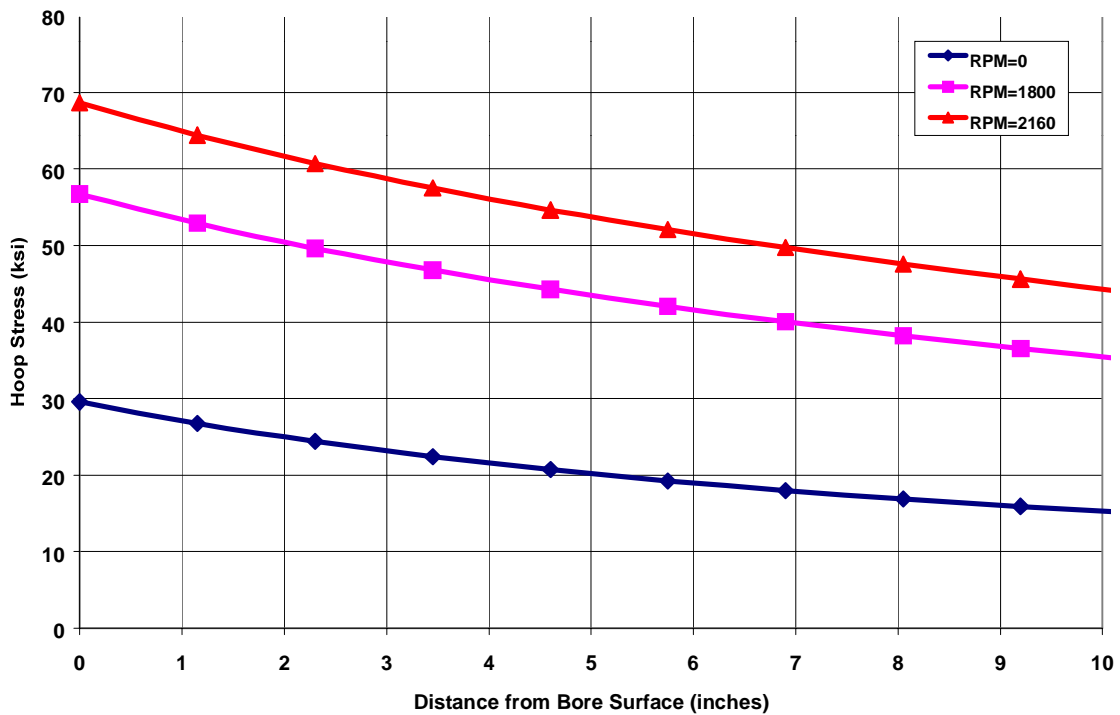
Figure 5-21 Hoop stress gradient from the bore of the failed Yankee Rowe no.1 disk (estimated using loss of shrink-fit at 120% rated speed)

Stress intensity factors were calculated and are presented in Figure 5-22 for a semi-circular crack (ratio of crack depth to axial length of 1:2) at the ID of a hollow cylinder. These results were generated using Structural Integrity's fracture mechanics code pc-CRACK^{TM} [7]. The semi-circular crack model is believed to be a reasonably good representation of most of the significant thumbnail surface-connected cracks, including the largest one, which is believed to have caused the failure. Results of the stress intensity calculations are plotted in Figure 5-22 based on both of the above stress estimates.

Yankee Row LP Rotor Disk No. 1
Stress Intensity Factors for an Axially Oriented Semi-Circular Crack at ID of a Hollow Cylinder
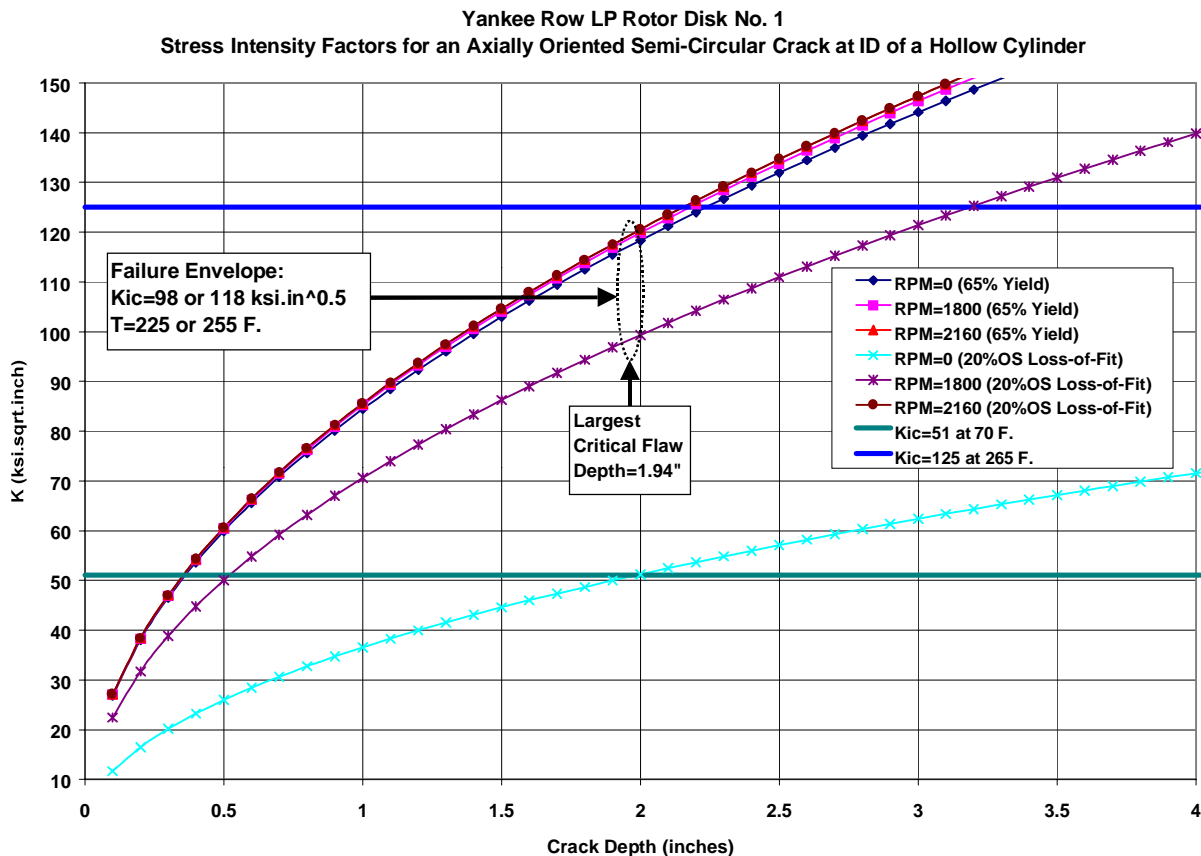
Figure 5-22 Stress intensity factor (K$_I$) versus crack size (a) results for the failed Yankee Rowe no.1 disk

The failure was reported to have occurred at 1800 rpm. From Figure 5-22 at 1800 rpm, and a critical crack depth of 1.94 inches, stress intensity factors of 118 and 98 ksi√inch were predicted for the two stress estimates. Corresponding operating temperatures of 255ºF and 225ºF were predicted to yield fracture toughness values corresponding to these calculated critical stress intensity factors. The first stress calculation method (65 percent yield), however, predicts the same 118 ksi√inch stress intensity factor at both zero speed and at 1800 rpm. Since the disk material is typically colder at standstill the material would exhibit lower fracture toughness. If

the first method for stress estimate were correct, then, failure should have occurred at standstill. The second stress estimate yields an inferred fracture toughness of 98 ksi√inch at a temperature of 225°F, and is believed to be more plausible for two reasons:

1. during unit startup, when the turbine first reaches 1800 rpm, the disk bore temperature is typically lower than the inlet steam temperature (265°F) because of the time required for heat transfer from the rim to the bore

2. the disk failure did not occur at zero speed, implying that higher stresses were experienced at 1800 rpm. Since the dimensions of the largest observed flaw was 1.94 inch deep by 1.62 inches in length, stress intensity factors shown in Figure 5-22 may be higher than that for this flaw. This would imply a slightly lower fracture toughness (~85-90 ksi√inch) and a lower bore temperature (~195-205°F), which could be even more plausible.

5.3.4 Concluding Comments; Yankee Rowe Disk Failure

In conclusion, the low fracture toughness in the bore area of this 1958-vintage disk forging during startup (51-90 ksi√inch) appears to have been the principal contributor to the failure. Yankee Rowe, which was retired in 1992 was one of the oldest nuclear plants in the U.S. Most modern turbine rotors manufactured using VCD or ESR forging techniques, yield fracture toughness values in excess of 180 ksi√inch at room temperature. Although the bore stresses were not evaluated using finite-element analysis techniques, the stress intensity model using pc-CRACK[TM] is perceived to have yielded accurate results based on the prediction that the crack tip stress intensity factor was very close to critical for the observed initiating cracks.

References

1. D. A. Rosario and P. C. Riccardella, "Evaluation of the Pilgrim Unit 1 Low Pressure Turbine Rotor 7th Stage Shrunk-on Disk," Structural Integrity Associates letter report No. SIR-93-047, Rev. 0, May 5, 1993 [Rev.2, issued April 14, 1994].
2. NRC memorandum from Jack R. Strosnider to Walter R. Butler, June 17 1993, re: "Pilgrim Unit 1: Assessment of Low Pressure Turbine Analysis."
3. "Pilgrim Critics Claim Danger from Cracked Low-Pressure Turbine Disks," Article from INSIDE N.R.C., June 28, 1993, written by Dave Airozo, Washington.
4. F. D'Isa, "Mechanics of Metals", 1975, Addison-Wesley Publishing Company,
5. J. E. Shigley, "Mechanical Engineering Design", 1972, 2nd Edition, McGraw-Hill Book Company.
6. EPRI Report, NP-3340, "Stress and Fracture Analysis of Shrunk-on Steam Turbine Disks", 1984.
7. Structural Integrity Associates, "pc-CRACK", Version 2.1, 1991.
8. EPRI Report, NP-2738, "Metallurgical Evaluation of a Failed LP Turbine Disc", Research Project 1398-6, December 1982.
9. Presentations by General Electric Co. to Boston Edison, 4/29/93, 4/28/93, 12/7/92 and 3/8/92, on axial keyway cracking of Pilgrim Unit 1 LP rotor shrunk-on disks.
10. Compilation of Proprietary GE, Westinghouse and CEGB Stress Corrosion Crack Growth Rates versus Wheel Operating Temperature.
11. W. G. Clark, B. B. Seth, and D. M. Shaffer, "Procedures for Estimating the Probability of Steam Turbine Disc Rupture from Stress Corrosion Cracking", presented at Joint ASME/IEEE Power Generation Conference, October 1981.
12. F. F. Lyle, Jr., "Low-Pressure Rotor Disc Cracking and Remaining Life Analysis", Proceedings of the Fossil Steam Turbine Disc Cracking Workshop, April 1991.
13. Telephone conversation between D. Rosario of SI and C. Jungclas of Boston Edison regarding Pilgrim Unit 1 turbine-generator overspeed testing, May 1, 1993.
14. D. A. Rosario, S. Dasgupta, D. L. Anthony, P. Sabourin and T. McCloskey, "Evaluation of Bore/Keyway and Dovetail Cracking in an LP Rotor," Proceedings of the 5th EPRI Steam Turbine/Generator Workshop, July 29-August 1, 1997, Lake Buena Vista, Florida.
15. J. H. Presson et al, "Improved Nuclear LP Turbine Inspection Strategy- A Team Approach," Proceedings: Fourth EPRI Turbine/Generator Workshop, August 1-4, 1995, Milwaukee, Wisconsin.
16. R. C. Schwant and D. P. Timo, "Life Assessment of General Electric Large Steam Turbine Rotors," EPRI CS-4160, Proceedings of the Seminar on Life Assessment and Improvement of Turbo-Generator Rotors for Fossil Plants, September 12-14, 1984, Raleigh, North Carolina.
17. GE Power Generation, Service Engineering Report "Shrunk-on Wheel Inspection - LPB Rotor; Rewrite of the 11/27/90 Report Incorporating the Effect of Unit Orientation," October 28, 1992.
18. A. McMinn et al, "A Review of Stress Corrosion Cracking of Low-Pressure Turbine Discs in the Nuclear Industry," EPRI Research Project 1929-14, December 1989.

19. A. Goldberg and R. D. Streit, Lawrence Livermore Laboratory "Observations and Comments on the Turbine Failure at Yankee Atomic Electric Company, Rowe, Massachusetts," NUREG/CR-1884, UCID-18850, November 15, 1980.

6
SUMMARY AND RECOMMENDATIONS

The purpose of this report is to examine and explain areas of potential conservatism in the current approach to calculating turbine missile probability. These probability assessments are required by regulators, and form the basis for turbine disk re-inspection intervals and frequency of turbine valve surveillance tests. Operators of nuclear plants are seeking to identify and reduce conservatisms in the missile analyses, which would provide the technical justifications for relaxation of disk inspection and valve testing requirements that affect plant operation and maintenance activities.

6.1 Summary

This report has provided a complete overview of the background and details of the current procedure for missile probability assessment. The process involves several diverse areas of risk assessment and management, including disk inspection, fracture mechanics, valve failure rates, high-energy fragment penetration characteristics, strike probability for specific plant equipment, and damage probability of struck targets. All of these topics are covered in this report, and potential conservatisms were identified in many of the areas. It is likely that if each of the above areas were to be pursued in depth as part of a future program to create a refined missile probability assessment methodology, a significant reduction is missile probability could be demonstrated. This could, in turn, provide the basis for the desired relief in disk inspection intervals and valve test frequencies – subject to review and approved by regulators and appropriate changes by plant operators to meet the requirements of their license.

NRC acceptance of a revised basis for determining missile probability is critical, and will require significant interaction between licensees and the NRC to achieve. Recent conversations with the NRC staff have indicated their willingness to re-examine the subject of turbine missile probability, and it is likely that this current effort by EPRI could provide a crucial technical starting point for upcoming discussions.

Since the mid-1980s, the NRC has instructed licensees to focus only on the probability of missile generation, while assigning a fixed "industry-wide" set of probabilities for the subsequent strike and damage of plant safety-related equipment. Most licensees currently rely on their turbine OEMs to generate this missile generation probability and a standard report typically follows routine inspections of the disk bore and keyway region. Disks with few or no SCC flaw indications are given relatively longer re-inspection intervals than those disks exhibiting larger cracks. Plants that operate with relatively little SCC damage are also permitted a moderate extension of the frequency of valve and overspeed control system testing. These OEM-supplied analyses are based on a combination of fundamental principles, such as fracture mechanics, years of field observations from cracked disks, and operational event histories related to reliability of plant control systems. All analyses are structured as probabilistic calculations rather than deterministic calculations, and the NRC has reviewed and approved each OEM procedure.

6.1.1 Options Available

Table 6-1 summarizes the findings reported in this document. Table 6-1 is a high-level summary, and the reader is encouraged to find supporting details in Chapters 2-5 of this report. Six risk elements are identified, with comments relating to how conservatism could be reduced. The relative potential for reduced conservatism, and the R&D costs range associated with each element are listed. Detailed costs for development and implementation of each item are not yet available, so the information in Table 6-1 is based on the judgement of EPRI staff at this time.

It is noted that several of the items in Table 6-1 are interrelated, and in-fact these items are tightly integrated in the present OEM methodology for assessing risk. This is an important issue if the option of replacing only *portions* of the existing OEM-supplied analysis were considered. An example is the assessment of missile probability attributable strictly to failure of the turbine overspeed protection system. This probability is not clearly identified in the current OEM-supplied missile probability reports. De-coupling this risk element and replacing it with an independent assessment would likewise require OEM cooperation.

Currently, however, the assessment of P_1 is completely de-coupled from the evaluation of P_2 and P_3. This de-coupling was proposed originally by Bush, and has remained this way based on NRC recommendations. This suggests that developing a revised approach to assessment of P_2 and P_3 would have some advantages since licensees could still use the currently-supplied assessments of P_1, but with probability limits that are increased commensurate with the expected decrease in the combined probability $P_2 \times P_3$. Unfortunately, this approach to managing the overall probability P_4 by performing a more refined analysis of $P_2 \times P_3$ has been discouraged by the NRC, who have stated that licensees must manage P_1 through a program of testing and inspection. EPRI also cautions against seeking regulatory approval for increases in the current limits on missile generation probability, P_1. Plant operators should be aware of the significant safety risk to plant personnel and financial risk associated with a turbine missile event – even if there is no associated damage to plant safety related equipment. The lost generation and replacement power cost that would be associated with repairs following a turbine missile event, combined with the repair costs, are expected to outweigh any advantages to O&M associated with an increased allowable limit on P_1.

6.1.2 Recommendations

EPRI will organize a group of licensees to act both as utility advisors on this project, and the interface to the NRC. EPRI will also establish contracts with specialists in fracture mechanics and probabilistics. This combined group will meet with EPRI staff for a presentation of the technical issues covered in this report. Other items to be covered in this meeting include the licensing ramifications of a revised missile probability assessment methodology, and development of a plan for including or interfacing with the OEMs in the re-evaluation of missile probability.

It is recommended that these technical advisors organize a meeting with both NEI and NRC in which the technical material contained in this report is presented. EPRI will provide technical support for this meeting. Topics that should be explored in these discussions include:

It is recommended that these technical advisors organize a meeting with both NEI and NRC in which the technical material contained in this report is presented. EPRI will provide technical support. Topics that should be explored in these discussions include:

- NRC technical opinion on the areas of conservatism identified by this report
- NRC opinion on implementing potential new risk assessment procedures (individual licensee or industry-wide)
- NRC position on further extensions to overspeed control system test intervals; source of suitable industry data, and other constraints on maximum intervals
- Is the NRC open to the possibility of re-examining P_2 and P_3?
- NRC's vision of the future role of OEM's in missile risk assessment
- Procedure required for qualification of any software to be used in a future missile probability evaluation tools

Based on the outcome of the discussions with NEI/NRC, and with the recommendations of the project technical advisors, EPRI will proceed with development of a select set of the refinements described in Table 6-1. Based on EPRI's assessment of the potential gains associated with improving the assessment of various risk elements, it is likely that the plan will include development of a new fracture mechanics analysis tool, which will require the appropriate level of software quality control as required by the NRC. It is also likely that the plan would include the creation of an independent database for assessments of turbine overspeed control failure rates.

Regarding the potential advantages offered by phased-array NDE in keyway inspections, EPRI will approach potential commercializers for this service.

Table 6-1 Elements of current methodology for assessing risk of damage to safety-related by turbine missiles, with potential for improved methodology

Item	Probability component*	Risk element	Current basis	Strategy for refinement	Potential gains**	R&D cost range**	comments
1	P_1	Turbine overspeed control failure	Pre-1991 industry event data	Use current industry data, refine to include	M	M/L	This risk element is currently integrated with overall P_1 evaluation is likely available
2	P_1	Disk brittle failure due to SCC	Linear analysis with probability assessment via closed-form solutions	Employ refined models and numerical techniques for critical crack size evaluation, use Monte-Carlo techniques	H	H	Case histories demonstrate significant reduction in conservatism possible. NRC demonstrated willingness to pursue. Analysis more complex and requires specialist. Availability of key input data still undetermined
3	P_1	Assessment of existing flaw characteristics	Fixed-angle UT techniques	Phased-array UT techniques	M	M	Needs additional verification of improved detection and sizing, particularly with Westinghouse-style disks. Implementation would require commercializer.
4	P_1	Fragment penetration probability	OEM-proprietary analysis, supported by tests	Revised analysis based on results of EPRI sled-tests performed at Sandia Labs	L	M/H	Implementation level dependent on separation of burst and missile probabilities from OEM calculations or development of alternative calculation/analysis methodology using EPRI test data.
5	P_2	Strike probability	Monte-Carlo approach developed by Semanderes	Review details to assess possible improvements; make more plant-specific	L	M	NRC currently discouraging. Current methodology may already be sufficiently refined. New method would require specialist to implement
6	P_3	Probability of damage to struck safety-related equipment	Conservative value of 1.0 assigned	Integrate with analysis of P_2 to account for range of missile size and energy	M/H	M	NRC currently discouraging. New method would require specialist to implement

* see Chapter 2 for definition

** three categories are high (H), moderate (M), and low (L)

About EPRI

EPRI creates science and technology solutions for the global energy and energy services industry. U.S. electric utilities established the Electric Power Research Institute in 1973 as a nonprofit research consortium for the benefit of utility members, their customers, and society. Now known simply as EPRI, the company provides a wide range of innovative products and services to more than 1000 energy-related organizations in 40 countries. EPRI's multidisciplinary team of scientists and engineers draws on a worldwide network of technical and business expertise to help solve today's toughest energy and environmental problems.

EPRI. Electrify the World